

Winter 2013

Rheological study of asphalt binders with a wax-based Warm Mix Additive and its relationships to mix compaction and rutting

Rajan Saha

Follow this and additional works at: <https://digitalcommons.latech.edu/dissertations>

 Part of the [Civil Engineering Commons](#)

RHEOLOGICAL STUDY OF ASPHALT BINDERS WITH A WAX-BASED
WARM MIX ADDITIVE AND ITS RELATIONSHIPS
TO MIX COMPACTION AND RUTTING

by

Rajan Saha, B.S.

A Dissertation Presented in Partial Fulfillment
Of the Requirements for the Degree
Doctor of Philosophy

COLLEGE OF ENGINEERING AND SCIENCE
LOUISIANA TECH UNIVERSITY

March 2013

UMI Number: 3570073

All rights reserved

INFORMATION TO ALL USERS

The quality of this reproduction is dependent upon the quality of the copy submitted.

In the unlikely event that the author did not send a complete manuscript and there are missing pages, these will be noted. Also, if material had to be removed, a note will indicate the deletion.



UMI 3570073

Published by ProQuest LLC 2013. Copyright in the Dissertation held by the Author.

Microform Edition © ProQuest LLC.

All rights reserved. This work is protected against unauthorized copying under Title 17, United States Code.



ProQuest LLC
789 East Eisenhower Parkway
P.O. Box 1346
Ann Arbor, MI 48106-1346

LOUISIANA TECH UNIVERSITY

THE GRADUATE SCHOOL

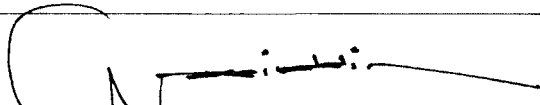
09-21-12

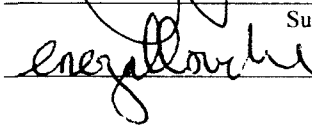
Date

We hereby recommend that the dissertation prepared under our supervision by Rajan Saha

entitled Rheological Study of Asphalt Binders with a Wax-Based Warm Mix Additive and Its Relationships to Mix Compaction and Rutting


be accepted in partial fulfillment of the requirements for the Degree of Doctor of Philosophy in Engineering (Civil)

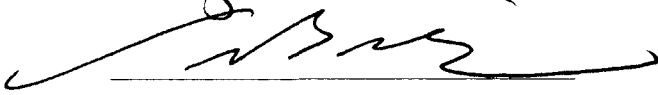


Supervisor of Dissertation Research



Head of Department
Civil Engineering
Department

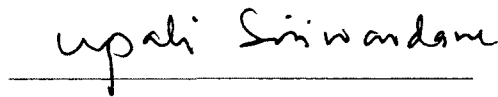
Recommendation concurred in:






Advisory Committee



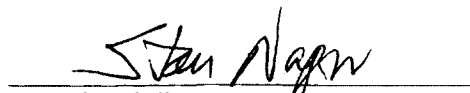


Approved: 

Director of Graduate Studies

Approved: 

Dean of the Graduate School



Dean of the College

ABSTRACT

Although the energy saving Warm Mix Asphalt (WMA) technology that produces asphalt mixes at lower temperatures are around for about a decade, there still exist some concerns that are hindering its wide spread implementation. The overall objective of this study is to investigate if the viscosity reductions at higher temperatures have any impacts on asphalt mix compaction and rutting performances. This study reveals that there exists a critical temperature for each asphalt binder below which viscosity will increase with addition of Sasobit[®]. Therefore, compaction below the critical temperature can negatively impact density.

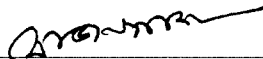
For PG 64-22, the critical temperature is 104 °C and for PG 76-22M, the critical temperature is about 101 °C. Another significant finding of this study is that with the addition of Sasobit[®], asphalt binders become a shear-thinning liquid even at compaction temperature ranges. The shear rate dependency increases with an increase in percent of Sasobit[®]. This indicates if the actual shear rate during the compaction process is higher than 6.8 s^{-1} , then the currently recommended viscosity as well as temperature is overestimated and compaction temperature can be reduced. On the other hand, if the actual shear rate during the compaction process is lower than 6.8 s^{-1} , then the currently recommended viscosity as well as temperature is underestimated and a higher compaction temperature should be used.

This study further reveals that an optimum amount of Sasobit[®] exists between 2% and 4% based on phase angle and non-recoverable creep compliance analyses of PG 64-22 and based on percent recovery of PG 76-22M. Currently used rutting factor $G^*/\sin\delta$ fails to indicate any optimum amount. Phase angle values suggest if rutting is performed at one grading higher temperature, an overdose of Sasobit[®] will increase rutting potential. Creep and recovery tests at equal-stiffness temperature indicate that addition of Sasobit[®] increases rutting resistance at lower stress while it increases rutting potential at higher stress. APA rut depths indicate that Sasobit[®] mixes prepared at WMA temperatures performed better than HMA without Sasobit[®]. However, from aging evaluation of extracted asphalt binders it was revealed that reduced production temperatures reduces aging and may increase rutting susceptibility. Finally, from an exploratory study it was concluded that wax modified asphalt binders may be differentiated by its morphology using an AFM. Overall, this study provides fundamental findings with respect to rheology and performance which will help implement warm mix asphalt in the U.S.

APPROVAL FOR SCHOLARLY DISSEMINATION

The author grants to the Prescott Memorial Library of Louisiana Tech University the right to reproduce, by appropriate methods, upon request, any or all portions of this Dissertation. It is understood that "proper request" consists of the agreement, on the part of the requesting party, that said reproduction is for his personal use and that subsequent reproduction will not occur without written approval of the author of this Dissertation. Further, any portions of the Dissertation used in books, papers, and other works must be appropriately referenced to this Dissertation.

Finally, the author of this Dissertation reserves the right to publish freely, in the literature, at any time, any or all portions of this Dissertation.

Author 
Date 11-15-12

DEDICATION

I wish to dedicate this dissertation to my parents, Engr. Rabindra Ranjan Saha and Dr. Chinu Rani Roy; my sister, Dr. Anamika Saha; my wife, Dr. Sharmi Saha, and my cousin, Ajit Roy. Without their love and support, I would not be where I am today.

TABLE OF CONTENTS

| | |
|---|-----|
| ABSTRACT..... | iii |
| DEDICATION..... | vi |
| LIST OF TABLES..... | xi |
| LIST OF FIGURES..... | xvi |
| LIST OF ABBREVIATIONS..... | xix |
| ACKNOWLEDGEMENTS..... | xxi |
| CHAPTER 1 INTRODUCTION..... | 1 |
| 1.1 Objectives..... | 4 |
| 1.2 Scope of the Research..... | 4 |
| 1.3 Organization of the Dissertation..... | 5 |
| CHAPTER 2 LITERATURE REVIEW | |
| 2.1 Introduction..... | 6 |
| 2.1.1 Sasobit®..... | 8 |
| 2.1.2 Asphaltan B®..... | 11 |
| 2.1.3 Aspha-Min®..... | 11 |
| 2.1.4 Foamed Asphalt..... | 13 |
| 2.1.5 Evotherm®..... | 14 |
| 2.1.6 Advera®..... | 14 |

| | |
|--|----|
| 2.2 Rheological Study of Wax-Based WMA..... | 15 |
| 2.3 Low Temperature Rheological Study of Wax-Based WMA..... | 17 |
| 2.4 Effects on Rutting Characteristics | 18 |
| 2.5 Summary on Rutting Characteristics | 29 |
| CHAPTER 3 EFFECTS OF A WAX-BASED WARM MIX ADDITIVE (SASOBIT[®]) ON LOWER COMPACTION TEMPERATURES | |
| 3.1 Introduction..... | 30 |
| 3.2 Objectives | 33 |
| 3.3 Material Description | 34 |
| 3.4 Experimental Plan..... | 35 |
| 3.4.1 Asphalt Binder Testing | 35 |
| 3.4.2 Mix Testing..... | 36 |
| 3.5 Experimental Procedure..... | 37 |
| 3.5.1 DSR Sample Preparation | 37 |
| 3.5.2 Superpave Mix Design Sample Preparation | 38 |
| 3.6 Results and Discussions..... | 39 |
| 3.6.1 Effects on Binder Stiffness, $G^*/\sin\delta$ | 39 |
| 3.6.2 Effects of Sasobit [®] at Compaction Temperatures on Viscosity..... | 41 |
| 3.6.3 Implications of Viscosity Changes on Field Density..... | 48 |
| 3.6.4 Effect of Sasobit [®] on Density of Gyratory Compacted Samples..... | 50 |
| 3.7 Conclusions..... | 53 |
| CHAPTER 4 EFFECT OF SHEAR RATE ON VISCOSITY OF SASOBIT[®] MODIFIED ASPHALT BINDER | |
| 4.1 Introduction..... | 55 |

| | |
|--|-----|
| 4.2 Objectives | 56 |
| 4.3 Material Description | 57 |
| 4.4 Experimental Plan..... | 57 |
| 4.5 Results and Discussions..... | 58 |
| 4.5.1 Effect of Shear Rate on Viscosity | 58 |
| 4.5.2 Viscosity Model | 65 |
| 4.5.3 Zero Shear Viscosity | 66 |
| 4.5.4 Steady State Viscosity and Dynamic Viscosity | 69 |
| 4.6 Conclusions..... | 71 |
| CHAPTER 5 LABORATORY EVALUATION OF RUTTING PERFORMANCE OF SASOBIT [®] MODIFIED WARM MIX ASPHALT | |
| 5.1 Introduction..... | 73 |
| 5.2 Objectives | 73 |
| 5.3 Materials and Test Matrix | 74 |
| 5.4 Rheological Evaluation of Sasobit [®] Modified Asphalt Binders with Dynamic Modulus Master Curves | 79 |
| 5.5 Evaluation of Sasobit [®] Modified Asphalt Binder's Rutting Factor $G^*/\sin\delta$ from Temperature Sweep Test..... | 83 |
| 5.6 Evaluation of Percent Recovery and J_{nr} as Rutting Factors Using MSCR Test for Sasobit [®] Modified Asphalt Binders..... | 86 |
| 5.7 Evaluation of Rutting Susceptibility of Sasobit [®] Modified WMA..... | 96 |
| 5.7.1 Effects of Sasobit [®] on Rutting Susceptibility of HMA..... | 98 |
| 5.7.2 Evaluation of Rutting Susceptibility of Sasobit [®] Modified WMA | 100 |
| 5.7.3 Development of a Linear Multiple Variable Rutting Model | 102 |

| | |
|---|------------|
| 5.8 Evaluation of Aging..... | 104 |
| 5.9 Conclusions..... | 106 |
| CHAPTER 6 EVALUATION OF ATOMIC FORCE MICROSCOPE (AFM) AS A SCREENING TOOL FOR ASPHALTIC MATERIALS – AN EXPLORATORY STUDY | |
| 6.1 Introduction..... | 110 |
| 6.2 Objective | 111 |
| 6.3 Asphalt Binder Film Preparation | 111 |
| 6.4 Results and Discussions..... | 112 |
| 6.5 Conclusions..... | 120 |
| CHAPTER 7 CONCLUSIONS AND RECOMMENDATIONS..... | 121 |
| REFERENCES | 129 |
| APPENDIX A RHEOLOGICAL DATA | 137 |
| APPENDIX B MIX DESIGN DATA | 160 |
| APPENDIX C RUT TEST DATA | 162 |
| APPENDIX D AGING DATA..... | 173 |

LIST OF TABLES

| | | |
|------------|--|----|
| Table 2-1. | WMA technologies (D'Angelo et al., 2008)..... | 6 |
| Table 2-2. | Green house gas reductions for WMA (Gandhi, 2008)..... | 7 |
| Table 2-3. | Literature review on rheological study of WMA..... | 15 |
| Table 2-4. | Minimum flow number requirements | 19 |
| Table 2-5. | NCHRP 09-33 rutting resistance from flow number testing results (Bonaquist, 2011) | 20 |
| Table 2-6. | APA rut test results (Hossain et al., 2009)..... | 22 |
| Table 2-7. | APA rut test results (Middleton and Forfylow, 2009) | 24 |
| Table 2-8. | HWTT results for plant-produced mixes (Diefenderfer and Hearon, 2008)..... | 26 |
| Table 2-9. | Results of laboratory produced samples (Diefenderfer and Hearon, 2008)..... | 27 |
| Table 3-1. | Aggregate gradation..... | 34 |
| Table 3-2. | Material sources | 34 |
| Table 3-3. | Experimental plan for rheological testing..... | 35 |
| Table 3-4. | Experimental plan for mix design sample testing..... | 36 |
| Table 3-5. | Aggregate test data..... | 38 |
| Table 3-6. | Density test result of mix | 38 |
| Table 3-7. | Volumetric data..... | 38 |
| Table 3-8. | Effect on binder stiffness | 39 |
| Table 3-9. | Effect of Sasobit® at higher compaction temperature (130 °C)..... | 41 |

| | | |
|-------------|---|----|
| Table 3-10. | Effect of Sasobit [®] at lower compaction temperature (100 °C)..... | 42 |
| Table 3-11. | Nuclear gauge field density (average of six locations from Cooper, 2009) | 49 |
| Table 3-12. | G _{mb} data of gyratory compacted samples | 51 |
| Table 4-1. | Experimental plan for shear rate study | 58 |
| Table 4-2. | Zero shear viscosity and CROSS model parameters | 66 |
| Table 4-3. | Correlation between zero shear viscosity and G*/sinδ | 68 |
| Table 4-4. | Steady state (rotational) viscosity and dynamic (sinusoidal) viscosity | 70 |
| Table 5-1. | Test matrix for dynamic modulus master curve | 74 |
| Table 5-2. | Test matrix for rutting Parameter G*/sinδ | 75 |
| Table 5-3. | Test matrix for MSCR test..... | 76 |
| Table 5-4. | Test matrix for rutting performance..... | 78 |
| Table 5-5. | Average values of G*/sinδ, G* and phase angle of PG 64-22 with and without Sasobit [®] | 84 |
| Table 5-6. | Average values of G*/sinδ, G* and phase angle of PG 76-22M | 85 |
| Table 5-7. | Average percent recovery of PG 64-22 with and without Sasobit [®] | 87 |
| Table 5-8. | Average J _{nr} of PG 64-22 with and without Sasobit [®] | 88 |
| Table 5-9. | Average percent recovery of PG 76-22M with and without Sasobit [®] | 90 |
| Table 5-10. | Average non-recoverable creep compliance (J _{nr}) of PG 76-22M..... | 91 |
| Table 5-11. | Percent recovery of PG 64-22 at equal-stiffness temperature | 92 |
| Table 5-12. | J _{nr} of PG 64-22 at equal-stiffness temperature..... | 93 |
| Table 5-13. | Percent recovery of PG 76-22M at equal-stiffness temperature | 94 |
| Table 5-14. | J _{nr} of PG 76-22M at equal-stiffness temperature | 94 |
| Table 5-15. | Coefficient of determination values for creep stress and percent recovery relationships | 95 |

| | | |
|-------------|---|-----|
| Table 5-16. | Effects of Sasobit [®] on rutting of HMA..... | 99 |
| Table 5-17. | Effects of Sasobit [®] on rutting of HMA with higher air voids | 99 |
| Table 5-18. | Effects of Sasobit [®] on rutting of HMA with higher asphalt content | 100 |
| Table 5-19. | Rutting susceptibility of Sasobit [®] modified WMA | 101 |
| Table 5-20. | Rutting susceptibility of Sasobit [®] modified WMA in case of warm mixing temperature of 133 °C | 102 |
| Table 5-21. | Summary output of multiple regression model..... | 103 |
| Table 5-22. | Actual and predicted rut depths | 104 |
| Table 5-23. | G*/sinδ of original and extracted asphalt binders..... | 105 |
| Table 5-24. | Aging indices of extracted asphalt binders | 106 |
| Table 6-1. | AFM data analysis for PG 64-22 + 0% wax - sample 1 | 116 |
| Table 6-2. | AFM data analysis for PG 64-22 + 0% wax - sample 2 | 117 |
| Table 6-3. | AFM data analysis for PG 64-22 + 0% wax - sample 3 | 118 |
| Table 6-4. | AFM data analysis for PG 64-22 + 1% wax - sample 1 | 118 |
| Table 6-5. | AFM data analysis for PG 64-22 + 1% wax - sample 2 | 119 |
| Table 6-6. | Summary of analysis..... | 119 |
| Table A-1. | PG 64-22 with 0% Sasobit [®] sample 1 | 142 |
| Table A-2. | PG 64-22 with 0% Sasobit [®] sample 2 | 143 |
| Table A-3. | PG 64-22 with 1% Sasobit [®] sample 1 | 144 |
| Table A-4. | PG 64-22 with 1% Sasobit [®] sample 2..... | 145 |
| Table A-5. | PG 64-22 with 2% Sasobit [®] sample 1 | 146 |
| Table A-6. | PG 64-22 with 2% Sasobit [®] sample 2 | 147 |
| Table A-7. | PG 64-22 with 4% Sasobit [®] sample 1 | 148 |
| Table A-8. | PG 64-22 with 4% Sasobit [®] sample 2 | 149 |

| | | |
|-------------|---|-----|
| Table A-9. | PG 76-22M with 0% Sasobit [®] sample 1 | 150 |
| Table A-10. | PG 76-22M with 0% Sasobit [®] sample 2 | 151 |
| Table A-11. | PG 76-22M with 1% Sasobit [®] sample 1 | 152 |
| Table A-12. | PG 76-22M with 1% Sasobit [®] sample 2 | 153 |
| Table A-13. | PG 76-22M with 2% Sasobit [®] sample 1 | 154 |
| Table A-14. | PG 76-22M with 2% Sasobit [®] sample 2 | 155 |
| Table A-15. | PG 76-22M with 4% Sasobit [®] sample 1 | 156 |
| Table A-16. | PG 76-22M with 4% Sasobit [®] sample 2 | 157 |
| Table A-17. | Sample density data 1 | 158 |
| Table A-18. | Sample density data 2 | 159 |
| Table C-1. | APA rut samples and rut depths of test 1 | 163 |
| Table C-2. | APA rut samples and rut depths of test 2 | 164 |
| Table C-3. | APA rut samples and rut depths of test 3 | 165 |
| Table C-4. | APA rut samples and rut depths of test 4 | 166 |
| Table C-5. | APA rut samples and rut depths of test 5 | 167 |
| Table C-6. | APA rut samples and rut depths of test 6 | 168 |
| Table C-7. | APA rut samples and rut depths of test 7 | 169 |
| Table C-8. | APA rut samples and rut depths of test 8 | 170 |
| Table C-9. | APA rut samples and rut depths of test 9 | 171 |
| Table C-10. | APA rut samples and rut depths of test 10 | 172 |
| Table D-1. | Phase angle, dynamic modulus and stiffness of asphalt binders extracted from 166 °C mix with 0% Sasobit [®] | 174 |
| Table D-2. | Phase angle, dynamic modulus and stiffness of asphalt binders extracted from 166 °C mix with 2% Sasobit [®] | 174 |

| | | |
|------------|---|-----|
| Table D-3. | Phase angle, dynamic modulus and stiffness of asphalt binders extracted from 133 °C mix with 0% Sasobit [®] | 175 |
| Table D-4. | Phase angle, dynamic modulus and stiffness of asphalt binders extracted from 133 °C mix with 2% Sasobit [®] | 175 |
| Table D-5. | Phase angle, dynamic modulus and stiffness of original PG 64-22 with 0% Sasobit [®] | 176 |
| Table D-6. | Phase angle, dynamic modulus and stiffness of original PG 64-22 with 2% Sasobit [®] | 176 |

LIST OF FIGURES

| | | |
|--------------|--|----|
| Figure 2-1. | Sasobit [®] prills..... | 9 |
| Figure 2-2. | Force ductility curve at 5 °C and DMA at temperatures below 5 °C (Edwards and Redelius, 2006) | 18 |
| Figure 2-3. | APA rut depth in mm in wet condition (Hossain et al., 2009)..... | 22 |
| Figure 2-4. | Rut depth analysis by LWT (Cooper, 2010)..... | 25 |
| Figure 2-5. | Rut depth analysis by flow number (Cooper, 2010)..... | 25 |
| Figure 2-6. | Rut depth results obtained for gravel mixes (Ali, 2010)..... | 28 |
| Figure 2-7. | Rut depth results obtained for limestone mixes (Ali, 2010)..... | 28 |
| Figure 3-1. | Rotational viscosity of PG 64-22 and PG 70-28 (Wasiuddin et al, 2007)..... | 31 |
| Figure 3-2. | Viscosity vs. temperature for pure asphalt and asphalt binder with Sasobit [®] | 32 |
| Figure 3-3. | A dynamic shear rheometer | 33 |
| Figure 3-4. | Combined aggregate gradation | 35 |
| Figure 3-5. | Sample on metal plate of DSR..... | 37 |
| Figure 3-6. | Dynamic viscosity for PG 64-22 0% Sasobit [®] | 43 |
| Figure 3-7. | Dynamic viscosity for PG 64-22 1% Sasobit [®] | 43 |
| Figure 3-8. | Dynamic viscosity for PG 64-22 2% Sasobit [®] | 44 |
| Figure 3-9. | Dynamic viscosity for PG 64-22 4% Sasobit [®] | 44 |
| Figure 3-10. | Dynamic viscosity for PG 76-22M 0% Sasobit [®] | 45 |

| | | |
|--------------|---|----|
| Figure 3-11. | Dynamic viscosity for PG 76-22M 1% Sasobit [®] | 45 |
| Figure 3-12. | Dynamic viscosity for PG 76-22M 2% Sasobit [®] | 46 |
| Figure 3-13. | Dynamic viscosity for PG 76-22M 4% Sasobit [®] | 46 |
| Figure 3-14. | Combined data for PG 64-22 with and without Sasobit [®] | 47 |
| Figure 3-15. | Combined data for PG 76-22M with and without Sasobit [®] | 48 |
| Figure 3-16. | Sample density chart..... | 53 |
| Figure 4-1. | Effect of temperature on shear rate at 64 °C, 100 °C and 124 °C | 59 |
| Figure 4-2. | Effect of shear rate at 64 °C on PG 64-22 with Sasobit [®] | 60 |
| Figure 4-3. | Effect of shear rate at 100 °C on PG 64-22 with Sasobit [®] | 60 |
| Figure 4-4. | Effect of shear rate at 124 °C on PG 64-22 with Sasobit [®] | 61 |
| Figure 4-5. | Effect of shear rate at 76 °C on PG 76-22M with Sasobit [®] | 62 |
| Figure 4-6. | Effect of shear rate at 100 °C on PG 76-22M with Sasobit [®] | 62 |
| Figure 4-7. | Effect of shear rate at 124 °C on PG 76-22M with Sasobit [®] | 63 |
| Figure 5-1. | Dynamic modulus values of three replicates of PG 64-22 with 0% Sasobit [®] | 79 |
| Figure 5-2. | Average dynamic modulus values of three replicates of PG 64-22 with 0% Sasobit [®] | 80 |
| Figure 5-3: | Relationship between time-temperature shift factor and temperature for PG 64-22 with 0% Sasobit [®] | 80 |
| Figure 5-4. | Dynamic modulus master curve for PG 64-22 with 0% Sasobit [®] | 81 |
| Figure 5-5: | Dynamic modulus master curves of PG 64-22 with and without Sasobit [®] | 82 |
| Figure 5-6. | Dynamic modulus master curves of PG 76-22M with and without Sasobit [®] | 82 |
| Figure 5-7: | Dynamic modulus master curves of PG 64-22 and PG 76-22M with and without Sasobit [®] | 83 |

| | | |
|-------------|---|-----|
| Figure 5-8. | (a) Asphalt pavement analyzer (APA), (b) Gyrotory rut samples, (c) Rut samples in mold, (d) Molds placed in the APA, (e) and (f) Rubber hose setup, (g) Steel wheel rolling, (h) Software taking rut measurements, (i) and (j) Rut samples after 8000 cycles (k) and (l) Manual rut measurement with a strain gauge | 97 |
| Figure 5-9. | Typical rut depths data obtained from the APA | 98 |
| Figure 6-1. | Asphalt binder under atomic force microscope | 112 |
| Figure 6-2. | Topographic image of asphalt binders PG 64-22 (20 μ m x 20 μ m)..... | 113 |
| Figure 6-3: | Phase identification..... | 113 |
| Figure 6-4. | PG 64-22 with 0, 0.5, 1% wax and aged condition..... | 114 |
| Figure 6-5. | PG 76-22M with aging and 1% wax..... | 115 |
| Figure 6-6. | Image analysis by Gwyddion..... | 116 |
| Figure A-1: | DSR applied shearing stress and strain..... | 140 |
| Figure A-2: | Complex modulus elaboration | 141 |

LIST OF SYMBOLS AND ABBREVIATIONS

| | | |
|--------|---|--|
| HMA | : | Hot Mix Asphalt |
| WMA | : | Warm Mix Asphalt |
| FT | : | Fischer Tropsch |
| WAM | : | Warm Asphalt Mix |
| PMA | : | Polymer Modified Asphalt |
| SBS | : | Styrene-Butadiene-Styrene |
| DSR | : | Dynamic Shear Rheometer |
| DMA | : | Dynamic Mechanical Analysis |
| BBR | : | Bending Beam Rheometer |
| MSCR | : | Multiple Stress Creep and Recovery |
| APA | : | Asphalt Pavement Analyzer |
| HWTT | : | Hamburg Wheel Track Test |
| AFM | : | Atomic Force Microscope |
| AMPT | : | Asphalt Mix Performance Tester |
| NCHRP | : | National Cooperative Highway Research Program |
| AASHTO | : | American Association of State and Highway Transportation Officials |
| NCAT | : | National Center for Asphalt Technology |
| NAPA | : | National Asphalt Pavement Association |
| VTRC | : | Virginia Transportation Research Council |

| | | |
|----------|---|--------------------------------------|
| MESAL | : | Million Equivalent Single Axle Loads |
| SGC | : | Superpave Gyrotory Compactor |
| RAP | : | Recycled Asphalt Pavement |
| LWT | : | Loaded Wheel Tracker |
| G^* | : | Complex Shear Modulus |
| G' | : | Loss Modulus |
| G'' | : | Storage Modulus |
| η' | : | Dynamic Viscosity |
| δ | : | Phase Angle |
| J_{nr} | : | Non Recoverable Creep Compliance |

ACKNOWLEDGEMENTS

I would like to sincerely thank my academic advisor and supervisor Dr. Nazimuddin M. Wasiuddin, for all his guidance, both academic and personal, during the course of my doctoral program.

I would like to thank Dr. Alfred Gunasekaran and Dr. Upali Siriwardane for the study of asphalt binder by atomic force microscope.

I would like to thank my supervisor for the guidance on rheological study of asphalt binder by the dynamic shear rheometer.

I would like to acknowledge Dr. Erez Allouche's help for allowing me to use some of the resources in the trenchless technology center (TTC).

I would also thank Nibert Saltibus for the experimental setup of the asphalt pavement analyzer.

Thanks are also extended to my colleagues, Saied Salehi Ashani, Mohammad Readul Islam, Kislser Wilson, Amanda Marshall and Braden Smith.

Most importantly, I would like to thank my wife Sharmi, my parents, brothers and sisters for their continued support and sacrifice during these years.

CHAPTER 1

INTRODUCTION

In 1970, the United States Clean Air Act was passed into law, the first Earth Day was held, and the U.S. industries started working to make the environment better. The asphalt industry became a leader in seeking innovations to promote a cleaner planet and better working conditions for the employees. The National Asphalt Pavement Association (NAPA) took the lead in a number of initiatives that have made asphalt plants better neighbors in the community and enhanced working conditions for those involved in the production and construction of asphalt pavements. A variety of government regulations, economic factors and changes in public attitudes were closely followed by the asphalt industry. For example, to comply with the Clean Air Act of 1970, emission control technologies were improved, and the current technology of bag house filtration greatly reduced particulate emissions from asphalt plants. During 1970s, rising oil prices and tightened supply resulted the development of new methods for reclaiming and recycling of asphalt pavements. Therefore, recycled asphalt pavement is now the most recycled material in the U.S. According to the public survey about impact of asphalt plants on communities, it was necessary to develop NAPA's Diamond Achievement Commendation. This refers to commitment towards better environment. In the year of 2002, NAPA identified new technologies in Europe which reduced the production and construction temperatures.

In 2007, National Center for Asphalt Technology (NCAT) showed that lowering the plant mix temperature by 6 °C (10.8 °F) significantly reduced the production of emissions from asphalt mixes (Lange and Stroup-Gardiner, 2007). Followed by a later study tour of NAPA leaders, its partners began to pursue the research and development work necessary for implementation of the Warm Mix Asphalt (WMA) (Prowell et al., 2012; Bonaquist, 2011; D'Angelo et al., 2008).

WMA belongs to a group of technologies which allows a significant reduction in the temperatures at which asphalt mixes are produced and placed. These several technologies provide complete aggregate coating at lower temperatures and act as compaction aids. However, better coating and compaction vary from one technology to another. Hot mix asphalt (HMA) is typically produced at temperatures from 138 °C to 160 °C (280 °F to 320 °F) while WMA is produced at 100 °C to 138 °C (212 °F to 280 °F) (Prowell, 2012).

The potential range of benefits of WMA are energy savings due to lower production temperatures, improved compaction aid, the ability to pave in cool ambient temperatures, longer hauling distances, the ability to incorporate higher percentages of RAP, longer paving seasons, reduced wear and tear of the plants, reduced oxidative aging of asphalt binders and, thus, reduced cracking in the pavements, and ability of opening the site to traffic sooner. Paving with WMA also provides the workers with a safer working environment (Hurley and Prowell, 2006; Prowell et al., 2012).

Currently, more than 20 WMA technologies are available in the market including some U.S. technologies. Many of the WMA technologies involved either waxes or

foamed asphalt. Waxes reduce the viscosity of the asphalt binder and improve lubrication at higher production temperatures.

To this end, overall, this study investigates if the viscosity reductions at higher temperatures have any impacts on asphalt mix compaction and rutting performances. In order to pursue this hypothesis the following investigations were performed.

First, dynamic viscosity (η') of asphalt binders with and without a wax-based WMA additive, Sasobit[®] was measured at wider temperature ranges. Laboratory densities of Superpave gyratory samples compacted at different temperatures, at different gyrations and at different asphalt contents were determined to evaluate the effect of viscosity on density. Also, field densities after different compaction steps were analyzed to evaluate the effect of Sasobit[®] on viscosity.

Second, as hot mix asphalt is prepared and compacted at different temperature ranges at different shear rates, it is imperative to know the influence of shear rate on viscosity at those temperature ranges. Therefore, effect of shear rate on asphalt binder has been studied in this regard.

Third, in order to address the concern that warm temperatures will increase rutting susceptibility because of reduced aging, different rutting factors of Sasobit[®] modified asphalt binders were determined and laboratory rutting test of the warm mix were performed. Evaluation of aging of extracted asphalt binders from mixes produced at different mixing temperatures were also performed.

Fourth, to understand the surface microstructure of Sasobit[®] modified asphalt binders, an atomic force microscope has been used. Also, the effectiveness of using an atomic force microscope as a screening tool for asphalt binder has been briefly studied.

1.1 Objectives

The overall objective of this study was to investigate the rheology of asphalt binders modified with a wax-based warm mix additive and its relationships with asphalt mix, compaction and rutting. The specific objectives of this research were as follows:

1. Effects of Sasobit[®] modified asphalt binder on lower compaction temperatures,
2. Effects of shear rate on viscosity of Sasobit[®] modified asphalt binders,
3. Laboratory evaluation of rutting factors and rutting performance of Sasobit[®] modified asphalt binders, and
4. Evaluation of atomic force microscope (AFM) as a screening tool for asphaltic materials.

1.2 Scope of the Research

In this study, rheological testing of asphalt binders modified with different percentages of Sasobit[®] were performed using a DSR. Temperature sweep, frequency sweep, multiple stress creep and recovery, and steady state shear tests were performed in this regard. A wide range of temperatures were used in the rheological testing by using different thermal liquids, by reducing the parallel plate gaps, strains, etc. Different innovative techniques were used for testing and data analyses in this regard. The DSR was used for viscosity measurements at visco-elastic state. Rheological behavior obtained was verified by mix performance. Densities of the laboratory compacted samples and also field compacted samples were used in this purpose. For in-depth investigations, densities were varied by number of gyrations and asphalt contents. In case of field densities, data obtained at different compaction steps were analyzed.

The DSR was used at rotational mode instead of sinusoidal mode to obtain rotational viscosity and it was compared with dynamic viscosity. Different shear rates were used in the case of rotational mode to analyze the effects of shear rate. Besides rutting factor $G^*/\sin\delta$, some other parameters that can be used as rutting factors were also analyzed such as, phase angle, percent recovery and non-recoverable creep compliance. A multiple variable linear regression rut depth model was developed varying mixing temperature, air voids, etc. An asphalt pavement analyzer was used in this purpose. For evaluation of aging, asphalt binders were extracted using a centrifuge and a rotary evaporator. Finally, an exploratory study has been performed using an atomic force microscope to distinguish between asphalt binders with and without wax modifications.

1.3 Organization of the Dissertation

This dissertation is divided into seven chapters. Chapter 1 contains an introduction to the problem and the objectives and scope of the research. A detailed literature review of related research is included in Chapter 2. The literature review includes background information about warm mix asphalt, some of the advantages and disadvantages, and earlier laboratory and field studies on warm mix asphalt. Chapter 3 contains results and discussions on the effects of Sasobit[®] on lower compaction temperatures. Chapter 4 contains investigations on the effect of shear rate and the viscosity model. Chapter 5 describes the effects of Sasobit[®] on rutting performances and its relationship to asphalt rheology. Chapter 6 contains discussions about the exploratory study using atomic force microscope for asphalt binder characterization. Finally, conclusions and recommendations are given in Chapter 7.

CHAPTER 2

LITERATURE REVIEW

2.1 Introduction

A number of WMA technologies were developed since 1990. Earlier WMA processes involved either waxes or foamed asphalt. Table 2-1 summarizes the different warm mix technologies. Table 2-2 shows greenhouse gas reductions by different WMA technologies.

Table 2-1. WMA technologies (D'Angelo et al., 2008)

| WMA process | Additive Percent | Production Temperature at Plant | Approximate Production till 2008 |
|--------------------------------|---|--|---|
| Sasobit® (Fischer-Tropsch Wax) | 2.5% by weight is used in Germany and 1-1.5% used in U.S. | 20-30 °C less than HMA | > 10 million tons |
| Asphaltan-B® (Montan Wax) | 2.5% by weight in Germany | 20-30 °C less than HMA | Not Known |
| Licomont BS 100 | 3% by weight of binder | 20-30 °C less than HMA | > 322,500 square meters since 1994 |
| 3E LT of Ecoflex | 2-3% | 30-40 °C drop from HMA | Not Known |

Table 2-1 continued...

| | | | |
|----------------------------------|------------------------------|------------------------|---------------------------|
| Aspha-Min [®] | 0.3% by weight of total mix | 20-30 °C less than HMA | 300,000 tons |
| Ecomac [®] | Not Known | 45 °C | > 100,000 tons |
| LEA, also EBE and EBT | 0.2-0.5% by weight of binder | < 100 °C | Seven commercial Projects |
| LEAB | 0.1% by weight of binder | 90 °C | Not known |
| LT Asphalt | 0.5-1.0% | 90 °C | > 60,000 tons |
| WAM-Foam | - | 110-120 °C | > 17,000 tons |
| U.S. Technology | | | |
| Evotherm [®] | 1-3% | 85-115 °C | > 4,000 tons |
| Double-Barrel Green [®] | 0.25% | 116-135 °C | >10,000 tons |
| Advera [®] (Zeolite) | Dilute surfactant | 20-30 °C less Than HMA | Not known |

Table 2-2. Greenhouse gas reductions for WMA (Gandhi, 2008)

| Compounds | % Reductions |
|----------------------------|---------------------|
| CO ₂ | 30-40 |
| SO ₂ | 30-40 |
| Volatile organic compounds | 50 |
| CO | 10-30 |
| NO _x | 60-70 |

2.1.1 Sasobit[®]

Sasobit[®] has been used most widely for WMA projects (Prowell et al., 2012). Sasobit[®] is a Fischer-Tropsch (FT) wax produced from coal gasification. Usually, it is obtained in pellet form and added at the rate of 1.5% by weight of binder. Sasobit[®] is a product of Sasol Wax, South Africa. It is a fine crystalline, long-chain aliphatic polyethylene hydrocarbon produced from coal gasification using the FT process (Sasol Wax, 2012). It is also known as “FT hard wax.” In the process of FT synthesis, coal or natural gas, methane, is oxidized partially to carbon monoxide (CO) and subsequently reacts with hydrogen (H₂) under catalytic conditions producing a mix of hydrocarbons which has the molecular chain length of carbon C5 to C100 carbon atoms. The Sasobit[®] is obtained in the carbon chain length C45 to C100. The longer carbon chains in the FT wax increase the melting point of Sasobit[®]. Sasobit[®] is termed as an “asphalt flow improver” and causes a reduction in viscosity; thus mixing and compaction temperature reduction by 18-54 °C (32-97 °F) (Kristansdottir et al., 2007). Sasobit[®] is completely soluble in asphalt binder at a temperature higher than 120 °C (248 °F) and its congealing temperature of about 102 °C (216 °F). Below the melting point temperature, Sasobit[®] has a crystalline network structure in the binder that causes stability (Hurley and Prowell, 2005; Gandhi, 2008).

The effects of Sasobit[®] in asphalt binders and HMA have been studied previously by several researchers (Kanitpong et al., 2007; Wasiuddin et al., 2007; Wasiuddin et al., 2008; Hurley and Prowell, 2005). Sasobit[®] is known to improve the flow of asphalt mixes (viscosity depressant) and reduce the mixing and compaction temperatures by about 18-54 °C (32-97 °F) (Kanitpong et al., 2007). Xiao et al., (2009) concluded that the addition of 1.5% Sasobit[®] will generally allow for mixing and paving temperatures about

11 °C to 31 °C (20 °F to 55 °F) (depending on the mix) lower than those for conventional HMA. The maximum compaction temperature was at least 31 °C (55 °F) less than HMA mixes in a study by Sargand et al., 2011. The manufacturer recommendation of Sasobit® addition is not more than 3% and not less than 0.8% (Sasol Wax, 2012).

For the commercial applications in Europe, South Africa and Asia, Sasobit® is added directly onto the aggregate mix as solid prills (Figure 2-1) or as molten liquid through a dosing meter. In the United States, Sasobit® is blended with the binder at the terminal and is blown directly into the mixing chamber (Prowell et al., 2012). Sasobit® is commercially available in 25 kg bags and 600 kg super-sacks. One hundred and forty-two projects were being paved using Sasobit® which is equivalent to 2,716,254 square yards of pavement since 1997 (Prowell et. al, 2012). Several projects were constructed in 18 countries including the United States. A wide range of aggregate types and mix types were used, such as dense graded mixes, stone mastic asphalt and Gussasphalt.

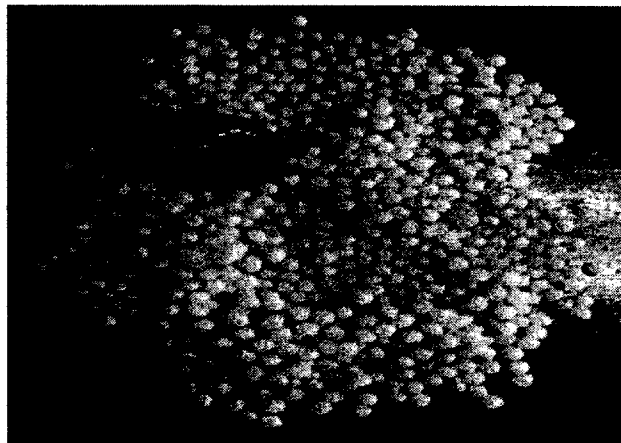


Figure 2-1. Sasobit® prills

It was found that Sasobit[®] improved the compactability of mixes in both the Superpave gyratory and vibratory compactor, improved compaction was observed at temperatures as low as 88 °C (190 °F). But the addition of Sasobit[®] does not affect the resilient modulus of an asphalt mix. In fact, it decreased the rutting potential of an asphalt mix as measured by the Asphalt Pavement Analyzer (APA) (Hurley and Prowell, 2005). Sasobit[®] additive is found to decrease the APA rut depths significantly, and these rut depths correlate well with the rutting factor $G^*/\sin\delta$. It was also observed that rutting resistance decrease with decreasing mixing and compaction temperatures (Wasiuddin et al., 2007). Sasobit[®] may have adversely affected the low end temperature properties of the binder PG 76-22M due to waxy component; however the use of Sasobit[®] additive had no significant effect in terms of rut resistance and moisture susceptibility as found by Cooper, 2009. In the case of fatigue cracking evaluation, data showed no significant difference between HMA mixes and Sasobit[®] mixes (Haggag et al., 2011). Sasobit[®] had a significant effect, however, on the pull-off tensile strength of the binder under dry conditions (Mogawer et al., 2011). The addition of Sasobit[®] significantly impacted the PG grading of binders and reduced both mixing and compaction temperatures of mixes. The flow number F_N increased with an increase of Sasobit[®] which indicates better rutting resistance (Liu et al., 2011). Sasobit[®] mixes demonstrated acceptable moisture damage resistance as measured by the TSR (Tensile Strength Ratio) value (Sargand et al., 2009).

2.1.2 Asphaltan B[®]

Asphaltan B[®] is a product of Romonta GmbH, Amsdorf, Germany (Corrigan, 2012; Kristansdottir, et al. 2007). It is a mix of substances based on montan wax constituents and higher molecular weight hydrocarbons. It was created specifically for hot-rolled asphalt (a fine grained HMA for pavement surfacing).

Crude montan wax is found in Germany, Eastern Europe, and in the U.S. in lignite coal deposits. Lignite coal deposits were formed over geologic time by the transformation of fossilized vegetation.

The manufacturer recommends adding Asphaltan B[®] to asphalt at 2-4% by weight. It can also be added at the asphalt mixing plant or by the binder producer and to polymer modified binders. It has a melting point of approximately 98 °C (210 °F). Similar to F-T waxes, it improves asphalt flow at reduced temperatures, but the manufacturer does not specify how much the production temperature can be lowered. The manufacturer reports increased compactability, resistance to rutting and moisture resistance of asphalt mix. Edwards et al. (2006) supports increased compactability by this product.

2.1.3 Aspha-Min[®]

Aspha-Min[®] is supplied by Eurovia Services GmbH, Germany (Aspha-Min[®], 2012). It is a finely powdered synthetic zeolite (sodium aluminium silicate hydrate) and has been hydro-thermally crystallized. When Aspha-Min[®] is added to the binder as well as mix, water is released. This released water creates a foaming of the asphalt binder and, thereby, increases workability temporarily and increases aggregate coating at lower temperatures. Aspha-Min[®] is added typically at 0.3% by total weight of HMA mix. When

it is heated above 85 °C (185 °F) to 182 °C (360 °F), it releases 21% water by mass. This released water microscopically foams the asphalt to aid coating of the aggregate. This foaming action acts as a temporary asphalt volume extender and mix lubricant, activating the aggregate particles to be rapidly coated and the mix to be workable and compactable at temperatures significantly lower than HMA (Federal Highway Administration, 2012).

According to Eurovia, Aspha-Min[®] can yield a reduction in mixing temperature greater than 50 °C (28 °F), thus saving 30% energy. Aspha-Min[®] is available in a very fine white powdered form in 50 lb or 100 lb bags (Kuennen, 2004). In a batch plant, it is added directly into the pugmill; in a drum mix plant, it is pneumatically fed into the drum via the RAP Collar (Barthel and Von Devivere, 2003).

According to Corrigan (2006), zeolites are framework silicates that have large vacant spaces in their structures allowing spaces for large cations such as sodium, potassium, barium, calcium and water molecule. In zeolites, the spaces are interconnected and form long, wide channels. These channels allow easy movement of the resident ions and molecules in and out of the zeolite structure. Zeolites are characterized by their ability to lose and absorb water without damaging their crystalline structures (Corrigan, 2006).

The addition of Aspha-Min[®] does not affect the resilient modulus of an asphalt mix nor it decreases the rutting potential of an asphalt mix by APA. The lower mixing and compaction temperature may cause moisture damage (Hurley and Prowell, 2005). No significant changes in grading were observed with the addition of Aspha-Min[®], yet a smaller reduction in rut depths was observed (Wasiuddin et al., 2007). Aspha-Min[®] showed APA rutting characteristics similar to the control HMA mix (Xiao et al., 2010). Binders containing Aspha-Min[®] had minor or no changes compared to the base binders in

terms of flow properties, stiffness and response to creep. Results from the Gel permeation chromatography test showed Aspha-Min[®] had no significant effect on the binders (Biro et al., 2009).

2.1.4 Foamed Asphalt

Foamed asphalt is produced by the combination of hot asphalt binder with cold water. When there is a contact between the cold water and the hot asphalt binder, the mix turns into tiny steam bubbles trapped inside the asphalt binder. Thus, expansion in the volume of the binder occurs, which ultimately improves the coating potential of the binder. WMA using foamed asphalt technology (WAM-foam) is a patented process which is jointly developed by Shell Global Solutions and KoloVeidekke in Norway. In this WAM-foam production process, two different kinds of asphalt grades, soft asphalt binder and hard asphalt binder, are combined with the mineral aggregate.

At first, the aggregate is mixed with the softer binder, which is a fluid at lower temperatures, and after that, harder binder is foamed and mixed with the aggregate and softer binder. By this process, the asphalt mix is produced at temperatures between 100 °C and 120 °C (212 °F and 250 °F) and compacted at 80 °C to 110 °C (175 °F to 230 °F) (Koenders, 2000).

Foamed asphalts were found to be more workable and easily compactable in comparison to HMA mixes. Furthermore, foamed asphalt mixes are not susceptible to moisture induced damage. Generally, foamed asphalt mixes tend to increase the rut depth in the APA test in comparison to HMA mixes (Ali, 2010).

2.1.5 Evotherm™

This process uses a chemical additive technology and a “Dispersed Asphalt Technology” (DAT) delivery system. It has been stated by the producer that by using this technology, a unique chemistry customized for aggregate compatibility is being delivered into a dispersed asphalt phase. During the production, the asphalt emulsion is mixed with the Evotherm™ chemical package and the produced emulsion is then mixed with the aggregate in the HMA plant.

It has been reported by the manufacturer that the chemistry provides good aggregate coating, workability, adhesion and improved compaction with no change in materials. However, the manufacturer reported a 55 °C (100 °F) reduction in production temperatures. It is the first chemical additive used in the U.S. and was introduced in 2005 by MeadWestvaco (MeadWestvaco, 2007).

Evotherm® improved the compactibility of mixes in both the Superpave gyratory compactor and vibratory compactor. Improved compaction was noted at temperatures as low as 88 °C (190 °F); it did not affect the resilient modulus of an asphalt mix and also did not increase the rutting potential of an asphalt mix by APA. WMA with Evotherm® can be quickly opened to the traffic, but it may increase the potential for moisture damage (Hurley and Prowell, 2006).

2.1.6 Advera®

Advera® is a synthetic zeolite, similar to Aspha-Min®, and contains about 18% of crystallized water by total weight according to the manufacturer. It works in gradually, releasing the water contained inside it. Advera® is a fine graded product (i.e. 100%

passing sieve #200). Advera[®] is directly added to the pugmill in batch plants and through a fiber port in drum plants.

The manufacturer suggests that a reduction in asphalt mixes' production temperatures of 10 °C to 21 °C (50 °F to 70 °F) is expected. At temperatures less than 80 °C, the addition of Advera[®] zeolite tended to stiffen the mix (Tao and Mallick, 2009). Limited research has been done with Advera[®].

2.2 Rheological Study of Wax-Based WMA

Table 2-3 summarizes some important literature on rheological study of wax-based WMA. However, the low temperature study performed by Edwards and Redelius (2006) has been discussed in Section 2.3.

Table 2-3. Literature review on rheological study of WMA

| Author, year | Materials Used | Tests |
|--|--|--|
| Edwards and Redelius, 2003 | <ul style="list-style-type: none"> - Non-waxy asphalt binder - Asphalt binder with 2% (w/w) wax - Asphalt binder with 4% wax - Slack wax | <ul style="list-style-type: none"> - Temperature sweep - Frequency Sweep |
| Results | | |
| Slack wax in asphalt gives significant negative effects by lowering the complex modulus at temperatures over about 40 °C. The slope of the logarithm of the complex modulus can be considered as the rutting factor. | | |

Table 2-3 continued...

| Author, year | Materials Used | Tests |
|---|---------------------------|--|
| Kim et al., 2010 | - PG 76-22M - Sasobit® | - Temperature sweep |
| Results | | |
| <p>The addition of Sasobit® decreased the viscosity of PMA binders at 135°C. PMA binders containing Sasobit® had higher failure temperature.</p> | | |
| Author, year | Materials Used | Tests |
| Biro et al., 2009 | - PG 64-22 - Sasobit® | - Viscosity - Frequency sweep - Creep and recovery |
| Results | | |
| <p>Binders follow Newtonian flow at 60 °C. The addition of WMA additives significantly increases the viscosities of the binders at 60 °C. Aspha-Min® does not affect the flow properties of the tested binders; whereas, the addition of Sasobit® causes shear thinning flow characteristics in the binders at 60 °C. Sasobit® recrystallizes in the binders at midrange temperatures, increasing the viscosity and stiffness. In case of frequency sweep, Sasobit® increases the stiffness of the binders. Aspha-Min® did not increase the stiffness of the binders as much as Sasobit®. Aspha-Min® also showed lower compliance values.</p> | | |

2.3 Low Temperature Rheological Study of Wax-Based WMA

Edwards and Redelius (2006) conducted laboratory study on rheological effects of wax at low temperature. The effect of wax or acid on the low temperature performance of asphalt was studied using DMA, BBR and force ductility measurements. Higher modulus at low temperatures makes the asphalt concrete sensitive to thermal and load induced cracking (Edwards and Redelius, 2006).

DMA results revealed that addition of natural wax or slack wax has a stiffening effect down to at least -5 °C. This effect indicates lower resistance to thermal cracking. Addition of slack wax decreased the stiffness of the non-waxy asphalt at temperatures lower than -5 °C. BBR analysis at -15 °C, -20 °C and -25 °C showed similar results (Edwards and Redelius, 2006).

Addition of FT-paraffin, montan wax or polyethylene wax showed a stiffening effect at temperatures down to at least 5 °C. Addition of commercial waxes also, in some cases, resulted in stiffening effects at temperatures lower than 5 °C (Edwards and Redelius, 2006).

In case of force ductility at 5 °C, maximum force was increased by the addition of FT paraffin or montan wax to asphalt. Polyethylene wax or polyphosphoric acid does not show any increment in force. The effect of wax and polyphosphoric acid at lower temperatures has been shown in Figure 2-2.

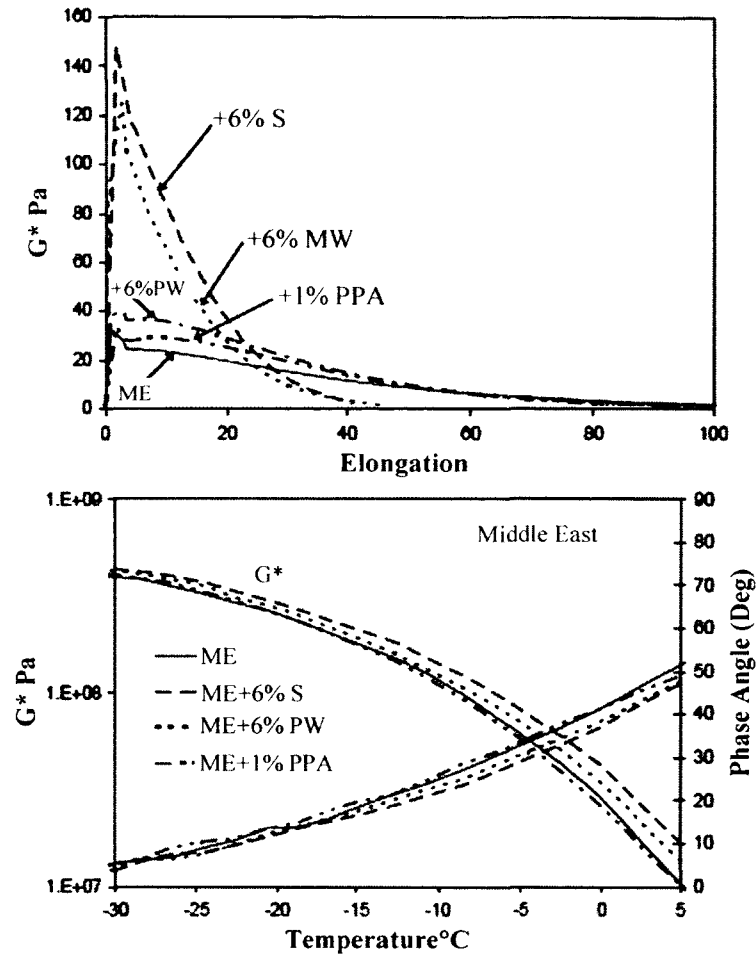


Figure 2-2. Force ductility curve at 5 °C and DMA at temperatures below 5 °C (Edwards and Redelius, 2006)

2.4 Effects on Rutting Characteristics

Studies conducted at the National Center for Asphalt Technology (NCAT) on WMA has shown that due to the reduced mixing temperature, the mixes show increased tendencies toward rutting and moisture susceptibility. This is because incomplete drying of the aggregate at the time of mixing (Prowell et al., 2007; Hurley and Prowell, 2005). Research conducted by Xiao et al. (2010) showed that hydrated lime improved the indirect tensile strength (ITS) and tensile strength ratio values of WMA mixes whether there was moisture in the aggregate or not. In a recent NCHRP study, Bonaquist (2011)

studied rutting of WMA based on flow number. Table 2-4 shows the minimum flow number criteria developed in NCHRP 09-19 study (Witczak et al., 2002).

Table 2-4. Minimum flow number requirements

| Traffic Level Million ESALs | Minimum Flow Number |
|--|--------------------------------|
| < 3 | --- |
| 3 to < 10 | 53 |
| 10 to < 30 | 190 |
| ≥ 30 | 740 |

In this NCHRP study, the flow number test was conducted using the asphalt mixture performance tester (AMPT). It was found that the flow numbers for WMA are significantly lower compare to the HMA. The average difference was approximately 40% and it was similar for all WMA processes. A relationship between the flow number (for a rut depth of 0.5 in.) and the allowable traffic was developed;

$$MESAL = \frac{F_n^{0.873}}{6.222} \quad 2.1$$

Where MESAL = Estimated traffic to 12 mm rutting, million equivalent single axle load, F_n = Flow number per NCHRP 09-33 test conditions, Cycles. Table 2-5 gives a summary about the allowable traffic from Equation 2.1 for all of the mixes included in that NCHRP Study. Table 2-5 implies that it will be difficult for WMA mixes designed for 10 MESAL or greater to meet the flow number rutting resistance criteria according to Table 2-4.

Table 2-5. NCHRP 09-33 rutting resistance from flow number testing results (Bonaquist, 2011)

| Mix | Gyrations Level | Design Traffic MESAL | RAP | HMA | | Advera® | | Evotherm™ | | Sasobit® | |
|-----|--------------------|----------------------------|-----|-----------|-------------------------|---------|-------------------------|-----------|-------------------------|----------|-------------------------|
| | | | | MESA L | Compaction Temp., °F | MESAL | Compaction Temp., °F | MESAL | Compaction Temp., °F | MESAL | Compaction Temp., °F |
| 1 | 50 | <0.3 | Yes | 6.1 | 310 | 2.4 | 215 | 2.0 | 215 | 3.5 | 260 |
| 2 | 50 | <0.3 | No | 2.2 | 310 | 1.0 | 260 | 1.8 | 260 | 1.6 | 215 |
| 3 | 75 | <3 | Yes | 13.5 | 310 | 4.7 | 260 | 5.9 | 260 | 9.5 | 260 |
| 4 | 75 | <3 | No | 2.8 | 310 | 2.6 | 215 | 2.2 | 260 | 1.6 | 215 |
| 5 | 100 | <10 | Yes | 12.3 | 310 | 3.5 | 260 | 5.0 | 260 | 4.1 | 215 |
| 6 | 100 | <10 | No | 4.9 | 310 | 3.9 | 215 | 3.9 | 215 | 5.9 | 260 |

Xiao et al., (2010) conducted another study for evaluation of rutting resistance in WMAs containing moist aggregate. The objective of that study was to investigate the influence of WMA additive, hydrated lime and moisture content of aggregate on the rutting resistance of the mixes using the APA. Dry and conditioned specimens were used in the study. Statistical significant analyses were done to know the effects on rutting characteristics.

In dry rut depth analysis, it was found that additional moisture and 1% lime decreased the rut depth of the mix containing Sasobit[®] and the control mix. For all aggregate types, the mixes containing Sasobit[®] had the lowest rut depth value. In general, rut values from various aggregate sources were different irrespective of the same WMA additive and moisture. With respect to the effect of WMA additive, the mix containing Evotherm[™] showed a higher rut depth compared to Sasobit[®]. Further, statistical analysis illustrated that the rut values were not different between control specimens and those containing the Aspha-Min[®] additive. This study also showed that irrespective of the lime content, moisture percentage and aggregate source, Sasobit[®] exhibited the highest rut resistance compare to other WMA additives (Xiao et al., 2010).

Hossain et al., (2009) studied rutting potential of Aspha-Min[®] (6% by weight of total mix) and Sasobit[®] (1.5% by weight of the asphalt binder) mixes using Superpave gyratory compactor (SGC) samples and an APA. A controlled temperature of 40 °C was maintained in the air and in the water bath of the APA. Rut depth measurements were taken after 500, 1000, 2000, 4000 and 8000 cycles. Figure 2-3 shows the APA rut depth data for samples with and without WMA additive. Table 2-6 summarizes the result.

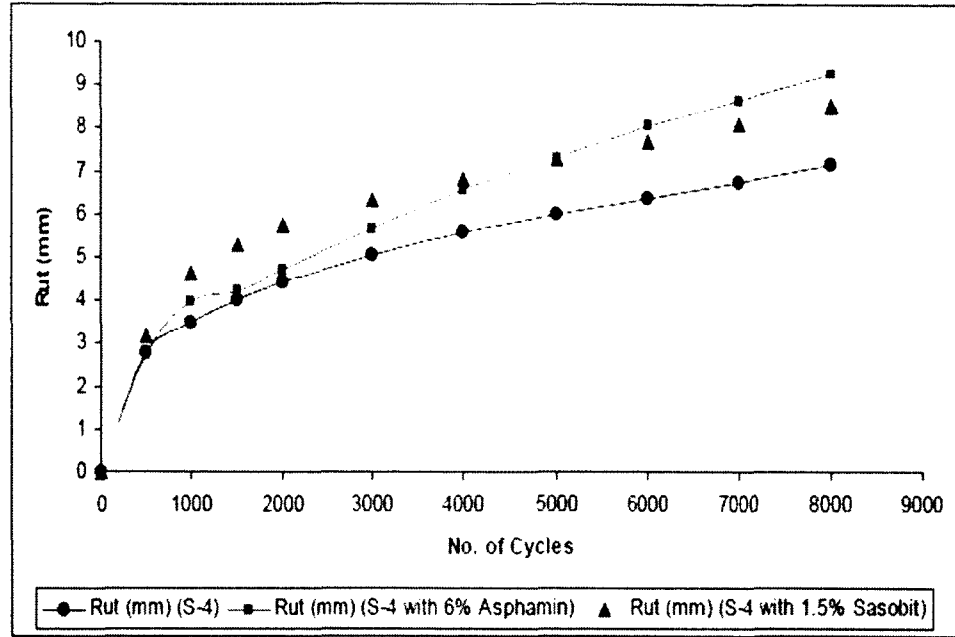


Figure 2-3. APA rut depth in mm in wet condition (Hossain et al., 2009)

Table 2-6. APA rut test results (Hossain et al., 2009)

| Number of Cycles | Rut (mm) | Rut (mm) 6% Aspha-Min [®] | Rut (mm) 1.5% Sasobit [®] |
|------------------|----------|------------------------------------|------------------------------------|
| 0 | 0 | 0 | 0 |
| 500 | 2.789 | 2.715 | 3.170 |
| 1000 | 3.473 | 3.950 | 4.620 |
| 1500 | 4.016 | 4.228 | 5.308 |
| 2000 | 4.404 | 4.709 | 5.733 |
| 3000 | 5.036 | 5.652 | 6.342 |
| 4000 | 5.566 | 6.551 | 6.811 |
| 5000 | 5.974 | 7.330 | 7.262 |
| 6000 | 6.353 | 8.067 | 7.688 |
| 7000 | 6.715 | 8.651 | 8.091 |
| 8000 | 7.134 | 9.262 | 8.493 |

It indicates that there is an increase in rut depth for mix samples with 1.5% Sasobit[®] and 6% Aspha-Min[®]. This increased rut depth is prominent at a very early stage (1000 cycles). After 8000 cycles, the APA rut depth of the control mix is 6.5 mm while the rut depths of 1.5% Sasobit[®] and 6% Aspha-Min[®] mixes are 8 mm and 9 mm, respectively. Sasobit[®] or Aspha-Min[®] modified mix samples showed higher rutting potential than the control mix. This could be due to weakness in the aggregate structure, inadequate binder stiffness or moisture damage.

A study by Middleton and Forfylyow (2009) on double barrel green WMA process evaluated the potential for rutting using the APA. Three sets of duplicate samples were prepared in the laboratory with SGC at an air void content of $7.0 \pm 0.5\%$. The APA testing was conducted at 58 °C. The APA testing was also conducted with the specimens submerged in water at 58 °C to assess the effects of moisture damage. Table 2-7 provides a summary of the APA rut test conducted by Middleton and Forfylyow (2009). Mixes with less than 8 mm of rut depth were not considered susceptible to rutting. It was expected that mixes containing relatively higher proportions of RAP would be more resistant to rutting because of the hardening effect of the asphalt binder.

Table 2-7. APA rut test results (Middleton and Forfylow, 2009)

| Mix type | Average air void Content (%) | APA rut depth after 8,000 cycles (mm) | |
|---------------------------|---------------------------------|--|------------|
| | | Dry result | Wet result |
| DBG Virgin | 7.1 | 4.783 | 7.976 |
| DBG 15% RAP | 7.3 | 5.245 | 5.205 |
| DBG 15% RAP and 5% MSM | 7.0 | 4.106 | 7.126 |
| DBG 50% RAP | 7.0 | 4.078 | 5.599 |

Cooper et al. (2010) conducted laboratory performance characteristics of sulfur-modified WMA. Three mixes, two hot mix asphalt (HMA) and one WMA, were used. First HMA mix used an unmodified asphalt binder classified as PG 64-22, second HMA mix used a Styrene-Butadiene-Styrene elastomeric modified binder classified as PG 70-22, and third mix was a WMA that incorporated a sulfur-based additive and a PG 64-22 binder. Rutting test was performed by using a Hamburg-type LWT (Loaded Wheel Tracker). A maximum allowable rut depth of 6 mm after 20,000 passes at 50 °C was used as the criteria. In this study, the flow number test was also performed. The test was conducted at 54 °C and a stress level of 207 kPa. Samples of 100 mm in diameter and 150 mm in height of a 37.5 mm NMS (Nominal Maximum Size) mix were used.

Figure 2-4 compares the rutting performance of the three mixes evaluated by Cooper (2010). As shown in Figure 2-4, mix WC64CO (PG 64-22) had the largest rut depth at 20,000 cycles, followed by WC64SU (Sulfur modified WMA) and WC70CO (PG 70-22). In Figure 2-5, the flow number values indicate that sulfur-modified WMA mix (WC64SU) performed well in both conventional mixes, including the PMA mix.

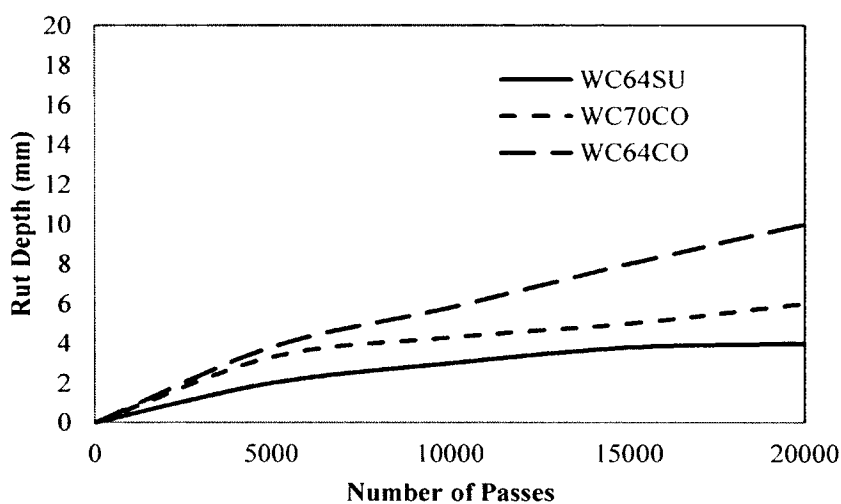


Figure 2-4. Rut depth analysis by LWT (Cooper, 2010)

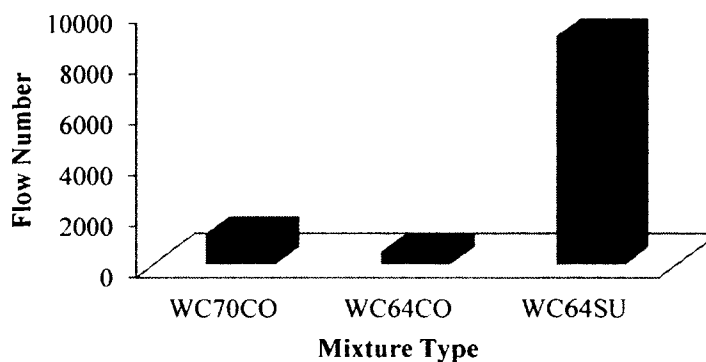


Figure 2-5. Rut depth analysis by flow number (Cooper, 2010)

A study by the Virginia Transportation Research Council (VTRC) on rutting performance of WMA (Diefenderfer and Hearon, 2008) included mixes produced both in the plant and in the laboratory. HMA was produced in the laboratory using the plant production temperatures, and WMA was produced in the laboratory at temperatures of 110 °C (230 °F), 130 °C (265 °F), and 149 °C (300 °F). In all cases, the mixing and compaction temperatures were the same.

The Hamburg wheel-track test (AASHTO T324) was performed in modified APA. Samples were submerged in water at 50 °C (122 °F) while a 158 lb load was applied. The test was considered to be complete at 20,000 cycles or a displacement of 1.575 in. The results of the tests performed on plant produced mixes are presented in Table 2-8.

Table 2-8. HWTT results for plant-produced mixes (Diefenderfer and Hearon, 2008)

| Mix Type | Average air Voids % | Standard deviation | Rut depth at 20,000 passes |
|-----------|---------------------|--------------------|----------------------------|
| Mix A HMA | 7.6 | 0.5 | 2.11 |
| Mix A WMA | 7.8 | 0.2 | 2.13 |
| Mix B HMA | 7.4 | 0.5 | 2.44 |
| Mix B WMA | 7.1 | 0.3 | 2.07 |

The maximum allowed deformation at 20,000 cycles is not specified in the AASHTO procedure, but a maximum of 10 mm after 20,000 cycles is specified by the Colorado DOT. The measured rut depths of the specimens were well below the 10 mm. Table 2-9 shows results of laboratory produced samples. It was concluded in this study that the rutting potential of WMA decreased with increasing production temperatures.

The rutting potential of WMA is, therefore, equal to or, in some cases, less than that of HMA based on this study (Diefenderfer and Hearon, 2008).

Table 2-9. Results of laboratory produced samples (Diefenderfer and Hearon, 2008)

| Sample | Average air Voids (%) | Standard Deviation | Rut depth at 20,000 passes (mm) | Stripping Inflection Point (passes) |
|-------------------------------|------------------------------|---------------------------|--|--|
| WMA 230 °F | 7.3 | 0.1 | 11.8 | 11000 |
| WMA 265 °F | 7.1 | 0.2 | 6.2 | |
| WMA 300 °F | 7.1 | 0.1 | 3.0 | - |
| HMA 300 °F | 7.0 | 0.1 | 6.2 | 17000 |
| WMA 300 °F long-term aging | 6.7 | 0.1 | 1.5 | - |
| HMA 300 °F long term aging | 7.1 | 0.1 | 2.2 | - |

Ali (2010) evaluated rutting potential of foam-based asphalt. Results shown in Figure 2-6 and Figure 2-7 indicate that, in general, the WMA-FA mixes tend to increase the rutting susceptibility in comparison to HMA mixes. This increase is mainly referred to as the softening of the asphalt binder due to foaming. This increase in the rutting susceptibility is considered statistically significant.

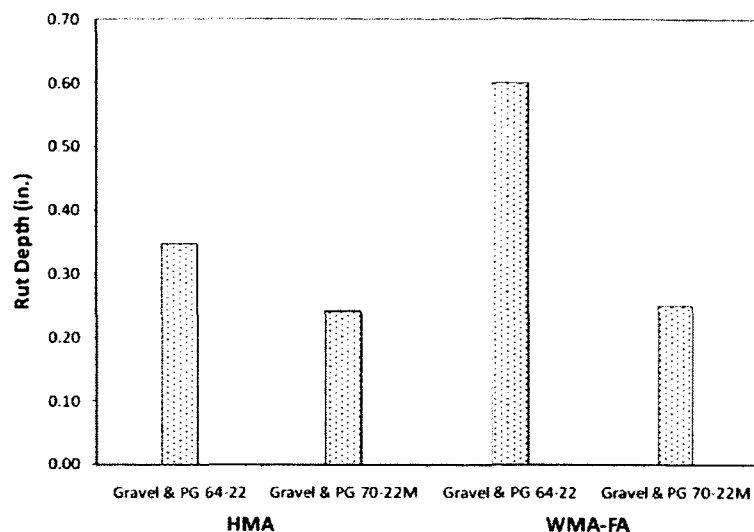


Figure 2-6. Rut depth results obtained for gravel mixes (Ali, 2010)

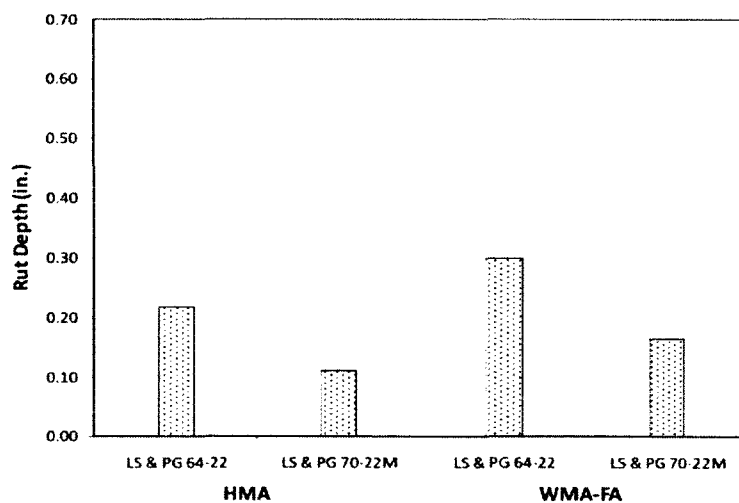


Figure 2-7. Rut depth results obtained for limestone mixes (Ali, 2010)

According to this study (Ali, 2010), adjustments might be necessary to the asphalt foaming procedure in order to improve the performance of WMA-FA mixes. Figure 2-6 and Figure 2-7 also show that the use of gravel increase the rutting susceptibility of WMA-FA mixes more than limestone mixes. Although the limestone mixes had higher asphalt binder contents, the limestone mixes have shown better rutting performance. This

could be due to the greater interlock and rough surfaces. Ali (2010) concluded that, a detailed investigation is necessary in this regard (Ali, 2010).

Kim et al. (2010) conducted a study on rutting of WMA and observed that Sasobit[®] increased the rutting resistance of asphalt binders from two different sources. However, the difference is statistically insignificant.

2.5 Summary on Rutting Characteristics

According to Prowel et al. (2007), Xiao et al. (2010) and Hurley and Prowell (2005), lower mixing and compaction temperatures result in incomplete drying of the aggregate in case of WMA. Xiao et al. (2010) concluded that WMA with gravel has higher rutting potential than WMA with limestone and also Sasobit[®] has the highest rut resistance compare to other additives. The NCHRP study (Bonaquist, 2011) showed WMA exhibited higher rut resistance than HMA and based on the flow number criteria, it will be difficult to prepare WMA mixes for 10 MESAL roads. Hossain et al. (2009) concluded that Sasobit[®] and Aspha-Min[®] had higher rutting potential in moist conditions. Wasiuddin et al. (2007) found significantly lower rut depth in the case of Sasobit[®] than that of Aspha-Min[®]. Cooper (2010) concluded that Sulfur modified WMA performed better in rutting performance.

The rutting potential of WMA decreased with increasing production temperatures as observed by Diefenderfer and Hearon (2008). Also, foam based WMA showed higher rut value than HMA (Ali, 2010). It can be concluded from this literature review that Sasobit[®] may have a positive effect on rutting performance if the rutting test is performed on dry samples.

CHAPTER 3

EFFECTS OF A WAX-BASED WARM MIX ADDITIVE (SASOBIT[®]) ON LOWER COMPACTION TEMPERATURES¹

3.1 Introduction

In the compaction process, the volume of air in an asphalt mix is reduced by the external forces. The removal of air makes the mix to occupy a smaller space causing increment in the unit weight or density of the mix. Compaction is a necessary factor in the design and production of asphalt mixes. The compaction temperature affects workability, which is related to the density of the mix. The current Superpave procedure for the compaction temperature for asphalt mixes is defined as the range of temperatures where an unaged asphalt binder has a kinematic viscosity of $280 \pm 30 \text{ mm}^2\text{s}^{-1}$; this was based on experience with unmodified asphalt binders. However, previous studies (Azari et al., 2003; Bahia, 2000; Stuart, 2000) showed that specimens could have the same volumetric properties over a very wide range of compaction temperatures (Lee et al., 2006).

¹ The contents of this chapter have been published in the Geo Frontiers Conference proceedings of 2011. This portion has been formatted for the dissertation.

A study on WMA conducted by Wasiuddin et al. (2007) reported that for asphalt binder PG 64-22, the three percentages of Sasobit[®] such as 2%, 3% and 4% reduced the mixing and compaction temperatures as measured by rotational viscometer (Figure 3-1). The reduction in mixing temperature was 16 °C (29 °F) from 163 °C (325 °F) for all the three percentages of Sasobit[®]. In the case of binder PG 70-28, 2, 3 and 4% of Sasobit[®] reduced the mixing temperature by 10 °C (18 °F), 12 °C (22 °F) and 13 °C (23 °F) respectively, from 163 °C (325 °F). A similar trend was observed for reduction in compaction temperature. However, Wasiuddin et al. (2007) did not investigate the effects of Sasobit[®] at lower compaction temperature ranges.

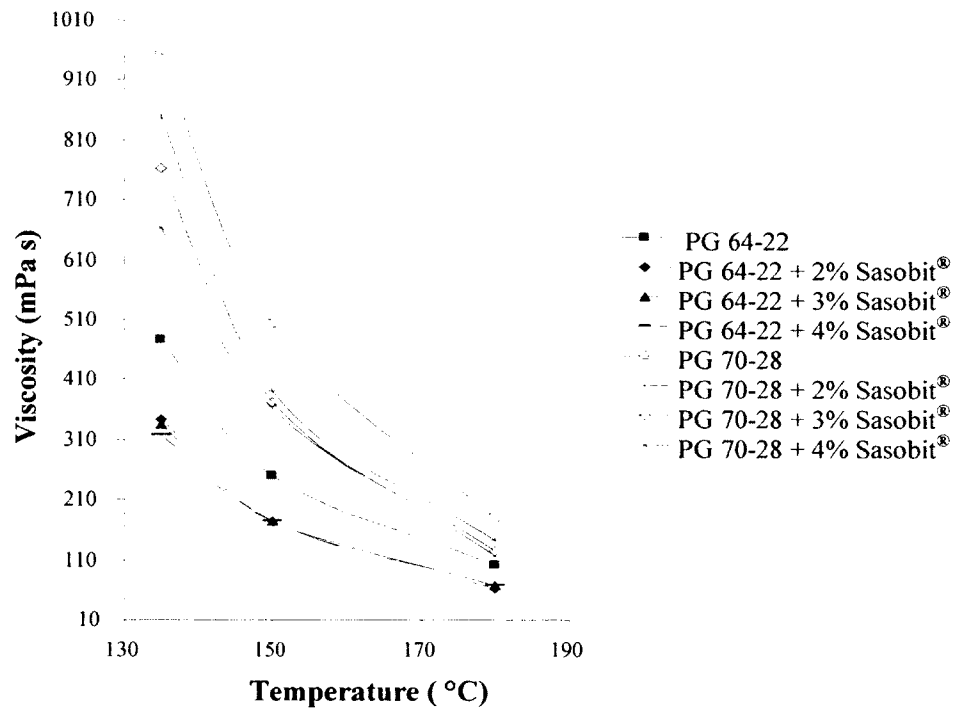


Figure 3-1. Rotational viscosity of PG 64-22 and PG 70-28 (Wasiuddin et al, 2007)

In the field, however, the compaction temperature usually ranges from 85 °C to 155 °C (185 °F to 311 °F). Finish rolling takes place from 70 °C to 85 °C (158 °F to 185 °F). In the current study, a Dynamic Shear Rheometer (DSR) was used to measure viscosity at lower compaction temperatures.

To this end, it has been observed previously that Sasobit[®] increased the stiffness of asphalt binder at service temperatures and reduced the viscosity at mixing and higher compaction temperatures. In other words, Sasobit[®] increased the viscosity at service temperatures and reduced the viscosity at production temperatures. Result indicates that the viscosity curves of asphalt binder and asphalt binder modified with Sasobit[®] will have a crossing point viscosity. A hypothetical viscosity model has been drawn in this study as shown in Figure 3-2. It is imperative that the temperature of the crossing point should be below the compaction temperatures of asphalt mix. Therefore, this study was initiated to find the effect of Sasobit[®] on lower compaction temperatures.

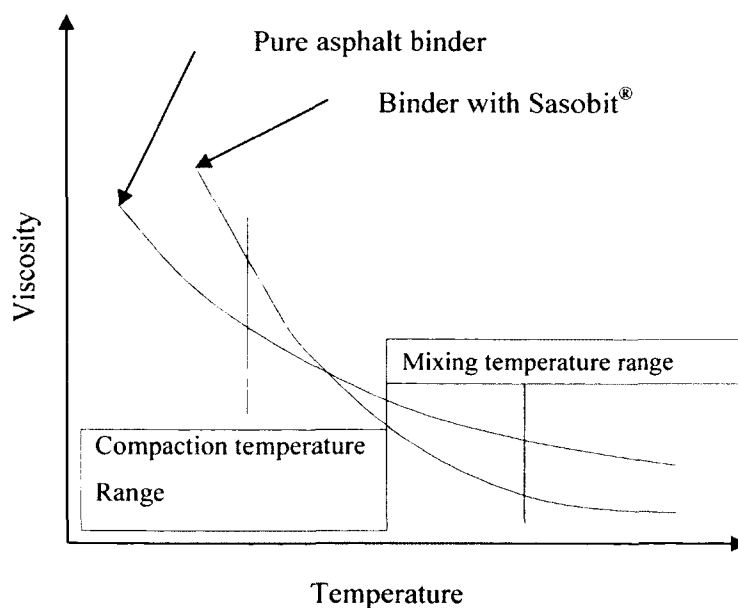


Figure 3-2. Viscosity vs. temperature for pure asphalt binder and asphalt binder with Sasobit[®]

Figure 3-3 shows a DSR that was used to measure dynamic viscosity as defined by G''/ω (see Appendix A for details).

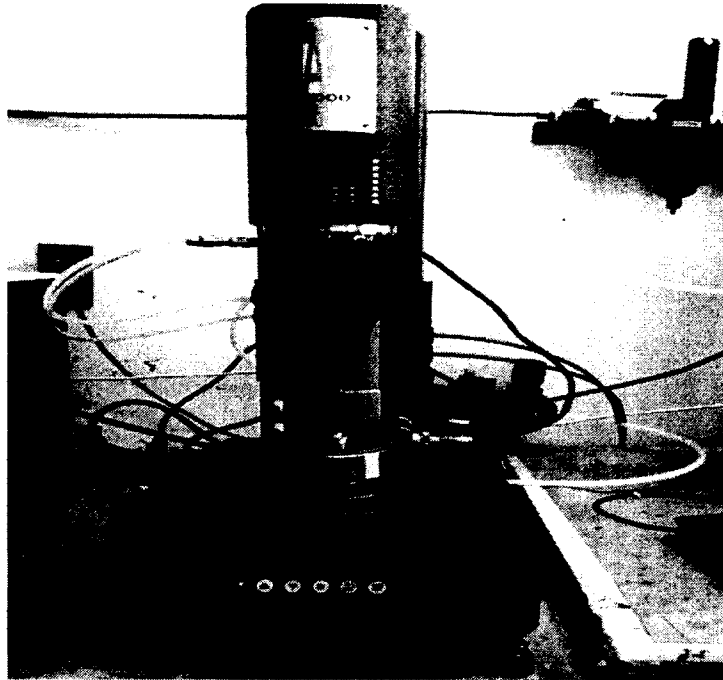


Figure 3-3. A dynamic shear rheometer

3.2 Objectives

The objective of this dynamic viscosity study is to investigate the effects of a wax-based warm mix additive on viscosity of asphalt binders and density of mixes at lower compaction temperature. The specific objectives are as follows:

1. Evaluation of $G^*/\sin\delta$ at pavement service temperatures with and without the addition of Sasobit[®],
2. Evaluation of dynamic viscosity using a DSR at lower compaction temperatures,
3. Evaluation of effect of Sasobit[®] on lab density of asphalt mixes, and
4. Evaluation of the effects of Sasobit[®] on field density.

3.3 Material Description

Both the asphalt binders, PG 64-22 and PG 76-22M, used in this study were obtained from Ergon Refining, Inc., Vicksburg, Mississippi. PG 64-22 is an unmodified binder, and PG 76-22M is a polymer modified binder. The binder used for the mix design was PG 64-22 obtained from Lion Oil, Inc. Table 3-1 and Table 3-2 show the aggregate gradations and aggregate sources respectively.

Table 3-1. Aggregate gradation

| Sieve size (mm) | Gradation Specs | Coarse Gravel 12% | Small Gravel 53% | Coarse Sand 18% | Fine Sand 17% |
|--------------------|-----------------|-------------------------|------------------------|-----------------------|---------------------|
| 19 | 100 | 100 | 100 | 100 | 100 |
| 12.5 | 90-100 | 54 | 99.12 | 100 | 100 |
| 9.5 | 90 | 2.66 | 83.59 | 100 | 100 |
| 4.75 | - | | 44.02 | 100 | 100 |
| 2.36 | 28-58 | | 21 | 91.9 | 100 |
| 0.6 | - | | 12 | 55.3 | 99.4 |
| 0.15 | - | | 3.1 | 5 | 40.4 |
| 0.075 | 2-10 | 0.1 | 2.3 | 2.4 | 28 |

Table 3-2. Material sources

| Materials type | Materials source, Code |
|-----------------|------------------------|
| Coarse Gravel | Standard, AA97 |
| Small Gravel | Standard, AA97 |
| Coarse Sand | Bidenharn, A505 |
| Fine Sand | Richard's |
| PG 64-22 Binder | Lion Oil, 41BF |

Figure 3-4 shows combined aggregate gradation. Appendix B shows the details of the mix design performed.

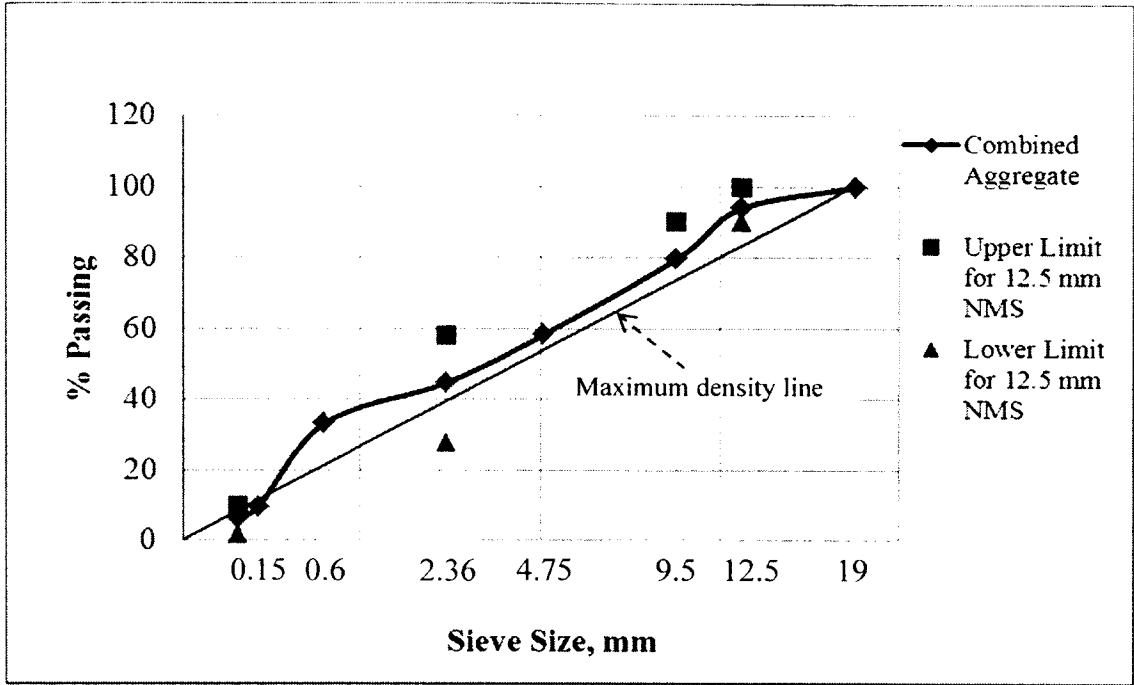


Figure 3-4. Combined aggregate gradation

3.4 Experimental Plan

3.4.1 Asphalt Binder Testing

Table 3-3 shows the test matrix for DSR testing of asphalt binders. Four percentages (w/w) of Sasobit® namely, 0%, 1%, 2% and 4% were used for this purpose.

Table 3-3. Experimental plan for rheological testing

| Binder | PG 64-22 | | | | PG 76-22M | | | |
|-------------------|---|---|---|---|---|---|---|---|
| | 0 | 1 | 2 | 4 | 0 | 1 | 2 | 4 |
| % of Sasobit® | 0 | 1 | 2 | 4 | 0 | 1 | 2 | 4 |
| Number of Samples | 3 | 3 | 3 | 3 | 3 | 3 | 3 | 3 |
| Test type | Temperature sweep 28 °C to 130 °C, 6 °C interval | | | | Temperature sweep 28 °C to 130 °C, 6 °C interval | | | |

3.4.2 Mix Testing

Table 3-4 shows test matrix for laboratory compacted samples prepared at different compaction temperatures. Two different gyration levels, two asphalt contents and one Sasobit[®] percentage were used in this study.

Table 3-4. Experimental plan for mix design sample testing

| First set, 4.8% AC, 115 Gyration max | | | | |
|---|--|--|---|---|
| Sample type | 0% Sasobit [®] , 85 °C Compaction | 2% Sasobit [®] , 85 °C Compaction | 0% Sasobit [®] , 120 °C Compaction | 2% Sasobit [®] , 120 °C Compaction |
| Number of samples to be tested for density | 4 | 4 | 4 | 4 |
| Second set, 5% AC, 75 Gyration max | | | | |
| Sample type | 0% Sasobit [®] , 85 °C Compaction | 2% Sasobit [®] , 85 °C Compaction | 0% Sasobit [®] , 130 °C Compaction | 2% Sasobit [®] , 130 °C Compaction |
| Number of samples to be tested for density | 4 | 4 | 4 | 4 |

3.5 Experimental Procedure

3.5.1 DSR Sample Preparation

A dynamic shear rheometer (AR 2000 Ex) with parallel metal plates was used according to AASHTO T315. There are two significant changes with respect to experimental procedure in this study. First, the circulation fluid was changed to a high temperature silicon fluid instead of water. This is because the testing temperature was as high as 130 °C. Secondly, 0.5 mm instead of 1 mm parallel plate gap was used. This is because at 130 °C the asphalt may come out of the parallel plates. Sasobit[®] was mixed to asphalt binders at 150 °C by using a spatula. After initial stirring of two minutes, the asphalt binder was heated in an oven for 10 minutes at 150 °C. This heating and stirring process was repeated for one hour. Figure 3-5 shows the sample on top of lower metal plate of a DSR.

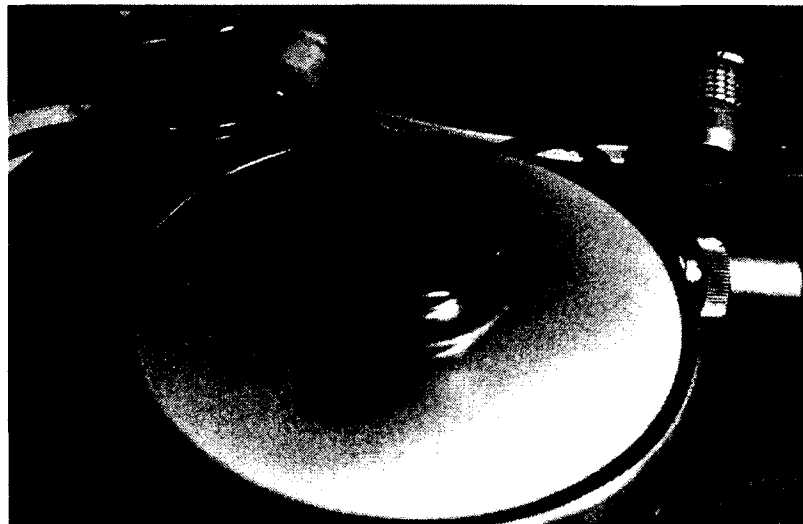


Figure 3-5. Sample on metal plate of DSR

3.5.2 Superpave Mix Design Sample Preparation

A 12.5 mm NMS (Nominal Maximum Size) Superpave asphalt mix was prepared according to the AASHTO specifications. Tables 3-5, 3-6 and 3-7 show the details of the mix produced.

Table 3-5. Aggregate test data

| | | |
|------------------------------------|-------|--------------------|
| Fine Agg. Angularity, % | 46 | Minimum 45 |
| Coarse Agg. Angularity, % | 100 | Minimum 95 |
| Flat or Elongated Particles | < 1 | Maximum. 10 |
| G_{se} | 2.6 | |
| G_{sb} | 2.554 | |

Table 3-6. Density test result of mix

| | Number of Gyration | Density % of G_{mm} | Density Required |
|------------------|---------------------------|------------------------------------|-------------------------|
| N _{ini} | 7 | 88.8 | 90% Max |
| N _{des} | 75 | 95.8 | 96.5 ± 1% |
| N _{max} | 115 | 96.4 | 98% Max |

Table 3-7. Volumetric data

| Optimum AC% | G_{mb} | G_{mm} | Density% of G_{mm} | Density Req. | % VMA | VMA Min. Req. | % VFA | % VFA Req. | Dust Prop. |
|--------------------|-----------------------|-----------------------|-----------------------------------|---------------------|--------------|----------------------|--------------|-------------------|-------------------|
| 4.8 | 2.321 | 2.423 | 95.8 | 96.5±1 | 13.5 | 13 | 69.1 | 68-78 | 1.56 |

3.6 Results and Discussions

3.6.1 Effects on Binder Stiffness,

$$\frac{G^*}{\sin\delta}$$

The complex shear modulus, G^* is an indicator of the stiffness or resistance of asphalt to deformation under load. The G^* and the phase angle, δ defines the resistance to shear deformation of the asphalt binder in the linear visco-elastic region. $G^*/\sin\delta$ is known as high temperature stiffness or rutting factor of asphalt binder. Table 3-8 shows that an increase in percent of Sasobit[®] increased the rutting factor of PG 64-22, thereby increasing the rutting resistance. Complex shear modulus, G^* and elastic or storage modulus, G' show similar increasing trends. For any viscous material, there exists a phase difference between stress and strain. For a purely viscous materials strain lags stress by 90° . For a visco-elastic material, such as asphalt binder, the phase lag is less than 90° . Table 3-8 also shows that phase angle reduced with an increase in percent of Sasobit[®] for PG 64-22.

Table 3-8. Effect on binder stiffness

| Sample type | Phase Angle, δ , Degree | Complex Shear Modulus, G^* , kPa | High temperature Stiffness, $G^*/\sin\delta$, kPa | Elastic or Storage Modulus, G' , Pa |
|------------------------------------|--------------------------------|------------------------------------|--|---------------------------------------|
| 64 °C | | | | |
| PG 64-22 | 84.4 | 3.1 | 3.1 | 302.8 |
| PG 64-22 + 1% Sasobit [®] | 82.0 | 4.3 | 4.4 | 602.3 |
| PG 64-22 + 2% Sasobit [®] | 80.1 | 6.7 | 6.8 | 1148.1 |
| PG 64-22 + 4% Sasobit [®] | 78.6 | 6.9 | 7.1 | 1375.3 |

Table 3-8 continued...

| 76 °C | | | | |
|---------------------------|------|-----|------|--------|
| PG 64-22 | 87.4 | 0.7 | 0.75 | 34.4 |
| PG 64-22 + 1% Sasobit® | 84.8 | 1.1 | 1.08 | 96.5 |
| PG 64-22 + 2% Sasobit® | 83.6 | 1.5 | 1.54 | 170.5 |
| PG 64-22 + 4% Sasobit® | 81.5 | 1.5 | 1.47 | 213.3 |
| 76 °C | | | | |
| PG 76-22M | 69.6 | 2.3 | 2.5 | 428.5 |
| PG 76-22M+ 1% Sasobit® | 67.8 | 2.9 | 3.1 | 1082.3 |
| PG 76-22M+ 2% Sasobit® | 67.5 | 3.3 | 3.6 | 1269.0 |
| PG 76-22M+ 4% Sasobit® | 68.5 | 2.9 | 3.1 | 1072.8 |

For PG 76-22M at 76 °C, up to 2% Sasobit® increased the rutting factor $G^*/\sin\delta$ and addition of 4% Sasobit® started reducing it. Similar trends can be observed for complex shear modulus, G^* and elastic modulus, G' . In the case of phase angle, similar trend but in the other direction was observed; firstly, this suggests that rate of Sasobit® must be optimized. Secondly, this effect can be justified by the fact that the Sasobit® is an asphalt flow improver and it reduces viscosity at production temperatures. Addition of excess Sasobit® may reduce stiffness properties. In this regard, rate effect can be explained by temperature effect and Table 3-8 shows the effect on stiffness values if the tests on PG 64-22 are done at 76 °C. It can be observed that changes of PG 64-22 were

similar to PG 76-22M at 76 °C with the addition of Sasobit[®]. Tables A-1 to A-16 in Appendix A show detailed rheological data on these tests.

3.6.2 Effect of Sasobit[®] at Compaction Temperatures on Viscosity

In the field, the compaction temperature usually ranges from 155 °C to 85 °C which includes breakdown and intermediate rolling. Finish rolling normally takes place within a temperature range of 85 °C down to 70 °C. In this study, the results showed that the dynamic viscosity of asphalt binders reduced with an increase in percent of Sasobit[®] at higher compaction temperatures, such as 130 °C. Table 3-9 shows that viscosity of PG 64-22 was 1.24 Pa s at 130 °C; whereas, viscosity of PG 64-22 with 1%, 2% and 4% Sasobit[®] were 1.08 Pa s, 1.00 Pa s and 0.73 Pa s, respectively. In case of PG 76-22M at 130 °C, a similar reducing trend was observed with an increase in percent of Sasobit[®].

Table 3-9. Effect of Sasobit[®] at higher compaction temperature (130 °C)

| Asphalt binder type | Dynamic Viscosity, η' (Pa s) at 130 °C |
|-------------------------------------|---|
| PG 64-22 | 1.24 |
| PG 64-22 + 1% Sasobit [®] | 1.08 |
| PG 64-22 + 2% Sasobit [®] | 1.00 |
| PG 64-22 + 4% Sasobit [®] | 0.73 |
| PG 76-22M | 4.28 |
| PG 76-22M + 1% Sasobit [®] | 3.61 |
| PG 76-22M + 2% Sasobit [®] | 3.47 |
| PG 76-22M + 4% Sasobit [®] | 2.93 |

However, this trend was reversed at lower compaction temperatures, such as 100 °C. Table 3-10 shows that at lower compaction temperature such as 100 °C, viscosity increases with an increase in percent of Sasobit[®], thus posing a potential negative effect on field compaction as well as density. Table 3-10 also shows that at 100 °C, the viscosity of PG 64-22 is 7.98 Pa s. This viscosity increases up to 10.74 Pa s for 2% Sasobit[®]. In case of PG 76-22M, 2% Sasobit[®] increased the viscosity from 30.04 Pa s to 32.47 Pa s. This increase in viscosity with Sasobit[®] was not sudden as found in temperature sweep tests performed in this study.

Table 3-10. Effect of Sasobit[®] at lower compaction temperature (100 °C)

| Asphalt binder type | Dynamic viscosity, η' (Pa s) at 100 °C |
|-------------------------------------|---|
| PG 64-22 | 7.98 |
| PG 64-22 + 1% Sasobit [®] | 7.76 |
| PG 64-22 + 2% Sasobit [®] | 10.74 |
| PG 64-22 + 4% Sasobit [®] | 10.33 |
| PG 76-22M | 30.94 |
| PG 76-22M + 1% Sasobit [®] | 30.29 |
| PG 76-22M + 2% Sasobit [®] | 32.47 |
| PG 76-22M + 4% Sasobit [®] | 30.82 |

Figure 3-6 to 3-9 and Figures 3-10 to 3-13 show the viscosity of PG 64-22 and PG 76-22M at a temperature range from 88 °C to 130 °C at 6 °C intervals.

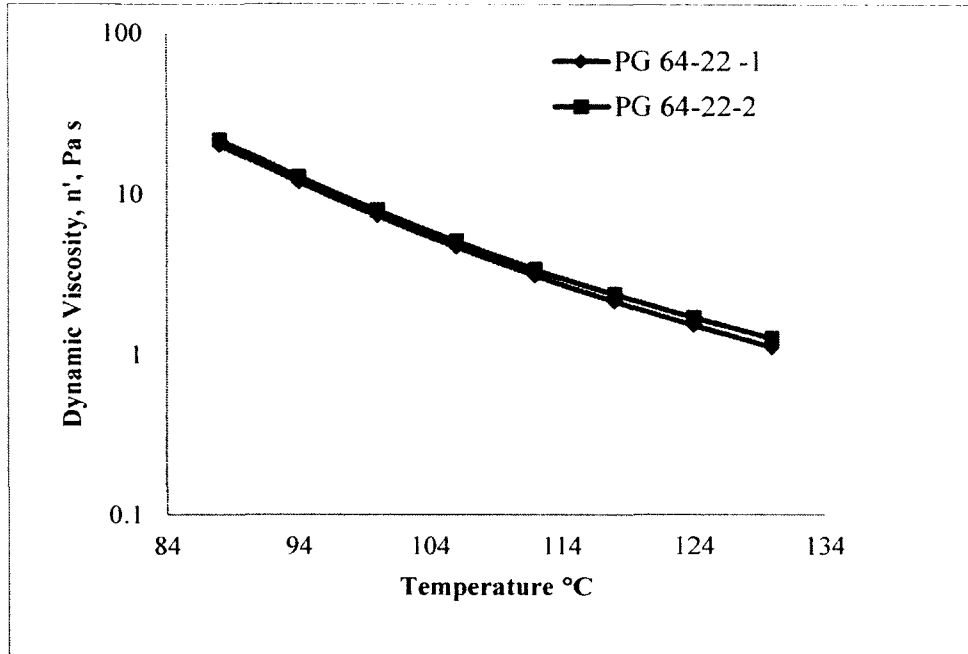


Figure 3-6. Dynamic viscosity for PG 64-22 0% Sasobit[®]

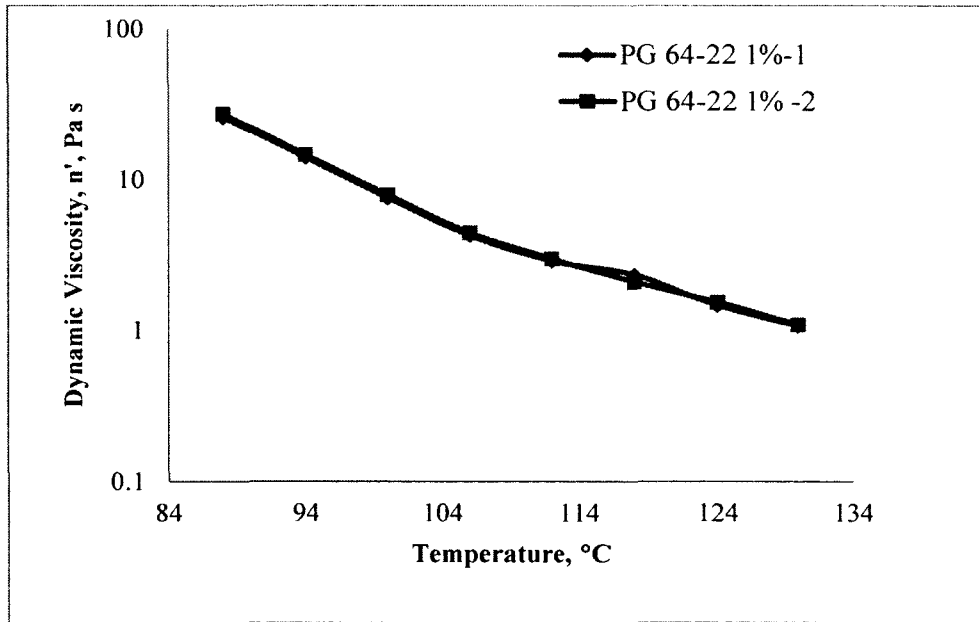


Figure 3-7. Dynamic viscosity for PG 64-22 1% Sasobit[®]

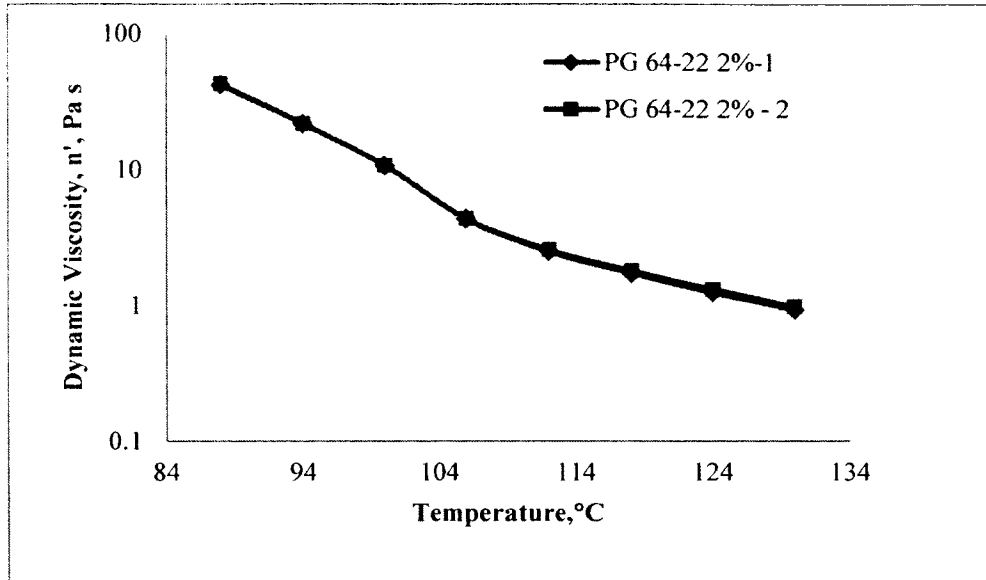


Figure 3-8. Dynamic viscosity for PG 64-22 2% Sasobit[®]

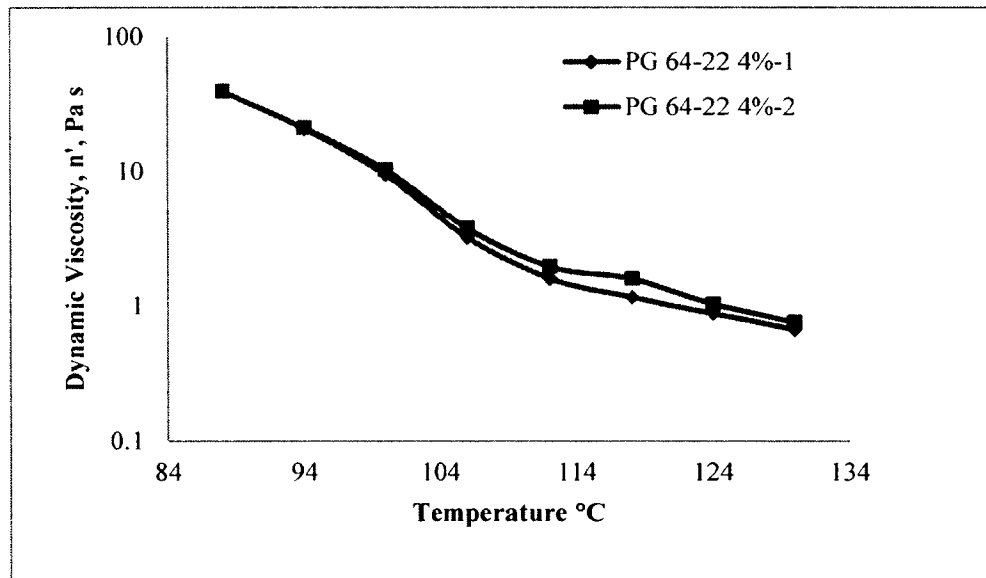


Figure 3-9. Dynamic viscosity for PG 64-22 4% Sasobit[®]

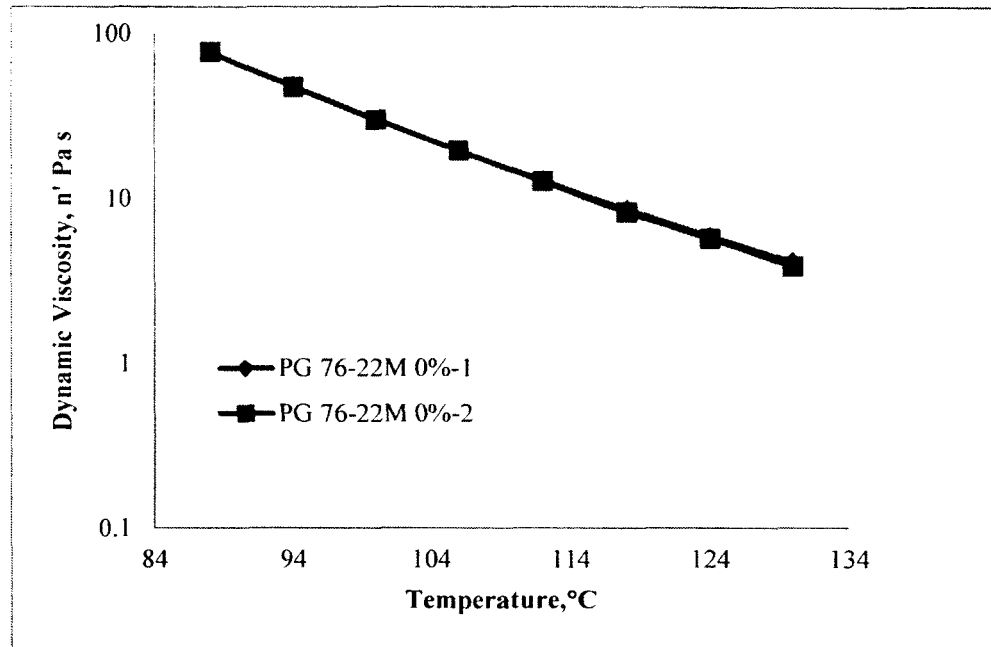


Figure 3-10. Dynamic viscosity for PG 76-22M 0% Sasobit®

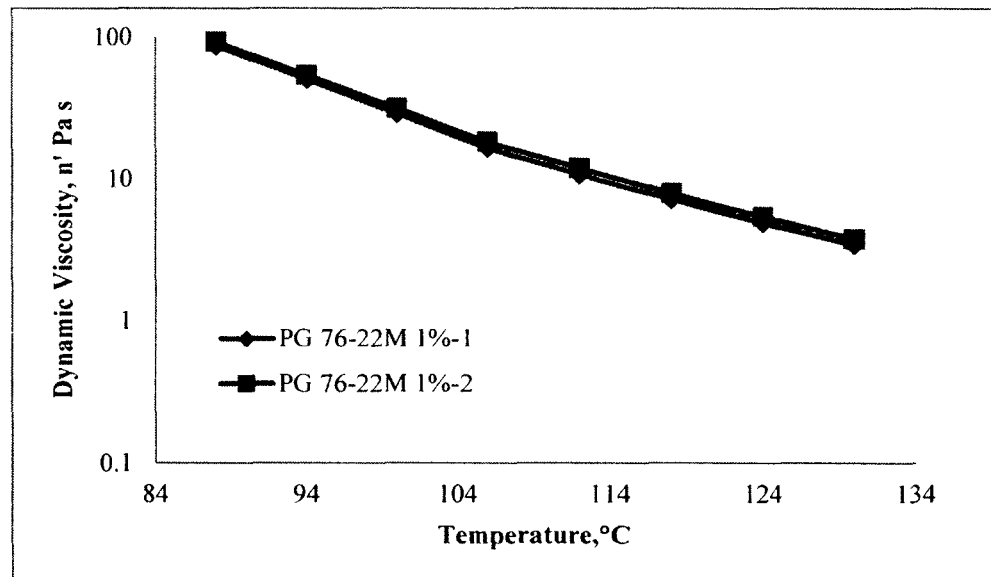


Figure 3-11. Dynamic viscosity for PG 76-22M 1% Sasobit®

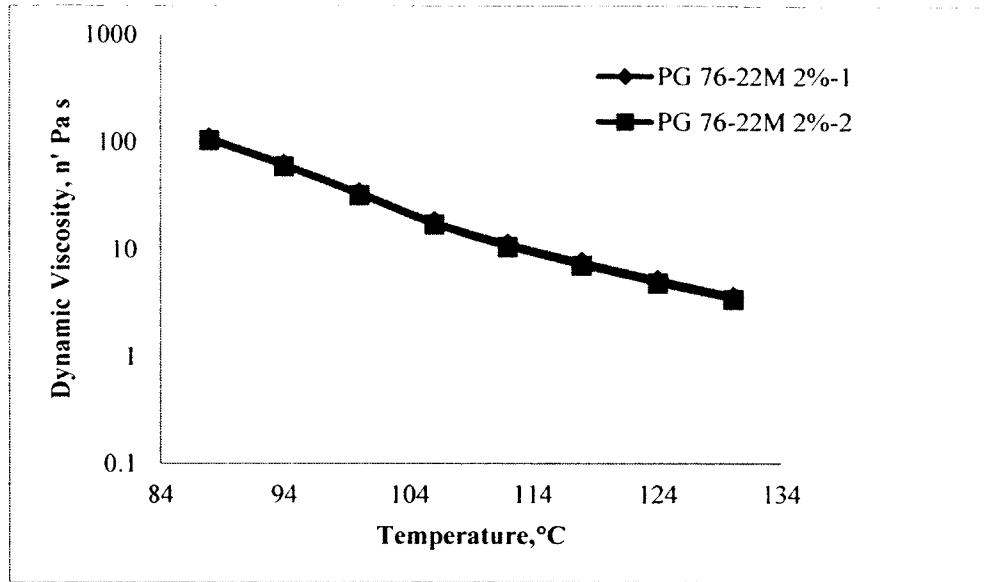


Figure 3-12. Dynamic viscosity for PG 76-22M 2% Sasobit[®]

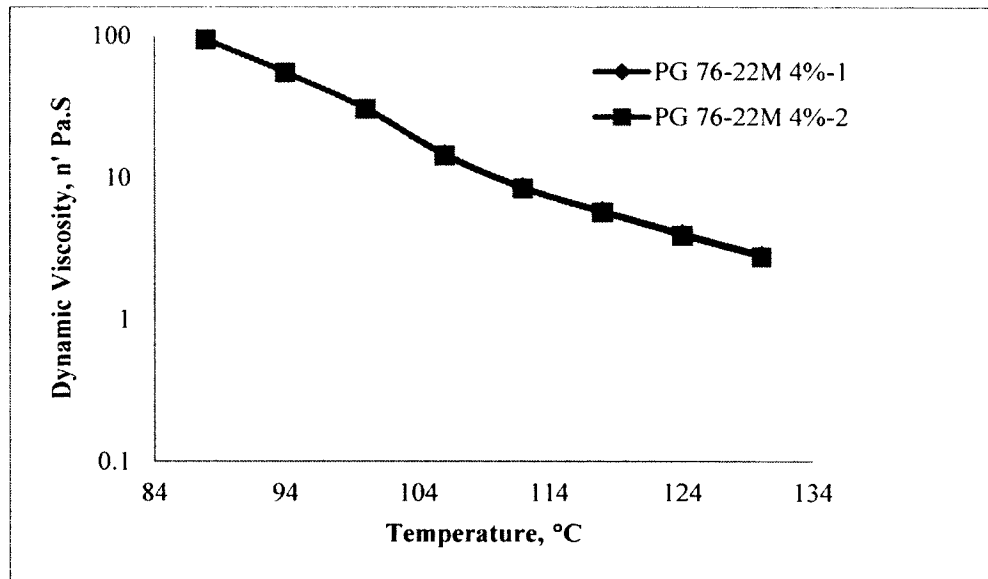


Figure 3-13. Dynamic viscosity for PG 76-22M 4% Sasobit[®]

Figure 3-14 and Figure 3-15 show the combined results. It is clearly evident from the figures that Sasobit[®] reduced viscosity at higher compaction temperatures but it increased viscosity at lower compaction temperatures. There exists a reverse or critical point for each asphalt binder below which viscosity will increase with addition of

Sasobit[®]. Therefore, compaction below the reverse point temperature can negatively impact density. For PG 64-22, the reverse point is 104 °C and for PG 76-22M, the reverse point is about 101 °C. These results indicate that for PG 64-22, a mix with Sasobit[®] will need comparatively more compaction effort below 104 °C and for PG 76-22M, this temperature is 101 °C.

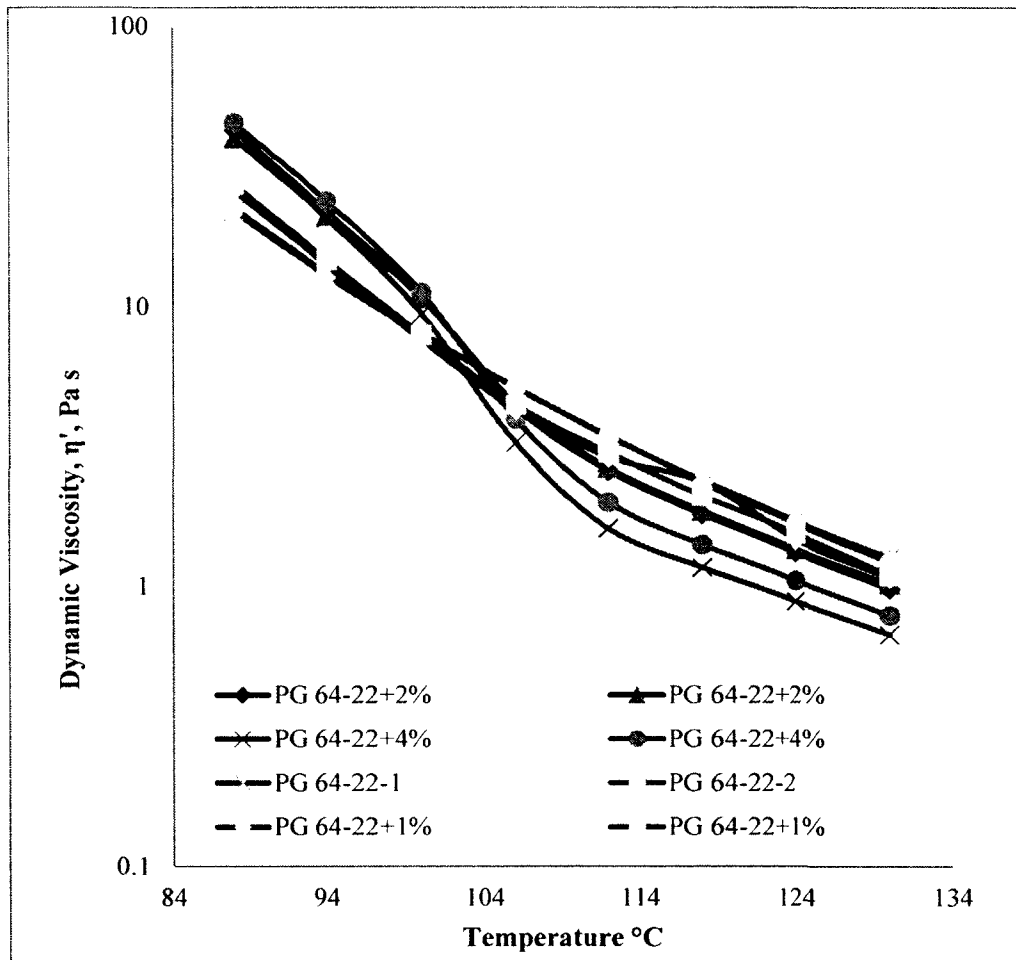


Figure 3-14. Combined data for PG 64-22 with and without Sasobit[®]

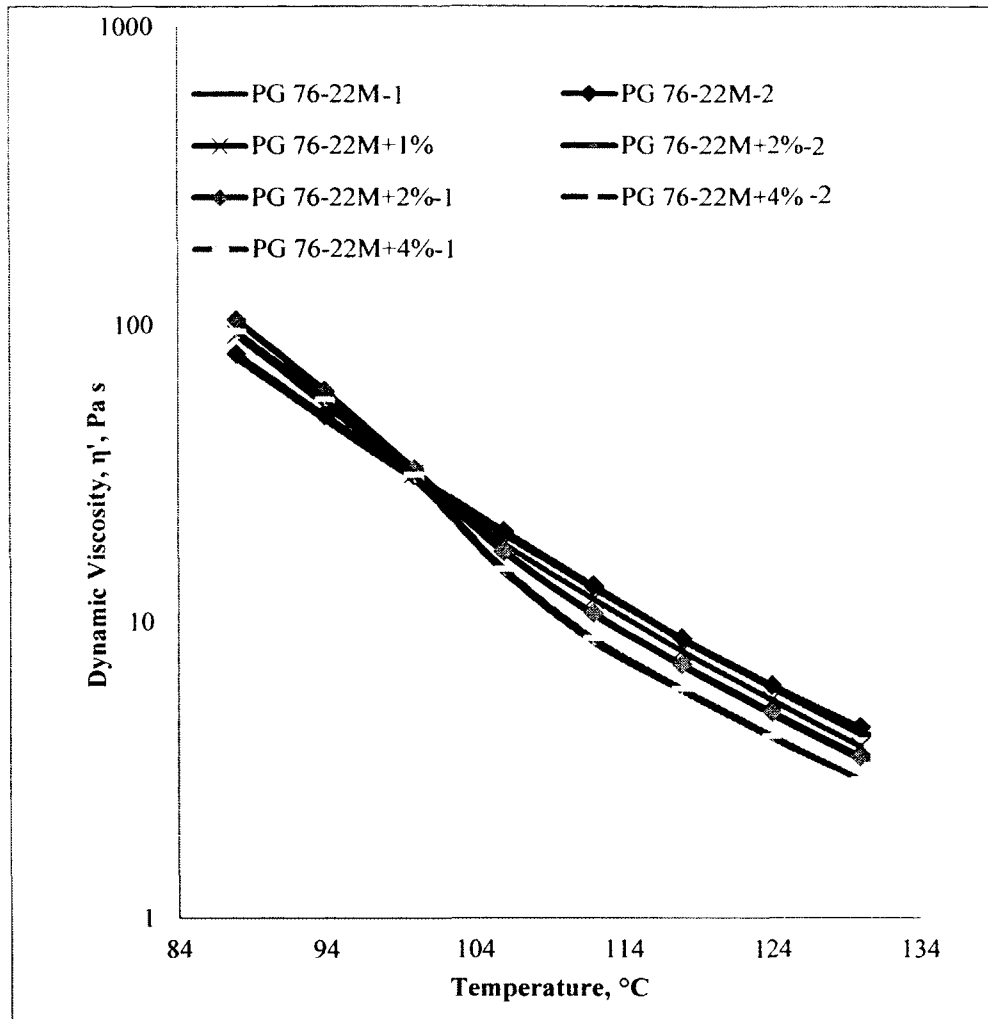


Figure 3-15. Combined data for PG 76-22M with and without Sasobit®

3.6.3 Implications of Viscosity Changes on Field Density

Cooper (2009) from Louisiana Transportation Research Center (LTRC) conducted a field study using Sasobit®. A mix with PG 76-22M was used with and without 1% Sasobit® in it. The HMA plant temperature was 166 °C for both PG 76-22M and Sasobit® mixes; this was done to better compare the Sasobit® mixes with control PG 76-22M mixes. The field asphalt contents were 3.7% and 4.1%, respectively for PG 76-22M and Sasobit® mixes. The breakdown and intermediate rolling were performed with

vibration and a steel wheel finished roller was used in static mode only. Nuclear gauge density was measured at six locations in both PG 76-22M and Sasobit[®] sections. Table 3-11 shows the average nuclear gauge density of six locations obtained by Cooper (2009).

Table 3-11. Nuclear gauge field density (average of six locations from Cooper, 2009)

| Nuclear gauge density (average of six locations) in percent | | |
|--|--|--|
| | HMA with Sasobit[®] in PG 76-22M | HMA without Sasobit[®] PG 76-22M |
| Directly behind screed | 78.7 | 75.2 |
| Roller 1 – Pass 1 | 87.0 | 85.6 |
| Roller 1 – Pass 2 | 89.4 | 88.9 |
| Roller 1 – Pass 3 | 90.0 | 90.1 |
| Roller 1 – Pass 4 | 91.3 | 91.3 |
| Roller 2 – Pass 1 | 91.6 | 91.1 |
| Roller 2 – Pass 2 | 92.4 | 91.9 |
| Roller 2 – Pass 3 | 92.5 | 91.9 |
| Roller 2 – Pass 4 | 93.4 | 92.3 |
| Roller 3 – Pass 1 | 92.9 | 92.3 |
| Roller 3 – Pass 2 | 93.0 | 92.8 |
| Roller 3 – Pass 3 | 93.3 | 92.2 |
| Roller 3 – Pass 4 | 93.2 | 93.0 |

It can be seen that the average density of six locations directly behind the screed were 78.7% and 75.2%, respectively, for PG 76-22M with 1% Sasobit[®] and PG 76-22M without Sasobit[®] while the densities after the finish roller were 93.2% and 93.0%, respectively. This indicates that Sasobit[®] indeed reduced the viscosity of binder as well as the mix at higher compaction temperature as can be seen from the density directly behind

the screed. The Sasobit[®] mix had 3.5% more density than the PG 76-22M mix. As the compaction continues, the mixes cooled down and the beneficial effects of Sasobit[®] cannot be seen anymore. By the time the finisher roller completed, both mixes produced similar densities, 93.3% and 93.0% respectively for Sasobit[®] and PG 76-22M mixes. This evidence strongly justifies the findings of this study that the beneficial effect of Sasobit[®] in viscosity reduction can only be obtained at higher compaction temperatures. However, the 0.3% increase in density with Sasobit[®] may not be related to viscosity reduction by Sasobit[®] and may be related to the 0.4% higher asphalt content of Sasobit[®] mixes. Table 3-11 reveals the effect of compaction temperature of Sasobit[®] on field density. As temperature goes down Sasobit[®] reduced the density compare to the other mix.

3.6.4 Effect of Sasobit[®] on Density of Gyratory Compacted Samples

At first, 12 gyratory compacted samples were prepared at optimum asphalt content of 4.8% PG 64-22 and at maximum gyrations of 115. Three samples of PG 64-22 and three samples of PG 64-22 with 2% Sasobit[®] were compacted at 120 °C, which was higher than critical compaction temperature of 104 °C. Another three samples of PG 64-22 and three samples of PG 64-22 with 2% Sasobit[®] were compacted at 85 °C which was lower than critical compaction temperature. Densities were determined following AASHTO T166 and the average density of three replicates was presented in Figure 3-16. The error bar in Figure 3-16 is based on standard deviation of three samples. It is evident that 2% Sasobit[®] increased the density of gyratory compacted samples at higher compaction temperature, whereas, it reduced the density at lower compaction temperature. Therefore, the effects of Sasobit[®] on density are similar to the effects on

viscosity as shown in previous sections. Table 3-12 shows the G_{mb} data of gyratory compacted samples.

Table 3-12. G_{mb} data of gyratory compacted samples

| First Set, 4.8% Asphalt Content, 115 Gyration | | |
|--|----------|---------|
| 0% Sasobit [®] , 85°C | G_{mb} | Average |
| Sample 1 | 2.31 | 2.31 |
| Sample 2 | 2.32 | |
| Sample 3 | 2.30 | |
| 2% Sasobit [®] , 85 °C | | Average |
| Sample 1 | 2.30 | 2.30 |
| Sample 2 | 2.30 | |
| Sample 3 | 2.29 | |
| 0% Sasobit [®] , 120 °C | | Average |
| Sample 1 | 2.32 | 2.32 |
| Sample 2 | 2.32 | |
| Sample 3 | 2.32 | |
| 2% Sasobit [®] , 120 °C | | Average |
| Sample 1 | 2.32 | 2.32 |
| Sample 2 | 2.32 | |
| Sample 3 | 2.32 | |
| Second Set, 5% Asphalt Content, 75 Gyration | | |
| 0% Sasobit [®] , 85 °C | | Average |
| Sample 1 | 2.31 | 2.30 |
| Sample 2 | 2.3 | |
| Sample 3 | 2.31 | |
| 2% Sasobit [®] , 85 °C | | Average |
| Sample 1 | 2.29 | 2.29 |
| Sample 2 | 2.31 | |
| Sample 3 | 2.29 | |

Table 3-12 continued...

| | | |
|----------------------------------|------|---------|
| 0% Sasobit [®] , 130 °C | | Average |
| Sample 1 | 2.32 | 2.31 |
| Sample 2 | 2.31 | |
| Sample 3 | 2.31 | |
| 2% Sasobit [®] , 130 °C | | Average |
| Sample 1 | 2.33 | 2.32 |
| Sample 2 | 2.32 | |
| Sample 3 | 2.32 | |

As can be seen in Figure 3-16, the standard deviations for the first 12 samples were close to the differences in average densities. At this point, it was hypothesized that use of reduced compactive efforts (design gyrations of 75 instead of maximum gyrations of 115) and increased asphalt content (5% instead of optimum asphalt content of 4.8%) may help demonstrating the reflection of viscosity changes in density. Therefore, the following 12 samples were prepared at 75 Gyrations and 5% asphalt content. Three samples of PG 64-22 and three samples of PG 64-22 with 2% Sasobit[®] were compacted at 130 °C. Another three samples of PG 64-22 and three samples of PG 64-22 with 2% Sasobit[®] were compacted at 85 °C, which is lower than critical compaction temperature. It can be seen that the standard deviation values have reduced in this case. Table A-17 and A-18 in Appendix A show detail density data.

The Superpave gyratory compactor provides the height of compacted samples. Densities of samples were also calculated based on these heights for cross checking. The densities found in this method were 2.27 ± 0.006 , 2.26 ± 0.009 , 2.28 ± 0.005 and 2.29 ± 0.005 gm/cc for 0% Sasobit[®] at 85 °C, 2% Sasobit[®] at 85 °C, 0% Sasobit[®] at 130 °C and

2% Sasobit[®] at 130 °C samples, respectively. The standard deviations of gyratory height densities were higher than those obtained from AASHTO T166.

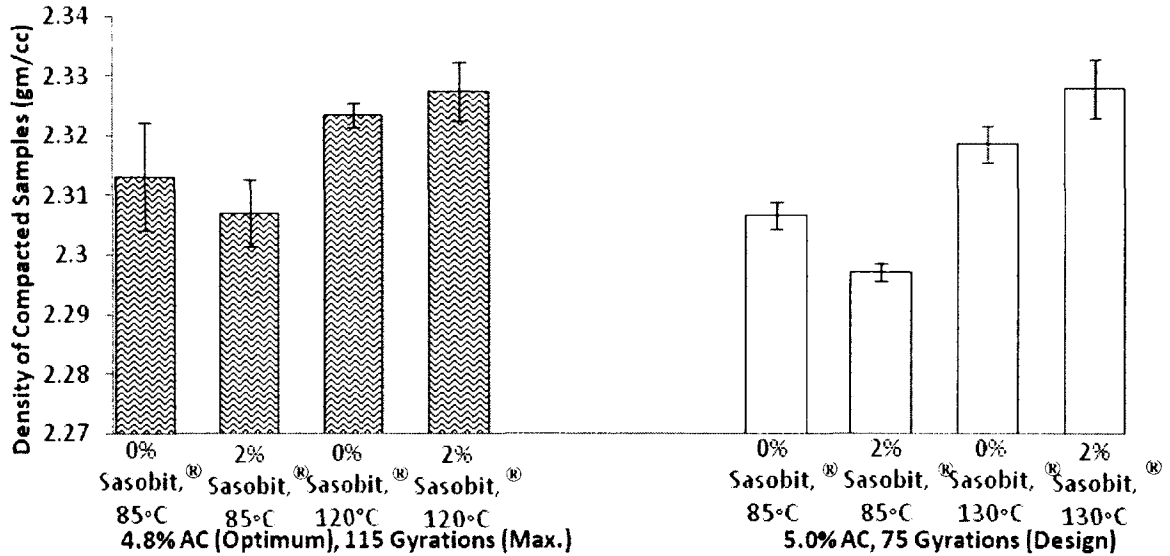


Figure 3-16. Sample density chart

3.7 Conclusions

In this study, the dynamic viscosity, η' at various compaction temperatures were analyzed with respect to gyratory compacted density and field density after different compaction steps. The following specific conclusions can be drawn from this study:

1. An increase in percent of Sasobit[®] increased the rutting factor $G^*/\sin\delta$ of PG 64-22, thereby increasing the potential for rutting resistance. For PG 76-22M at 76 °C, up to 2% Sasobit[®] increased the rutting factor $G^*/\sin\delta$ and addition of 4% Sasobit[®] started reducing it. Firstly, this finding suggests that rate of Sasobit[®] addition need to be optimized. Secondly, this effect can be justified by the fact that the Sasobit[®] is an asphalt flow improver and it reduces viscosity at production temperatures. Addition of excess Sasobit[®] may reduce

stiffness properties. In this regard, rate effect can be explained by temperature effect and it can be observed that changes of PG 64-22 is similar to PG 76-22M at 76 °C with the addition of Sasobit®.

2. Sasobit® reduces viscosity at higher compaction temperatures but it increases viscosity at lower compaction temperatures. There exists a critical temperature for each asphalt binder below which viscosity will increase with addition of Sasobit®. Therefore, compaction below the critical temperature can negatively impact density. For PG 64-22, this critical temperature is 104 °C and for PG 76-22M, the critical temperature is about 101 °C.
3. The gyratory compacted samples exhibit that Sasobit® added samples have higher densities than without Sasobit® samples at higher compaction temperature whereas, Sasobit® added samples have lower densities than without Sasobit® samples at lower compaction temperature.
4. Sasobit® indeed reduced the viscosity of binder as well as the mix at higher compaction temperature as can be seen from the density directly behind the screed. Sasobit® mix as monitored in this study had 3.5% more density than the PG 76-22M mix without Sasobit®. As the compaction continues, the mixes cooled down and the beneficial effects of Sasobit® could not be seen anymore. By the time the finisher roller completed, both mixes produced similar densities, 93.3% and 93.0% respectively for Sasobit® and PG 76-22M mixes. This finding strongly justifies the findings of this study that the beneficial effect of Sasobit® in viscosity reduction can only be obtained at higher compaction temperatures.

CHAPTER 4

EFFECT OF SHEAR RATE ON VISCOSITY OF SASOBIT[®] MODIFIED ASPHALT BINDER²

4.1 Introduction

Hot mix asphalt is prepared and compacted at different temperature ranges and shear rates. Therefore, it is imperative to know the influence of shear rate on viscosity at those temperature ranges. In a state highway agencies' survey, the need for determining the right mixing and compaction temperatures has been reported (Khatri et al., 2001). This is needed because almost all the contractors use extremely high temperatures to reach viscosity levels with modified asphalt binders. In most cases, the level of viscosity of approximately 0.3-0.5 Pa s is achieved at extremely high temperatures. This high temperature may degrade the binder properties. The contractors and state agencies require suitable temperatures for viscosity and compaction. Suppliers follow trial and error method to recommend temperatures to contractors. Superpave binder and mix volumetric procedures do not provide any specific recommendations in cases of binders with high viscosities (Khatri et al., 2001).

² The contents of this chapter have been published in the International Journal of Pavement Research and Technology, Vol. 5, No. 6, pp. 369-378, November 2012. This portion has been formatted for the dissertation.

There are three alternatives which could be used to achieve required compaction of modified asphalt in the field and in the laboratory (Khatri et al., 2001):

1. Using high temperatures for field and laboratory compaction. High temperatures can have adverse effects such as volatilization and degradation of binders,
2. Increasing compaction effort to overcome higher viscosity. This compaction effort will add cost and time, ultimately increases cost of the product, and
3. Increasing asphalt content will result in easier compaction but higher asphalt content can increase cost and it can result in excessive rutting.

Therefore, it is critical to optimize the WMA process. Generally, it has been believed that compaction in the field results in shear rates that are higher than the low shear rates used in the viscosity testing procedure (Kennedy et al., 2000). Asphalt binders exist in thin films in the asphalt mix, a small amount of movement may cause a very high shear rate (Khatri and Bahia, 2001; Yildirim et al., 2000). Therefore, it has been an interest to find the effect of shear rate in the case of asphalt modified by warm mix additives. This chapter focuses on studying shear rate dependency of viscosity of Sasobit[®] modified asphalt binders.

4.2 Objectives

Compaction temperatures can be determined by estimating the relation between viscosity and temperature. Previous studies showed that most modified asphalt binders show pseudo plastic characteristic (Khatri and Bahia, 2001; Yildirim et al., 2000). For these materials, viscosity depends on shear rate (Levy, 1962). Therefore, for modified asphalt binders, the effect of shear rate should be considered during viscosity

measurements to calculate the compaction temperatures. The specific objectives of the shear rate study were to:

1. Develop viscosity model and to find the effect of Sasobit[®] on model parameters,
2. Effect of Sasobit[®] on zero shear viscosity,
3. Evaluate the steady state rotational viscosity using a DSR at lower compaction temperatures, and
4. Evaluate the effect of shear rate on steady state viscosity of asphalt binders.

4.3 Material Description

Both the asphalt binders, PG 64-22 and PG 76-22M, used in this study were obtained from Ergon Refining, Inc., Vicksburg, Mississippi. PG 64-22 is an unmodified binder and PG 76-22M is a PMA binder. Sasobit[®] is obtained from Sasol Wax, North America Corp.

4.4 Experimental Plan

Three selected percentages of Sasobit[®], 1%, 2% and 4% were added to both the binders for rheological testing using a DSR consisting of parallel metal plates according to AASHTO T315. Metal plates of 25 mm diameter were used. The gap between the upper and lower plates was 0.5 mm instead of 1 mm. For effect of shear rate on steady state viscosity, three temperatures, namely 64 °C, 100 °C and 124 °C for PG 64-22 and three temperatures, 76 °C, 100 °C and 124 °C were used for PG 76-22M. Shear rates were used in the range between 0.0025 s⁻¹ to 250 s⁻¹. Table 4-1 shows the experimental plan for the shear rate study.

Table 4-1. Experimental plan for shear rate study

| Binder type | % of Sasobit [®] | | | | Temperature |
|---|---------------------------|---|---|---|--------------------|
| PG 64-22 | 0 | 1 | 2 | 4 | 64, 100 and 124 °C |
| Number of Samples tested | 3 | 3 | 3 | 3 | |
| Binder type | % of Sasobit [®] | | | | Temperature |
| PG 76-22M | 0 | 1 | 2 | 4 | 64, 100 and 124 °C |
| Number of Samples tested | 3 | 3 | 3 | 3 | |
| Shear Rate : 0.0025 s ⁻¹ – 250 s ⁻¹ | | | | | |

4.5 Results and Discussions

4.5.1 Effects of Shear Rate on Viscosity

In this study, shear sweep was performed under steady state rotational mode at various temperatures. Figure 4-1 shows that the viscosity of PG 64-22 does not vary with shear rate at 124 °C indicating that PG 64-22 is a Newtonian liquid. Figure 4-1 also shows that PG 64-22 behaves as a Newtonian liquid even at 100 °C. However, at 64 °C the behavior of PG 64-22 is complex under various shear rates. At lower shear rates, it behaves like a Newtonian fluid and at higher shear rates it becomes a shear thinning liquid meaning viscosity decreases as shear rate increases.

As indicated earlier, the behavior of asphalt binders is different in case of polymer modifications. Polymer-modified asphalt binders, such as PG 76-22M used in this study, exhibit shear rate dependency even at production temperatures where unknown shear rates are utilized and shear rate dependency is of practical interests. Figure 4-1 shows that at 124 °C, the viscosity of PG 76-22M does not change with change in shear rates. At 100 °C and at 76 °C, PG 76-22M becomes shear thinning. Therefore, PMA binders are non-

Newtonian at some production (compaction) temperatures, and it is a shear-thinning (pseudo plastic) liquid where liquid will display a decreasing viscosity with an increasing shear rate.

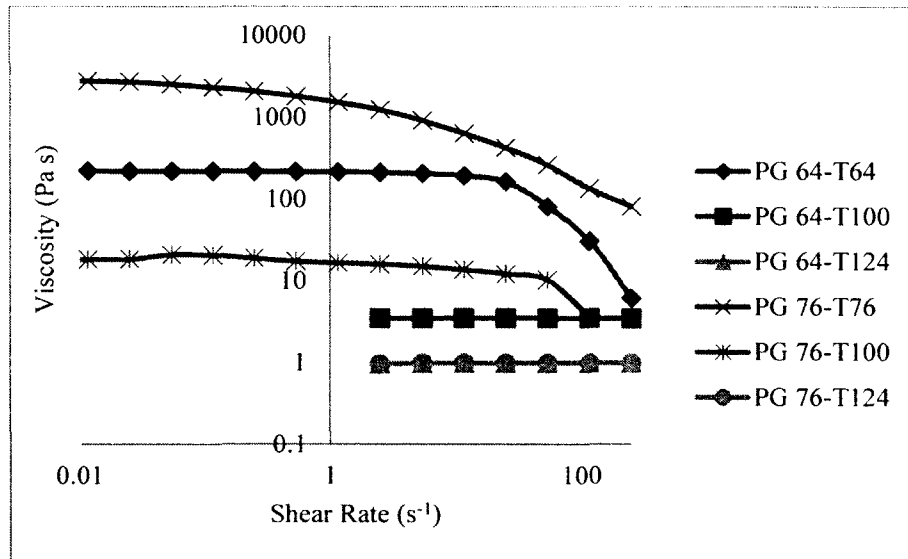


Figure 4-1. Effect of temperature on shear rate at 64 °C, 100 °C and 124 °C

However, shear rate dependency reduces as temperature increases. Figure 4-2 shows that adding Sasobit[®] to PG 64-22 at 64 °C changes PG 64-22 from Newtonian to shear thinning liquid at all ranges of shear rate.

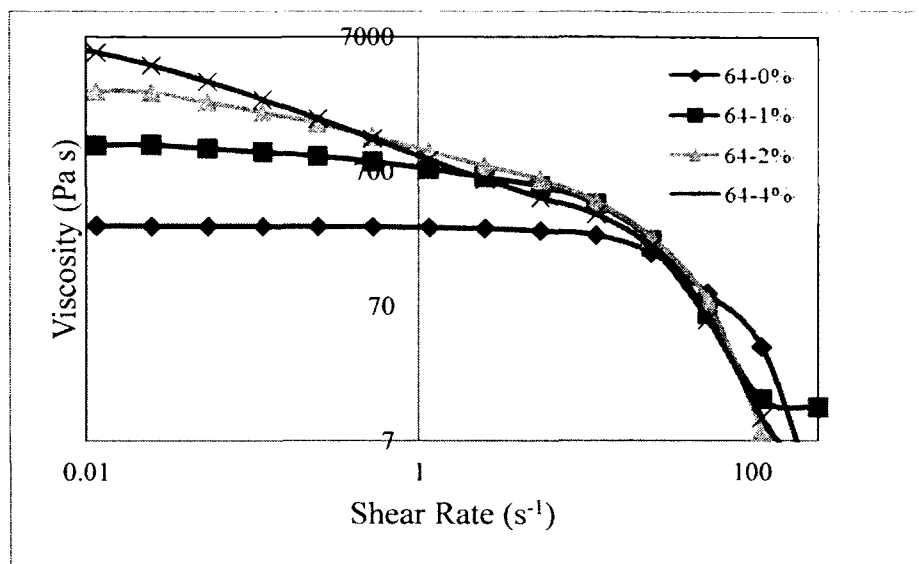


Figure 4-2. Effect of shear rate at 64 °C on PG 64-22 with Sasobit[®]

The shear rate dependency increased as the percent of Sasobit[®] increased. Similar effects of Sasobit[®] were observed at 100 °C in reduced level, and shear rate dependency with the addition of Sasobit[®] was almost negligible at 124 °C as evident from Figure 4-3 and Figure 4-4.

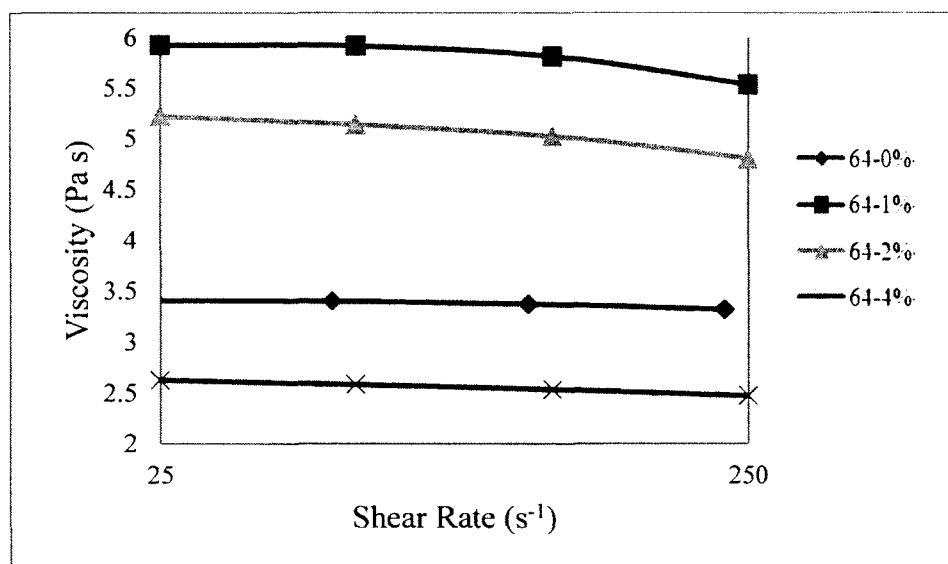


Figure 4-3. Effect of shear rate at 100 °C on PG 64-22 with Sasobit[®]

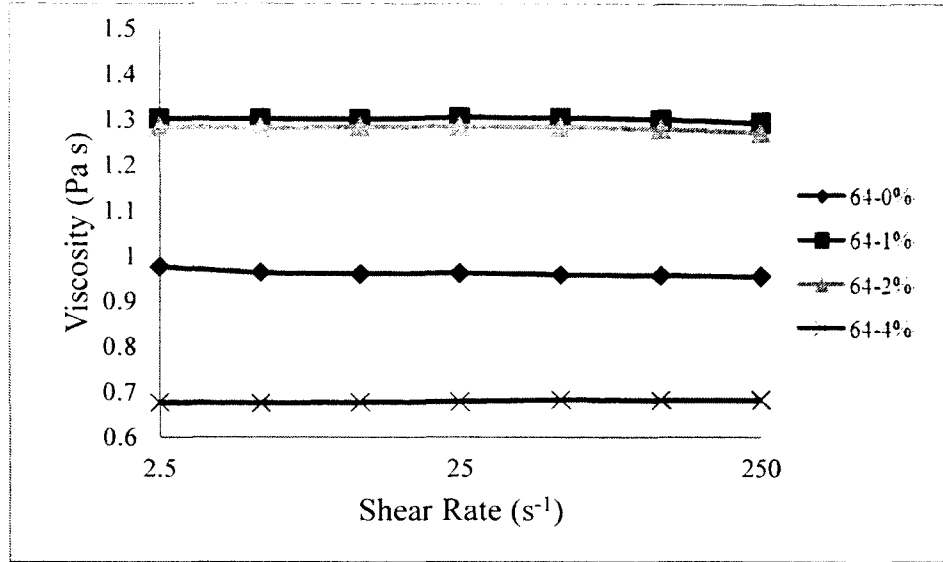


Figure 4-4. Effect of shear rate at 124 °C on PG 64-22 with Sasobit®

These figures also show that the shear rate dependency in general, reduces as temperature increases. Also, the rate of change of viscosity becomes higher with higher shear rates and lower at lower shear rates. The rate of change of viscosity become very high at shear rates of approximately 200 s⁻¹ (as shown in Figure 4-2) and the rate of change was negligible at low shear rates around 0.01 s⁻¹ indicating that the viscosity reached a constant value and it did not increase noticeably if the shear rate was further lowered.

As observed earlier, PG 76-22M is primarily a shear thinning liquid without the addition of Sasobit®. Addition of 1%, 2% and 4% Sasobit® reduces viscosity but the shear thinning behavior does not change (See Figures 4-5, 4-6 and 4-7). However, shear rate dependency reduces as temperature increases.

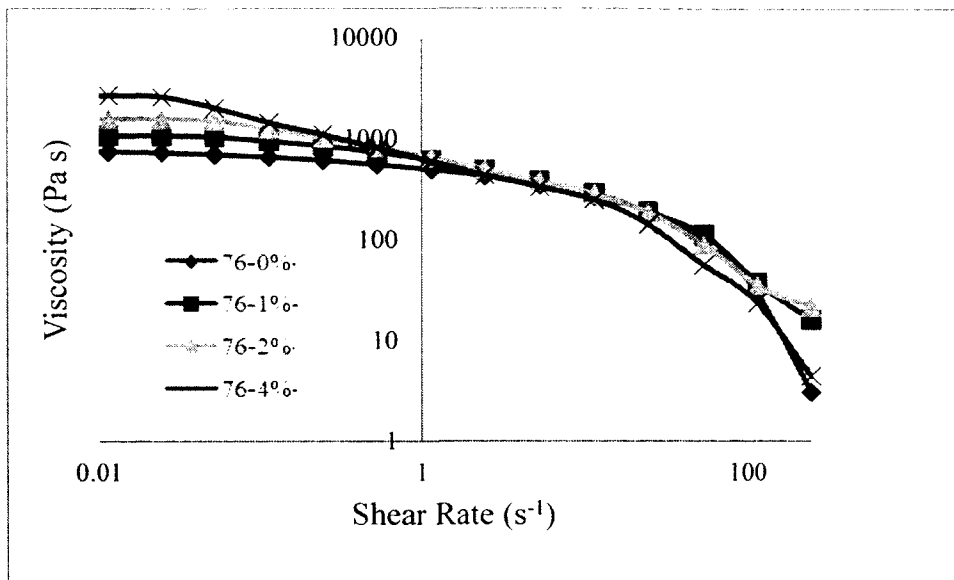


Figure 4-5. Effect of shear rate at 76 °C on PG 76-22M with Sasobit[®]

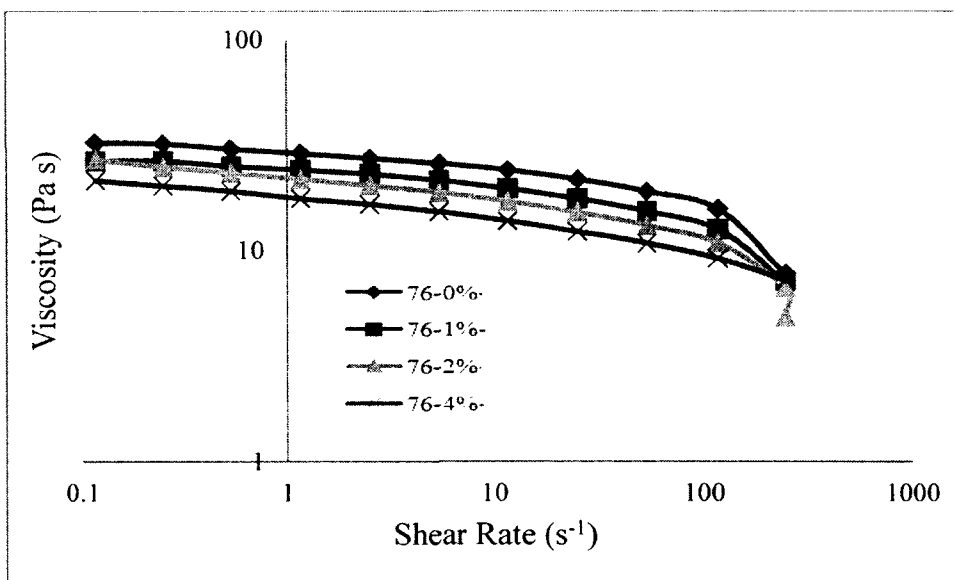


Figure 4-6. Effect of shear rate at 100 °C on PG 76-22M with Sasobit[®]

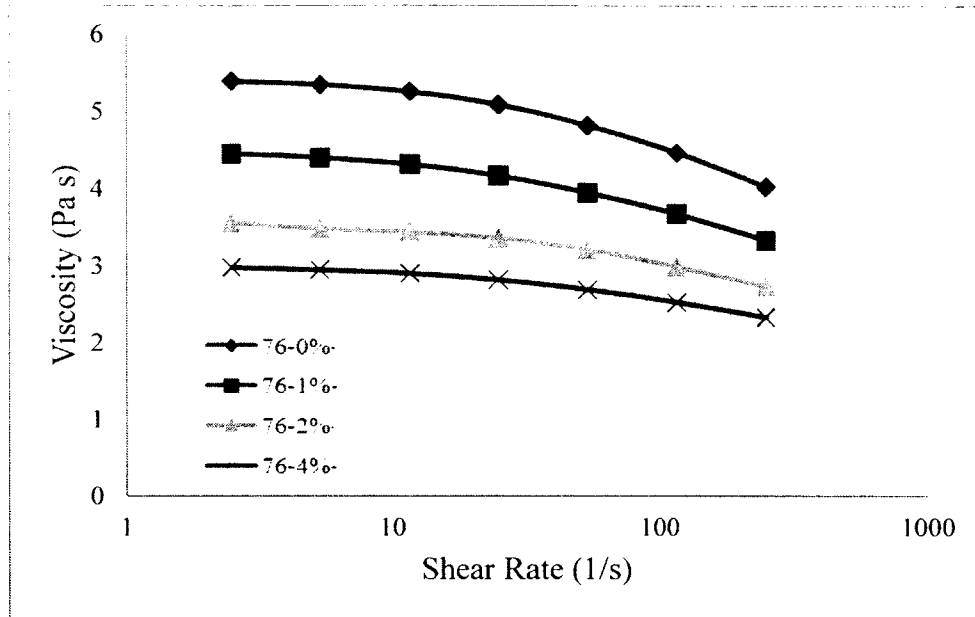


Figure 4-7. Effect of shear rate at 124 °C on PG 76-22M with Sasobit®

Unlike PG 64- 22, PG 76-22M with 1% and 2% Sasobit® showed shear rate dependency even at 124 °C. Similar to PG 64-22, PG 76-22M with and without Sasobit® also showed that shear rate dependency is higher at higher shear rates.

Superpave requires use of rotational viscometer for viscosity measurements for mixing and compaction temperatures. The recommended 20 rpm in RV type Brookfield viscometer corresponds to 6.8 s^{-1} . In this study, parallel plate steady state rotational loading was applied. In case of PG 64-22 with and without Sasobit®, the rate of change of viscosity is small at shear rate of 6.8 s^{-1} , as can be seen in Figure 4-3 and Figure 4-4 for 100 °C and 124 °C, respectively. In case of PG 76-22M, the rate of change of viscosity with respect to shear rate at 100 °C and 124 °C was significant with rate of change being higher at 100 °C as can be seen in Figure 4-5 and Figure 4-6. This indicates if the actual shear rate during the compaction process is higher than 6.8 s^{-1} , then the currently recommended viscosity as well as temperature is overestimated and compaction

temperature can be reduced. On the other hand, if the actual shear rate during the compaction process is lower than 6.8 s^{-1} , then the currently recommended viscosity as well as temperature is underestimated and a higher compaction temperature should be used. In the following paragraph, the actual shear rate during the compaction process will be discussed based on existing literature.

Khatri et al. (2001), reported that during the critical part of the compaction process the zero shear viscosity is the most important factor controlling the densification for a given aggregate source and structure. The concept of using low shear viscosity is validated by the rate of change of linear strain rate, which shows that for almost half the compaction period the mix experiences very low shear rate in the Superpave gyratory compactor. Based on this finding, a procedure to estimate zero shear viscosity using the existing rotational viscometer was developed and zero shear viscosity was proposed for use.

In contrast, Yildirim et al. (2000) argued that the binder coating on the aggregate is very thin, around 10 microns range, and just a very small movement might cause a very high shear rate on the binder. Yildirim et al. (2000) used equiviscous method and hypothesized that mix with unmodified and modified binders will produce similar G_{mb} at equal viscosity but at different temperatures. With known viscosity and the temperature, they found the shear rate using a Superpave gyratory compactor and viscosity-shear rate relationship and observed a very high shear rate and, therefore, proposed reduced mixing and compaction temperatures. In the present study, as discussed previously, it was found that Sasobit[®] changed PG 64-22 from Newtonian to shear thinning fluid. It also increased the shear rate dependency of PG 76-22M. This indicates that the viscosity as well as

temperature reductions due to the addition of Sasobit[®], is greater than what might be obtained using rotational viscometer at 6.8 s^{-1} as used currently.

4.5.2 Viscosity Model

Sybiliski (1996) proposed a simple equation to model non-Newtonian behavior of polymer-modified asphalt binders which is a simplified version of the CROSS model.

The CROSS model describes a flow curve of shear-thinning liquid in the form of a four-parameter equation:

$$\frac{\eta - \eta_{\alpha}}{\eta_0 - \eta_{\alpha}} = \frac{1}{1 + (K\gamma)^m} \quad 4.1$$

After rewriting

$$\frac{\eta_0 - \eta}{\eta - \eta_{\alpha}} = (K\gamma)^m \quad 4.2$$

where η_0 = zero shear viscosity, η_{α} = viscosity at infinite or very high shear rate,

K = constant, material parameter, γ = shear rate and m = constant, material parameter.

The value of η_{α} is sometimes hard to measure for high-viscosity, liquid and in the case of high-viscosity liquid, it can be assumed that $\eta \gg \eta_{\alpha}$. Therefore, the following simplified equation has been proposed.

$$\frac{\eta_0 - \eta}{\eta} = (K\gamma)^m \quad 4.3$$

At high service temperatures, such as $64 \text{ }^{\circ}\text{C}$ for PG 64-22 and $76 \text{ }^{\circ}\text{C}$ for PG 76-22M, the asphalt binder is a high-viscous liquid. Therefore, the viscosity of PG 64-22 and PG 76-22M with and without Sasobit[®] at $64 \text{ }^{\circ}\text{C}$ and $76 \text{ }^{\circ}\text{C}$, respectively were fitted with the simplified CROSS model as proposed by Sybiliski (1996). Table 4-2 shows the coefficient of determination, R^2 values for simplified CROSS model fit. It can be seen

that both the binders with and without Sasobit[®] fit the model very well with the coefficient of determination varying between 0.86 and 0.94 for PG 64-22 and between 0.88 and 0.97 for PG 76-22M.

The material parameter, K which is related to viscosity and called consistency by Sybilski (1996), increased with increased viscosity. It can be seen from Table 4-2 that K values increase as the percent of Sasobit[®] increased. The other material parameter, m is a shear compliance factor. The higher the m value, the lower is the shear compliance. Table 4-2 shows no general trend of increasing or decreasing m values.

4.5.3 Zero Shear Viscosity

Anderson et al. (2002) and Sybilski (1996) correlated zero shear viscosity with rutting of asphalt pavement. Table 4-2 shows the zero shear viscosity of asphalt binders with and without Sasobit[®]. Here, it can be seen that the zero shear viscosity of both the asphalt binders increases as percent of Sasobit[®] increases. The zero shear viscosities were determined at 64 °C for PG 64-22 and at 76 °C for PG 76-22M.

Table 4-2. Zero shear viscosity and CROSS model parameters

| Binder | Temp. | Zero shear Viscosity, Pa s | K | m | CROSS Model Fit, R² |
|------------------------------------|--------------|-----------------------------------|----------|----------|---------------------------------------|
| PG 64-22 | 64 °C | 278.1 | 0.02 | 0.83 | 0.94 |
| PG 64-22 + 1% Sasobit [®] | | 1116 | 0.45 | 0.80 | 0.93 |
| PG 64-22 + 2% Sasobit [®] | | 2770 | 1.45 | 0.88 | 0.91 |
| PG 64-22 + 4% Sasobit [®] | | 6374 | 5.47 | 0.89 | 0.86 |

Table 4-2 continued...

| | | | | | |
|--|-------|-------|------|------|------|
| PG 76-22M | 76 °C | 742.3 | 0.40 | 0.83 | 0.93 |
| PG 76-22M + 1% Sasobit [®] | | 1070 | 0.45 | 0.80 | 0.97 |
| PG 76-22M + 2% Sasobit [®] | | 1576 | 0.60 | 0.93 | 0.88 |
| PG 74-22M + 4% Sasobit [®] | | 2668 | 2.76 | 0.84 | 0.93 |

As discussed earlier, $G^*/\sin\delta$ is known to be the rutting factor for asphalt binders. Table 4-3 shows that $G^*/\sin\delta$ of PG 64-22 with and without Sasobit[®] at 64 °C and 34 °C. In case of PG 76-22M with and without Sasobit[®], the $G^*/\sin\delta$ were reported at 76 °C and 34 °C. For asphalt binders PG 64-22 with and without Sasobit[®], the R^2 values between zero shear viscosity and $G^*/\sin\delta$ at 64 °C and between zero shear viscosity and $G^*/\sin\delta$ at 34 °C were 0.63 and 0.53, respectively. In case of PG 76-22M with and without Sasobit[®], the R^2 values between zero shear viscosity and $G^*/\sin\delta$ at 76 °C and between zero shear viscosity and $G^*/\sin\delta$ at 34 °C were 0.26 and 0.58, respectively. The correlation is, therefore, better in case of PG 64-22 binders. For both the binders, the correlation was better for $G^*/\sin\delta$ at 34 °C.

Table 4-3. Correlation between zero shear viscosity and $G^*/\sin\delta$

| Binder | Zero shear viscosity At 64 °C, Pa s | $G^*/\sin\delta$ at 64 °C | $G^*/\sin\delta$ at 34 °C | R^2 (Zero shear viscosity vs. $G^*/\sin\delta$ at 64 °C) | R^2 (Zero shear Viscosity vs. $G^*/\sin\delta$ at 34 °C) |
|-------------------------------------|--|---|---|---|---|
| PG 64-22 | 278.1 | 3.12 | 234.55 | 0.63 | 0.53 |
| PG 64-22 + 1% Sasobit [®] | 1116 | 3.95 | 264.25 | | |
| PG 64-22 + 2% Sasobit [®] | 2770 | 6.88 | 547.75 | | |
| PG 64-22 + 4% Sasobit [®] | 6374 | 6.52 | 480.65 | | |
| | Zero shear viscosity At 76 °C, Pa s | $G^*/\sin\delta$ at 76 °C | $G^*/\sin\delta$ at 34 °C | R^2 (Zero shear viscosity vs. $G^*/\sin\delta$ at 76 °C) | R^2 (Zero shear Viscosity vs. $G^*/\sin\delta$ at 34 °C) |
| PG 76-22M | 742.3 | 2.45 | 245.9 | 0.26 | 0.58 |
| PG 76-22M + 1% Sasobit [®] | 1070 | 3.07 | 332.45 | | |
| PG 76-22M + 2% Sasobit [®] | 1576 | 3.54 | 495.95 | | |
| PG 74-22M + 4% Sasobit [®] | 2668 | 3.13 | 457.15 | | |

4.5.4 Steady State Viscosity and Dynamic Viscosity

Table 4-4 shows a comparison between steady state viscosity measured in rotational mode and dynamic viscosity measured in sinusoidal mode, using parallel plate DSR. It can be seen that at all temperatures, dynamic viscosity was higher than steady state viscosity. It can be assumed here that complex viscosity will even be greater than steady state viscosity.

Table 4-4 also shows that at higher temperature such as, 124 °C, the steady state and dynamic viscosity were comparable, e.g., for PG 64-22 without Sasobit[®] at 64 °C, the steady state and dynamic viscosity are 34.95 Pa s and 309.3 Pa s, respectively; whereas, at 124 °C, the corresponding viscosity were 0.95 Pa s and 1.69 Pa s.

The coefficient of determination between steady state and dynamic viscosity has been determined and shown in Table 4-4. It was evident that for PG 76-22M, the correlation was in general better than PG 64-22. Another observation is that at 100 °C, both the binders show lowest coefficient of determination because at 100 °C and nearby temperatures, there exists a critical temperature as discussed in previous chapter. Overall, based on the comparison between steady state and dynamic viscosity it can be concluded that the viscosity from the two methods are better comparable at higher temperature, such as 124 °C. Because of the critical temperature at around 100 °C, the coefficient of determination values are below 0.95, except in one case.

Table 4-4. Steady state (rotational) viscosity and dynamic (sinusoidal) viscosity

| Binder | Temperature 64 °C | | Temperature 100 °C | | Temperature 124 °C | |
|-------------------------|--------------------------------|---------------------------|--------------------------------|---------------------------|--------------------------------|------------------------------|
| | Steady state Viscosity Pa s | Dynamic Viscosity Pa s | Steady state Viscosity Pa s | Dynamic Viscosity Pa s | Steady state Viscosity Pa s | Dynamic Viscosity Pa s |
| PG 64-22 | 34.95 | 309.3 | 3.32 | 7.98 | 0.95 | 1.69 |
| PG 64-22 + 1% Sasobit® | 14.3 | 387.95 | 5.53 | 7.76 | 1.29 | 1.5 |
| PG 64-22 + 2% Sasobit® | 8.34 | 657.2 | 4.81 | 10.74 | 1.27 | 1.33 |
| PG 64-22 + 4% Sasobit® | 10.39 | 625.4 | 2.47 | 10.33 | 0.68 | 0.96 |
| R ² Value | 0.71 | | 0.08 | | 0.28 | |
| | Temperature 76 °C | | Temperature 100 °C | | Temperature 124 °C | |
| PG 76-22M | 3.05 | 216.05 | 7.78 | 30.94 | 4.02 | 6.04 |
| PG 76-22M + 1% Sasobit® | 16.02 | 263 | 10.51 | 30.29 | 3.33 | 5.17 |
| PG 76-22M + 2% Sasobit® | 21.63 | 302.4 | 6.66 | 32.47 | 2.73 | 4.91 |
| PG 76-22M + 4% Sasobit® | 4.42 | 270.95 | 7.22 | 30.82 | 2.33 | 4.08 |
| R ² Value | 0.59 | | 0.57 | | 0.95 | |

4.6 Conclusions

The following specific conclusions can be obtained from the investigation of shear rate dependency of viscosity of Sasobit[®] modified asphalt binders.

1. PG 64-22 is a Newtonian fluid at 124 °C and 100 °C. At 64 °C it is Newtonian at low to medium shear rates. Polymer modified binders such as PG 76-22M used in this study, exhibited shear-thinning behavior even at asphalt compaction temperature, 124 °C, where shear rate dependency and viscosity is of practical interests. Similar trends were observed at 100 °C and at 76 °C except that the shear rate dependency increased with reduced temperatures.
2. With the addition of Sasobit[®], PG 64-22 at 64 °C becomes a shear-thinning liquid from Newtonian liquid. The shear rate dependency increased with an increase in the percent of Sasobit[®]. Similar effects of Sasobit[®] were observed at 100 °C in reduced level and shear rate dependency with the addition of Sasobit[®] is almost negligible at 124 °C. The shear rate dependency in general reduces as temperature increases. Also, the rate of change of viscosity is higher at higher shear rates and lower at lower shear rates. For PG 76-22M, the shear rate dependency increased with an increase in percent of Sasobit[®] at all the three temperatures, 76 °C, 100 °C and 124 °C. This indicates if the actual shear rate during the compaction process is higher than 6.8 s^{-1} , then the currently recommended viscosity as well as temperature is overestimated and compaction temperature can be reduced. On the other hand, if the

actual shear rate during the compaction process is lower than 6.8 s^{-1} , then the currently recommended viscosity as well as temperature is underestimated and a higher compaction temperature should be used.

3. The coefficient of determination, R^2 values for simplified CROSS model fit showed that both the binders with and without Sasobit[®] fit the model very well with coefficient of determination varying between 0.86 and 0.94 for PG 64-22 and between 0.88 and 0.97 for PG 76-22M.
4. The zero shear viscosity were determined at $64 \text{ }^\circ\text{C}$ for PG 64-22 and at $76 \text{ }^\circ\text{C}$ for PG 76-22M. The correlation between zero shear viscosity and $G^*/\sin\delta$ was better in case of PG 64-22 binders. For both the binders, the correlation was better between zero shear viscosity and $G^*/\sin\delta$ at $34 \text{ }^\circ\text{C}$.
5. At all the temperatures used in this study, dynamic viscosities were higher than steady state viscosity. Overall, on the comparison between steady state and dynamic viscosity, it can be concluded that the viscosity from the two methods were better comparable at higher temperature, such as $124 \text{ }^\circ\text{C}$ and the coefficient of determination values were below 0.95 except in one case.

CHAPTER 5

LABORATORY EVALUATION OF RUTTING PERFORMANCE OF SASOBIT[®] MODIFIED WARM MIX ASPHALT

5.1 Introduction

Based on the comprehensive literature study on the rutting of WMA, it was found that one of the biggest concerns regarding WMA performance is that it may be rutting susceptible. The cause behind the concerns is that asphalt binder may not age (hardening due to oxidation at higher temperature) at warm temperatures and therefore, may remain softer than hot mix asphalt and cause rutting. Consequently, this study has been conducted to understand the rutting susceptibility of Sasobit[®] modified WMA.

5.2 Objectives

The overall objective of this study was to evaluate rutting performance of Sasobit[®] modified WMA. The specific objectives are as follows:

1. Develop dynamic modulus master curves and evaluate overall rheological behavior of Sasobit[®] modified asphalt binders,
2. Evaluate asphalt binder's rutting factors with and without Sasobit[®] modifications from temperature sweep tests and MSCR tests,

3. Develop a multiple variable regression model of rutting and evaluate rutting performance of Sasobit[®] modified WMA, and
4. Evaluation of aging of extracted asphalt binders from mixes prepared at hot and warm mix temperatures.

5.3 Materials and Test Matrix

A neat asphalt binder, PG 64-22 and a polymer modified asphalt binder, PG 76-22M were obtained from Lion Oil, Inc. and Ergon Refining, Inc., respectively. Sasobit[®] and asphalt mix used for this study have same properties and sources as in Chapter 3.

Table 5-1 shows the test matrix for dynamic modulus master curve. A total of 24 samples with and without Sasobit[®] were tested each at 10 °C, 25 °C, 46 °C, 70 °C and 94 °C at the frequency range from 0.1 to 100 rad/sec.

Table 5-1. Test matrix for dynamic modulus master curve

| Asphalt Binders | % Sasobit [®] | No. of Samples | Temperature | Frequency Range |
|---------------------------------|------------------------|----------------|--------------------------------------|-----------------|
| PG 64-22 | 0 | 3 | 10 °C, 25 °C, 46 °C, 70 °C and 94 °C | 0.1-100 rad/sec |
| | 1 | 3 | | |
| | 2 | 3 | | |
| | 4 | 3 | | |
| No. of PG 64-22 samples Tested | 12 | | | |
| PG 76-22M | 0 | 3 | 10 °C, 25 °C, 46 °C, 70 °C and 94 °C | 0.1-100 rad/sec |
| | 1 | 3 | | |
| | 2 | 3 | | |
| | 4 | 3 | | |
| No. of PG 76-22M samples Tested | 12 | | | |
| Total No. of samples Tested | 24 | | | |

Table 5-2 shows the test matrix for rutting factor, $G^*/\sin\delta$. For PG 64-22, tests were performed at 64 °C and 70 °C and for PG 76-22M, 70 °C, 76 °C and 82 °C were used.

Table 5-2. Test matrix for rutting Parameter $G^*/\sin\delta$

| Asphalt binders | % Sasobit® | No. of Sample | Temperature | Rutting factor |
|---------------------------------|------------|---------------|-------------|---|
| PG 64-22 | 0 | 3 | 64 °C | $G^*/\sin\delta$ (at 10 rad/sec and 12% strain) |
| | 1 | 3 | | |
| | 2 | 3 | 70 °C | |
| | 4 | 3 | | |
| No. of PG 64-22 samples Tested | 12 | | | |
| PG 76-22M | 0 | 3 | 70 °C | $G^*/\sin\delta$ (at 10 rad/sec and 12% strain) |
| | 1 | 3 | 76 °C | |
| | 2 | 3 | 82 °C | |
| | 4 | 3 | | |
| No. of PG 76-22M samples Tested | 12 | | | |
| Total No. of samples Tested | 24 | | | |

Table 5-3 shows the test matrix for rutting parameter percent recovery and J_{nr} . MSCR tests were performed according to AASHTO TP70 at 64 °C, 70 °C and 1 kPa stiffness temperatures for PG 64-22 and at 70 °C, 76 °C and 1 kPa stiffness temperatures for PG 76-22M. The 1 kPa stiffness temperatures were determined from the temperature sweep tests performed according to Table 5-2.

Table 5-3. Test matrix for MSCR test

| Asphalt binder | % Sasobit® | No. of Sample | Temperature | Creep stress | Rutting factor |
|-----------------------------------|-------------------|----------------------|---|--|--|
| PG 64-22 | 0 | 3 | 64 °C, 66 °C (1 kPa Stiffness Temperature), 70 °C | 0.1 kPa and 3.2 kPa (at 1 kPa Stiffness Temperature, Creep Test was Performed at 0.1 kPa, 0.2 kPa, 0.5 kPa and 3.2 kPa Stresses) | % Recovery, Non-Recoverable Creep Compliance |
| | 1 | 3 | 64 °C, 68 °C (1 kPa Stiffness Temperature), 70 °C | | |
| | 2 | 3 | 64 °C, 70 °C, 73 °C (1 kPa Stiffness Temperature) | | |
| | 4 | 3 | 64 °C, 70 °C, 78 °C (1 kPa Stiffness Temperature) | | |
| No. of PG 64-22 Samples Tested is | 12 | | | | |

Table 5-3 continued...

| | | | | | |
|-----------------------------------|----|---|---|--|---|
| PG 76-22 | 0 | 3 | 70 °C, 76 °C, 76.8 °C (1 kPa Stiffness Temperature), 82 °C | 0.1 kPa and 3.2 kPa (at 1 kPa stiffness Temperature, Creep test was Performed at 0.1 kPa, 0.2 kPa, 0.5 kPa and 3.2 kPa stresses) | % Recovery, non- Recoverable creep Compliance |
| | 1 | 3 | 70 °C, 76 °C, 78.7 °C (1 kPa Stiffness Temperature), 82 °C | | |
| | 2 | 3 | 70 °C, 76 °C, 81.2 °C (1 kPa Stiffness Temperature), 82 °C | | |
| | 4 | 3 | 70 °C, 76 °C, 82 °C (1 kPa Stiffness Temperature) | | |
| No. of PG 76-22 samples Tested | 12 | | | | |
| Total No. of samples Tested | 24 | | | | |

In Table 5-4, it can be seen that 10 sets each having six asphalt mix samples were tested for rutting performances. Percent air voids, percent asphalt contents, percent Sasobit[®], mixing temperatures and compaction temperatures were varied for rutting evaluation of Sasobit[®] modified WMA. For evaluation of aging, extraction and recovery were performed using a centrifuge and a rotary evaporator according to ASTM D 5404 followed by ASTM D 2172 (Test Method A).

Table 5-4. Test matrix for rutting performance

| No. of Mix Set | No. of Samples | % Air Voids | % Asphalt Content | % Sasobit [®] | Mixing Temperature | Compaction Temperature |
|---|----------------|-------------|-------------------|------------------------|--------------------|------------------------|
| Set 1 | 6 | 7.33 | 4.8 | 0 | 163 °C | 150 °C |
| Set 2 | 6 | 7.53 | 4.8 | 2 | 163 °C | 150 °C |
| Set 3 | 6 | 10.41 | 4.8 | 0 | 163 °C | 150 °C |
| Set 4 | 6 | 9.97 | 4.8 | 2 | 163 °C | 150 °C |
| Set 5 | 6 | 7.67 | 5.3 | 0 | 163 °C | 150 °C |
| Set 6 | 6 | 7.97 | 5.3 | 2 | 163 °C | 150 °C |
| Set 7 | 6 | 7.16 | 4.8 | 0 | 143 °C | 110 °C |
| Set 8 | 6 | 7.49 | 4.8 | 2 | 143 °C | 110 °C |
| Set 9 | 6 | 7.74 | 4.8 | 2 | 133 °C | 110 °C |
| Set 10 | 6 | 7.47 | 4.8 | 0 | 133 °C | 110 °C |
| Total no. of mix samples tested for rutting is 60 (10 Sets X 6 samples in each set) | | | | | | |

5.4 Rheological Evaluation of Sasobit[®] Modified Asphalt Binders with Dynamic Modulus Master Curves

Dynamic modulus master curves reflect overall rheological behavior of the asphalt binders. In this study, four master curves were constructed for PG 64-22 with 0%, 1%, 2% and 4% Sasobit[®] and four master curves were plotted for PG 76-22M with 0%, 1%, 2% and 4% Sasobit[®]. For each of the eight master curves, three asphalt binder samples were tested. Figures 5-1 to 5-4 describes how one master curve was constructed from three replicates; for example, in the case of PG 64-22 with 1% Sasobit[®]. At first, frequency sweep results from three individual samples were plotted in Figure 5-1. The average dynamic modulus from these three replicates was calculated and plotted in Figure 5-2. Time-temperature shift factor, $a_T (=t_T/t_{T0})$ using time-temperature superposition principle was determined and was plotted against temperature in Figure 5-3. Figure 5-4 shows how a master curve was obtained from polynomial fitting of frequency sweep data. The reference temperature for all the master curves was 25 °C.

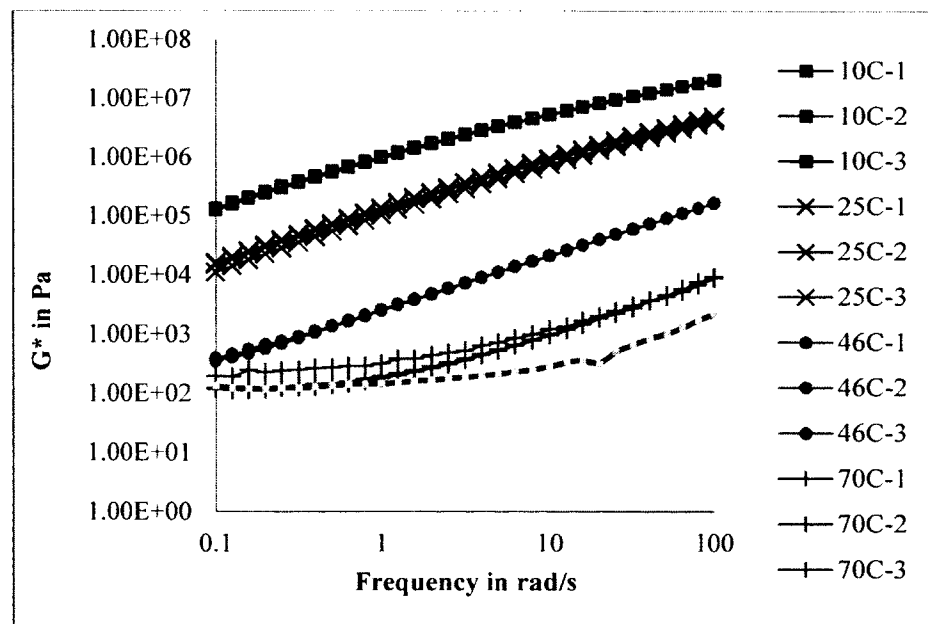


Figure 5-1. Dynamic modulus values of three replicates of PG 64-22 with 0% Sasobit[®]

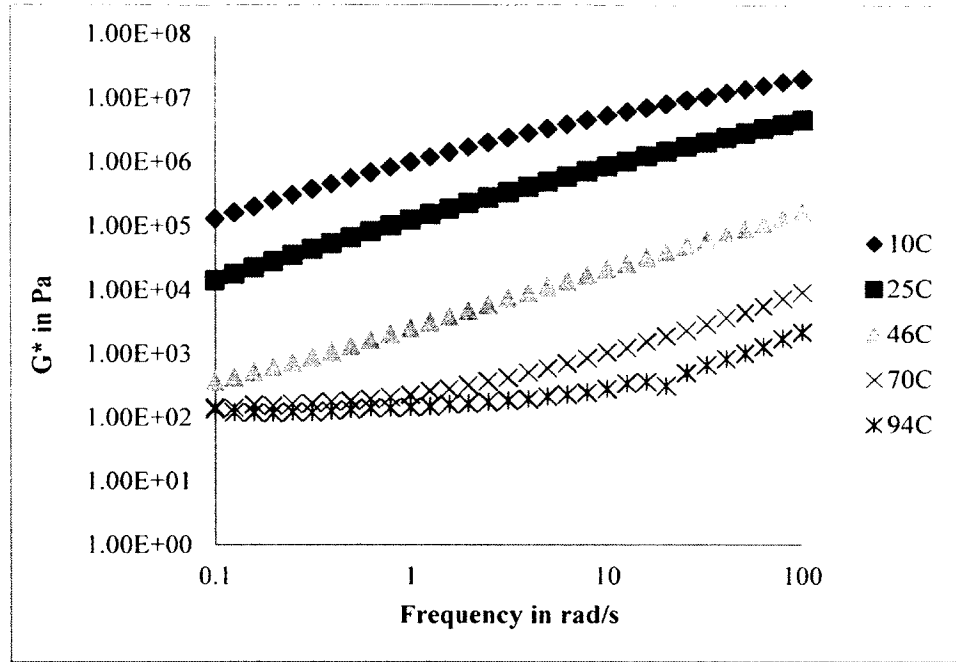


Figure 5-2. Average dynamic modulus values of three replicates of PG 64-22 with 0% Sasobit®

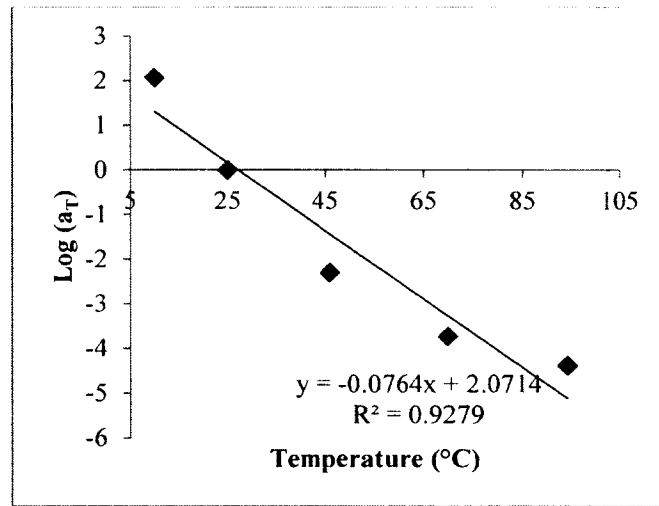


Figure 5-3. Relationship between time-temperature shift factor and temperature for PG 64-22 with 0% Sasobit®

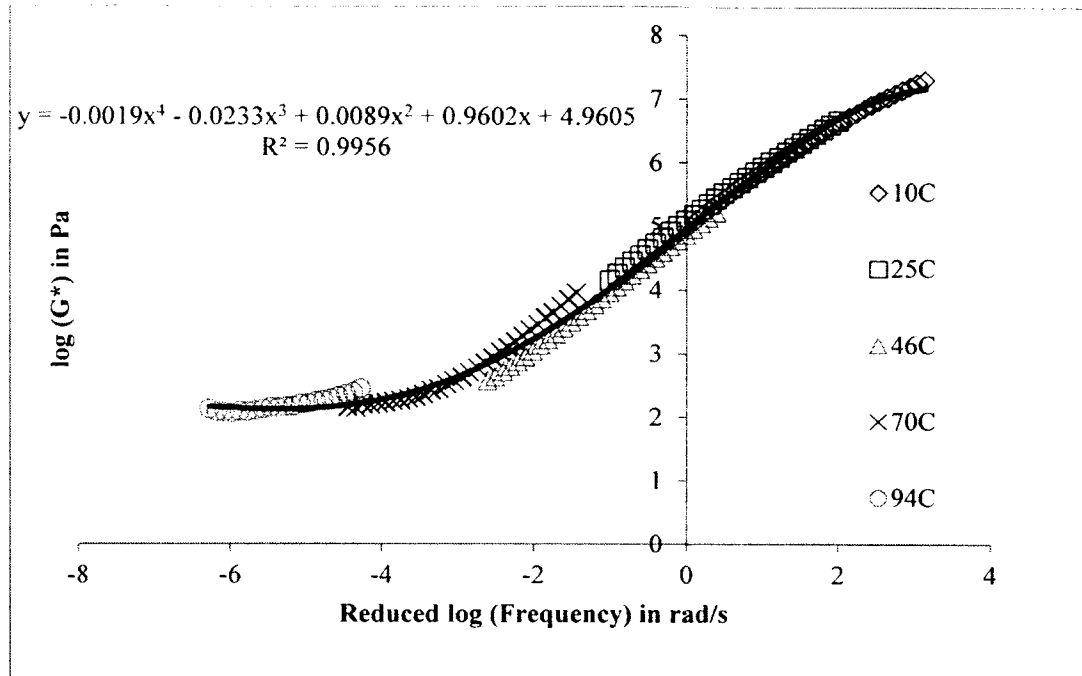


Figure 5-4. Dynamic modulus master curve for PG 64-22 with 0% Sasobit®

Figure 5-5 shows the four master curves of PG 64-22 with 0%, 1%, 2% and 4% Sasobit®. It can be observed that at lower frequency (higher temperature), Sasobit® increased dynamic modulus or stiffness of asphalt binder. The rate of increase in dynamic modulus depends on the increase in percent of Sasobit®. However, at higher frequency (lower temperature) all asphalt binders with and without Sasobit® tend to move towards a unique stiffness value. It is known that all asphalt binder exhibits about 1 GPa of stiffness at glass transition temperature.

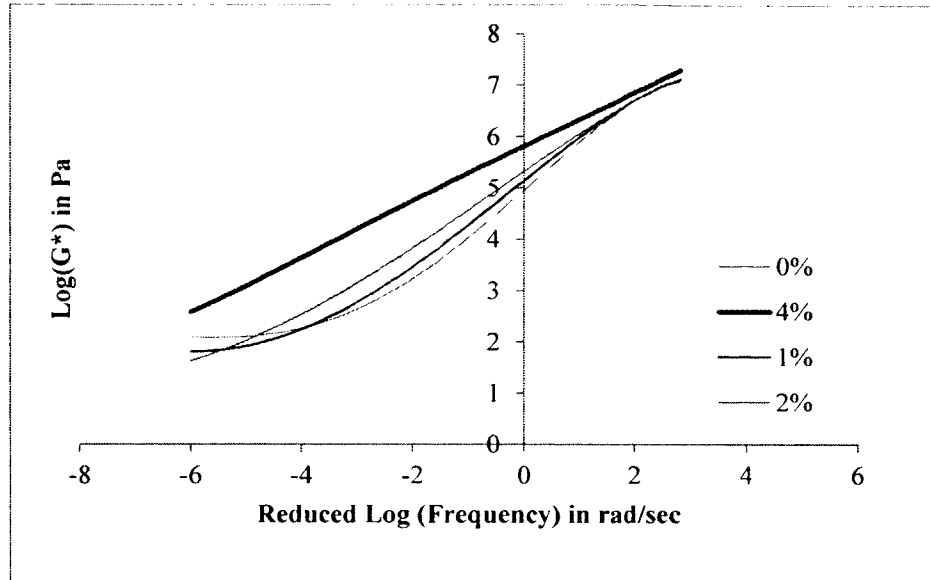


Figure 5-5. Dynamic modulus master curves of PG 64-22 with and without Sasobit[®]

Similarly, four master curves of PG 76-22M with 0%, 1%, 2% and 4% Sasobit were plotted in Figure 5-6. The overall rheological behavior of Sasobit[®] modified PG 76-22M was similar to PG 64-22 except that PG 76-22M had higher stiffness due to polymer modifications as can be seen in Figure 5-7.

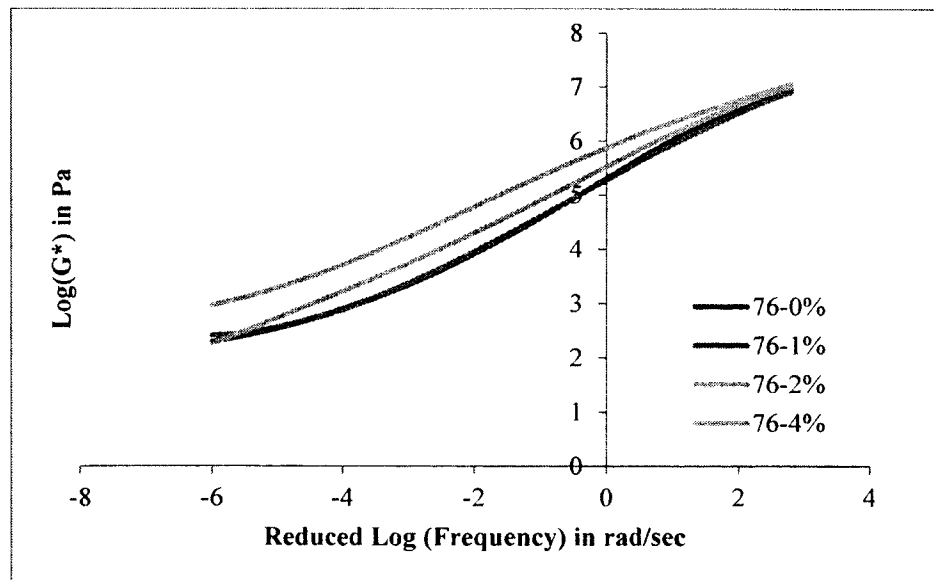


Figure 5-6. Dynamic modulus master curves of PG 76-22M with and without Sasobit[®]

Based on overall rheological behavior in Figure 5-7, it can be concluded that Sasobit[®] increased stiffness of asphalt binders and may have potential for reduced rutting of asphalt mixes. In next two sections, rutting factors of Sasobit[®] modified asphalt binders will be determined to evaluate more on rutting potential.

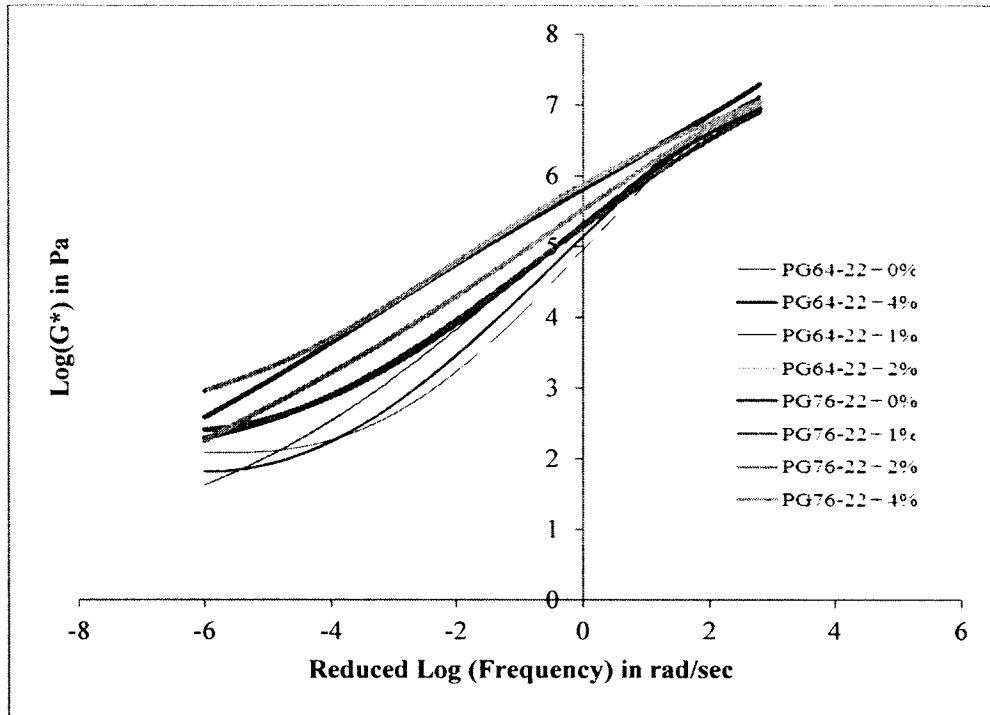


Figure 5-7. Dynamic modulus master curves of PG 64-22 and PG 76-22M with and without Sasobit[®]

5.5 Evaluation of Sasobit[®] Modified Asphalt Binder's Rutting Factor $G^*/\sin\delta$ from Temperature Sweep Test

Table 5-5 shows the average values of $G^*/\sin\delta$, G^* and phase angle of PG 64-22 with and without different percentages of Sasobit[®]. Two temperatures, 64 °C and 70 °C, were used for this purpose. Superpave uses $G^*/\sin\delta$ as the rutting potential of an asphalt binder. It can be observed in Table 5-5 that rutting factor $G^*/\sin\delta$ at 64 °C increased with an increase in percent of Sasobit[®]. At 64 °C, $G^*/\sin\delta$ values were 2.5, 4.1, 7.4 and 12.2

kPa, respectively for 0%, 1%, 2% and 4% Sasobit[®]. This finding indicates that Sasobit[®] has a rutting resistance potential if prepared at hot mix temperatures. A similar trend is observed at 70 °C.

Table 5-5. Average values of $G^*/\sin\delta$, G^* and phase angle of PG 64-22 with and without Sasobit[®]

| PG 64-22 at 64 °C | | | | | | |
|------------------------------|--------------------------------|-------------------------|------------|-------------------|------------------------|------------------------------|
| Percent Sasobit [®] | Phase Angle, δ (degree) | St. dev. of Phase Angle | G^* (Pa) | St. dev. of G^* | $G^*/\sin\delta$ kPa | St. dev. of $G^*/\sin\delta$ |
| 0% | 85.7 | 0.1 | 2491.7 | 82.6 | 2.5 | 0.1 |
| 1% | 82.1 | 0.2 | 4032.0 | 334.0 | 4.1 | 0.3 |
| 2% | 79.7 | 0.4 | 7308.0 | 319.8 | 7.4 | 0.3 |
| 4% | 76.6 | 1.1 | 11866.7 | 1099.7 | 12.2 | 1.2 |
| PG 64-22 at 70 °C | | | | | | |
| Percent Sasobit [®] | Phase Angle, δ (degree) | St. dev. of Phase Angle | G^* (Pa) | St. dev. of G^* | $G^*/\sin\delta$ (kPa) | St. dev. of $G^*/\sin\delta$ |
| 0% | 87.0 | 0.0 | 1168.7 | 9.8 | 1.2 | 0.01 |
| 1% | 85.3 | 0.2 | 1616.0 | 123.0 | 1.6 | 0.1 |
| 2% | 82.9 | 0.2 | 2847.3 | 114.0 | 2.9 | 0.1 |
| 4% | 80.7 | 0.6 | 4005.3 | 274.6 | 4.1 | 0.3 |

Table 5-5 also shows that phase angle, δ decreased with an increase in percent of Sasobit[®]. At 64 °C, the phase angle values were 85.7, 82.1, 79.7 and 76.6 degrees respectively for 0%, 1%, 2% and 4% Sasobit[®]. Reduced phase angle is often referred to as “increased elastic recovery” or “rutting resistance.” Therefore, both $G^*/\sin\delta$ and phase angle indicated increased rutting resistance for Sasobit[®] modified asphalt binder. At 70 °C, a similar reduction trend in phase angle was observed. In Table 5-5, with respect to

standard deviation, it can be noted that both $G^*/\sin\delta$ and phase angle values were repeatable.

Table 5-6 shows the average values of $G^*/\sin\delta$, G^* and phase angle of PG 76-22M with and without different percentages of Sasobit[®]. In this case, three temperatures 70 °C, 76 °C, and 82 °C were used to evaluate rutting factor. It can be observed that in all three temperatures, $G^*/\sin\delta$ increased with an increase in percent of Sasobit[®].

Table 5-6. Average values of $G^*/\sin\delta$, G^* and phase angle of PG 76-22M

| PG 76-22M at 70 °C | | | | | | |
|------------------------------|--------------------------------|-------------------------|------------|-------------------|----------------------|------------------------------|
| Percent Sasobit [®] | Phase Angle, δ (degree) | St. dev. of Phase Angle | G^* (Pa) | St. dev. of G^* | $G^*/\sin\delta$ kPa | St. dev. of $G^*/\sin\delta$ |
| 0% | 65.3 | 0.1 | 3717.0 | 131.4 | 4.1 | 0.1 |
| 1% | 63.3 | 0.4 | 4301.7 | 63.1 | 4.8 | 0.1 |
| 2% | 58.7 | 0.2 | 5111.7 | 130.2 | 6.0 | 0.2 |
| 4% | 58.1 | 0.7 | 9200.7 | 321.9 | 10.8 | 0.4 |
| PG 76-22M at 76 °C | | | | | | |
| Percent Sasobit [®] | Phase Angle, δ (degree) | St. dev. of Phase Angle | G^* (Pa) | St. dev. of G^* | $G^*/\sin\delta$ kPa | St. dev. of $G^*/\sin\delta$ |
| 0% | 68.1 | 0.1 | 2164.0 | 105.4 | 2.3 | 0.1 |
| 1% | 65.8 | 0.2 | 2469.0 | 42.6 | 2.7 | 0.04 |
| 2% | 59.6 | 0.3 | 2941.3 | 66.7 | 3.4 | 0.1 |
| 4% | 60.0 | 0.8 | 4517.3 | 147.5 | 5.2 | 0.2 |

Table 5-6 continued...

| PG 76-22M at 82 °C | | | | | | |
|------------------------------|--------------------------------|-------------------------|------------|-------------------|------------------------|------------------------------|
| Percent Sasobit [®] | Phase Angle, δ (degree) | St. dev. of Phase Angle | G^* (Pa) | St. dev. of G^* | $G^*/\sin\delta$ (kPa) | St. dev. of $G^*/\sin\delta$ |
| 0% | 71.4 | 0.2 | 1257.7 | 46.1 | 1.3 | 0.05 |
| 1% | 68.7 | 0.2 | 1460.0 | 41.6 | 1.6 | 0.04 |
| 2% | 60.4 | 0.3 | 1763.0 | 33.2 | 2.0 | 0.04 |
| 4% | 62.2 | 1.0 | 2605.3 | 106.2 | 2.9 | 0.1 |

PG 76-22M is polymer modified and a different behavior is observed in case of phase angle at higher temperatures. At 70 °C and 76 °C, Sasobit[®] reduced the phase angle as was observed for PG 64-22. However, for PG 76-22M at 82 °C, 1% and 2%, Sasobit[®] reduced the phase angle and 4% Sasobit[®] increased the phase angle. Therefore, there is an optimum percent of Sasobit[®] that must be used for better or reduced phase angle. A percent of Sasobit[®] more than that optimum will increase the phase angle and reduce rutting resistance. Based on phase angle evaluation of PG 76-22M, it can be observed that an optimum Sasobit[®] percent lies between 2% and 4%. However, increase in the percent of Sasobit[®] from 2% to 4% still increased the G^* value from 1.76 kPa to 2.61 kPa and $G^*/\sin\delta$ from 2.0 to 2.9 kPa.

5.6 Evaluation of Percent Recovery and J_{nr} as Rutting Factors Using MSCR Test for Sasobit[®] Modified Asphalt Binders

Percent recovery after creep stress in MSCR test is an indicator of recoverable deformation in asphalt pavements. Table 5-7 shows the average percent recovery of PG 64-22 with and without Sasobit[®] after 0.1 kPa and 3.2 kPa creep stresses. It can be observed that the addition of Sasobit[®] increased the percent recovery significantly. The

percent recovery of PG 64-22 without Sasobit[®] was 1.8 at 0.1 kPa creep stress. The percent recovery increased to 15.0, 26.5 and 34.9 for 1%, 2% and 4% Sasobit[®], respectively. For 3.2 kPa creep stress, similar trend can be observed. Table 5-7 shows the standard deviation values for average percent recovery of three samples. Better repeatability with respect to standard deviation can be noticed in case of percent recovery of 3.2 kPa creep stress than that of 0.1 kPa creep stress. The MSCR test was also performed at 70 °C and a similar trend with respect to increase in percent recovery was observed.

Table 5-7. Average percent recovery of PG 64-22 with and without Sasobit[®]

| PG 64-22 | | | | | |
|------------------------------|------------------|-----------------------|---------|--------------------|---------|
| Percent Sasobit [®] | Temperature (°C) | Avg. percent recovery | | Standard deviation | |
| | | Creep stress | | Creep stress | |
| | | 0.1 kPa | 3.2 kPa | 0.1 kPa | 3.2 kPa |
| 0% | 64 | 1.8 | 0.4 | 0.49 | 0.01 |
| | 70 | 0.4 | -0.5 | 0.58 | 0.01 |
| 1% | 64 | 15.0 | 2.6 | 1.52 | 0.18 |
| | 70 | 3.5 | -0.1 | 1.54 | 0.12 |
| 2% | 64 | 26.5 | 5.1 | 3.51 | 0.35 |
| | 70 | 10.5 | 1.0 | 0.94 | 0.09 |
| 4% | 64 | 34.9 | 11.7 | 18.1 | 1.9 |
| | 70 | 29.2 | 2.4 | 2.42 | 0.31 |

It is believed that, J_{nr} is an indicator of permanent deformation in asphalt pavement and can be used as rutting factor. Several DOTs, such as LA DOTD, have ongoing projects for implementation of J_{nr} in state specifications. Table 5-8 shows the effects of Sasobit[®] on average J_{nr} of PG 64-22. J_{nr} measures the non-recoverable creep

compliance; therefore, the lower the J_{nr} , the better it is. Some specifications including AASHTO MP19 consider J_{nr} only at 3.2 kPa stress. At 64 °C, the average J_{nr} of PG 64-22 without Sasobit[®] at 3.2 kPa creep stress is 0.4 kPa and addition of 1% and 2% Sasobit[®] reduced the J_{nr} to 0.3 kPa and 0.1 kPa, respectively. Note that addition of 4% Sasobit[®] increased the J_{nr} to 1.4 kPa from 0.4 kPa instead of reducing it as with lower percentages of Sasobit[®]. This result indicates that an overdose of Sasobit[®] can have negative impact on rutting of asphalt pavements.

Table 5-8. Average J_{nr} of PG 64-22 with and without Sasobit[®]

| PG 64-22 | | | | | |
|------------------------------|------------------|---|---------|--------------------|---------|
| Percent Sasobit [®] | Temperature (°C) | Avg. non-recoverable creep Compliance, J_{nr} (1/kPa) | | Standard deviation | |
| | | Creep stress | | Creep stress | |
| | | 0.1 kPa | 3.2 kPa | 0.1 kPa | 3.2 kPa |
| 0% | 64 | 0.4 | 0.4 | 0.01 | 0.01 |
| 0% | 70 | 0.8 | 0.9 | 0.01 | 0.01 |
| 1% | 64 | 0.1 | 0.3 | 0.10 | 0.03 |
| 1% | 70 | 0.6 | 0.7 | 0.04 | 0.05 |
| 2% | 64 | 0.002 | 0.1 | 0.0003 | 0.01 |
| 2% | 70 | 0.3 | 0.4 | 0.01 | 0.02 |
| 4% | 64 | 0.02 | 1.4 | 0.03 | 1.9 |
| 4% | 70 | 0.1 | 9.2 | 0.01 | 0.74 |

However, at 64 °C this 1.4 kPa J_{nr} at 3.2 kPa creep stress had a standard deviation of 1.9, and J_{nr} values at 70 °C may in need to be discussed. It can be observed that at 70 °C, the J_{nr} at 3.2 kPa stress is 0.9 kPa and addition of 1% and 2% Sasobit[®] reduced the J_{nr} to 0.7 kPa and 0.4 kPa, respectively, whereas, addition of 4% Sasobit[®] increases the J_{nr} from 0.9 kPa to 9.2 kPa. The standard deviation in this case of 9.2 kPa J_{nr} was 0.74. Therefore, it can be concluded from 3.2 kPa J_{nr} measurements of PG 64-22 that 1% and

2% Sasobit[®] reduced the rutting susceptibility while 4% Sasobit[®] increased the rutting susceptibility of asphalt pavements.

In the case of PG 76-22M, the MSCR test was performed at three temperatures, 70 °C, 76 °C and 82 °C. Table 5-9 shows the average percent recovery results of PG 76-22M with standard deviations. In case of PG 64-22, for both 64 °C and 70 °C and for both 0.1 kPa and 3.2 kPa creep stress, an increase in percent of Sasobit[®] caused an increase in average percent recovery. However, for polymer modified PG 76-22M such an increase in average percent recovery with an increase in percent of Sasobit[®] was observed for 3.2 kPa creep stress at 70 °C and 76 °C. This finding indicates that the positive effect of Sasobit[®] on rutting resistance of PG 76-22M was observed only at lower pavement service temperatures (70 °C and 76 °C and not at 82 °C). Analyses of 0.1 kPa creep stress data in Table 5-9 reveals that 1% and 2% Sasobit[®] increased the percent recovery of PG 76-22M and addition of 4% Sasobit[®] started reducing it.

Table 5-9. Average percent recovery of PG 76-22M with and without Sasobit®

| PG 76-22M | | | | | |
|------------------|------------------|-----------------------|---------|--------------------|---------|
| Percent Sasobit® | Temperature (°C) | Avg. percent recovery | | Standard deviation | |
| | | Creep stress | | Creep stress | |
| | | 0.1 kPa | 3.2 kPa | 0.1 kPa | 3.2 kPa |
| 0% | 70 | 42.6 | 25.0 | 1.5 | 1.2 |
| | 76 | 28.8 | 15.2 | 14.1 | 1.4 |
| | 82 | 28.1 | 6.2 | 1.5 | 0.4 |
| 1% | 70 | 72.9 | 42.2 | 2.2 | 1.1 |
| | 76 | 71.4 | 31.7 | 1.6 | 1.6 |
| | 82 | 58.5 | 23.2 | 3.0 | 6.5 |
| 2% | 70 | 87.1 | 64.1 | 6.7 | 2.7 |
| | 76 | 91.1 | 42.0 | 0.9 | 3.5 |
| | 82 | 79.1 | 13.9 | 2.2 | 2.1 |
| 4% | 70 | 87.0 | 67.3 | 0.4 | 2.0 |
| | 76 | 86.2 | 46.0 | 0.6 | 3.5 |
| | 82 | 74.3 | 22.4 | 3.2 | 3.2 |

For example, at 76 °C and 0.1 kPa creep stress, the average percent recovery of PG 76-22M is 28.8 and addition of 1% and 2% Sasobit® increase the percent recovery to 71.4 and 91.1, respectively, whereas, the percent recovery for 4% Sasobit® was 86.2. This finding indicates that an optimum amount of Sasobit® is needed for increasing rutting resistance of PG 76-22M.

Table 5-10 shows the average non-recoverable creep compliance, J_{nr} of PG 76-22M with and without different percentages of Sasobit® for 0.1 kPa and 3.2 kPa stress at 70 °C, 76 °C and 82 °C. AASHTO MP19 recommends the use of 3.2 kPa creep stress for analyses of J_{nr} values. A general trend observed in Table 5-10 is that an increase in percent of Sasobit® reduced J_{nr} , and thereby reducing rutting susceptibility.

Table 5-10. Average non-recoverable creep compliance (J_{nr}) of PG 76-22M

| PG76-22M | | | | | |
|------------------------------------|-------------------------|---|----------------|---------------------------|----------------|
| Percent Sasobit[®] | Temperature (°C) | Avg. non-recoverable creep Compliance, J_{nr} (1/kPa) | | Standard deviation | |
| | | Creep stress | | Creep stress | |
| | | 0.1 kPa | 3.2 kPa | 0.1 kPa | 3.2 kPa |
| 0% | 70 | 0.033 | 0.140 | 0.054 | 0.006 |
| | 76 | 0.007 | 0.314 | 0.001 | 0.019 |
| | 82 | 0.013 | 0.734 | 0.000 | 0.015 |
| 1% | 70 | 0.001 | 0.089 | 0.000 | 0.004 |
| | 76 | 0.002 | 0.222 | 0.000 | 0.005 |
| | 82 | 0.006 | 0.474 | 0.001 | 0.088 |
| 2% | 70 | 0.000 | 0.043 | 0.000 | 0.005 |
| | 76 | 0.000 | 0.147 | 0.000 | 0.016 |
| | 82 | 0.002 | 0.560 | 0.000 | 0.039 |
| 4% | 70 | 0.000 | 0.020 | 0.000 | 0.002 |
| | 76 | 0.000 | 0.078 | 0.000 | 0.009 |
| | 82 | 0.002 | 0.287 | 0.000 | 0.032 |

The conclusion from the above discussions is that at 64 °C for PG 64-22 and at 76 °C for PG 76-22M, addition of 1% and 2% Sasobit[®] increases the rutting resistance. Sasobit[®] is a synthetic wax and it reduces viscosity at hot mix production temperatures and increases stiffness ($G^*/\sin\delta$) at pavement service temperatures. To understand if the increase in rutting resistance is caused by the increase in stiffness or by the internal molecular associations, a different set of MSCR tests were performed. In this approach, equal-stiffness (1 kPa of $G^*/\sin\delta$) temperatures of 0%, 1%, 2% and 4% Sasobit[®] added asphalt binders were determined based on temperature sweep test performed earlier in this study. MSCR tests were performed on that equal-stiffness temperature.

The equal-stiffness ($G^*/\sin\delta$ value of 1 kPa) temperatures of PG 64-22 with 0%, 1%, 2% and 4% Sasobit[®] are 66 °C, 68 °C, 73 °C and 78 °C, respectively. Table 5-11 shows the percent recovery of PG 64-22 with and without Sasobit[®] at equal-stiffness temperature. It can be noted here that at high temperature and/or high creep stress (i.e., 3.2 kPa), some asphalt binders showed negative percent recovery values.

Table 5-11. Percent recovery of PG 64-22 at equal-stiffness temperature

| PG 64-22: Percent recovery at equal-stiffness ($G^*/\sin\delta$ Value of 1 kPa) temperature | | | | | | | | | |
|--|-----------------------------|------------------|---------|---------|---------|--------------------|---------|---------|---------|
| Percent Sasobit [®] | 1 kPa Stiffness Temperature | Percent recovery | | | | Standard deviation | | | |
| | | Creep stress | | | | Creep stress | | | |
| | | 0.1 kPa | 0.2 kPa | 0.5 kPa | 3.2 kPa | 0.1 kPa | 0.2 kPa | 0.5 kPa | 3.2 kPa |
| 0% | 66°C | 2.3 | 2.2 | 2.0 | 0.4 | 0.22 | 0.12 | 0.48 | 0.02 |
| 1% | 68°C | 11.7 | 10.0 | 6.8 | 0.4 | 0.69 | 0.58 | 0.44 | 0.02 |
| 2% | 73°C | 32.1 | 28.9 | 15.3 | 0.1 | 5.76 | 7.17 | 3.99 | 0.07 |
| 4% | 78°C | 43.7 | 32.9 | 14.1 | -1.2 | 8.50 | 7.71 | 3.89 | 0.18 |

Creep and recovery plots for these indicated that just after the 3.2 kPa creep stress was withdrawn, strain continued to grow for a while before it started recovering.

Therefore, these negative values are actual and not due to an experimental or calculation error. It can be observed from Table 5-11 that at lower creep stress such as 0.1 kPa, the addition of Sasobit[®] increased the percent recovery while at higher creep stress such as 3.2 kPa, addition of Sasobit[®] reduces the percent recovery. A similar trend is observed from J_{nr} values of Table 5-12 that at lower creep stress addition of Sasobit[®] reduces J_{nr} but at higher creep stress Sasobit[®] increases J_{nr} . This indicates at higher stress Sasobit[®] will make PG 64-22 rutting susceptible and at lower stress, it will make PG 64-22 rutting

resistant. Therefore, the true influence of Sasobit[®] on rutting of PG 64-22 is stress dependent.

Table 5-12. J_{nr} of PG 64-22 at equal-stiffness temperature

| PG 64-22: Non-recoverable creep compliance at equal-stiffness ($G^*/\sin\delta$ value of 1 kPa) temperature | | | | | | | | | |
|---|---|--|----------------|----------------|----------------|---------------------------|----------------|----------------|----------------|
| Percent Sasobit[®] | 1kPa Stiffness Temperature | Non-recoverable creep Compliance, J_{nr} (1/kPa) | | | | Standard deviation | | | |
| | | Creep stress | | | | Creep stress | | | |
| | | 0.1 kPa | 0.2 kPa | 0.5 kPa | 3.2 kPa | 0.1 kPa | 0.2 kPa | 0.5 kPa | 3.2 kPa |
| 0% | 66°C | 0.4 | 0.02 | 1.4 | 0.4 | 0.01 | 0.001 | 0.88 | 0.01 |
| 1% | 68°C | 0.3 | 0.02 | 1.7 | 0.5 | 0.01 | 0.000 | 0.03 | 0.00 |
| 2% | 73°C | 0.2 | 0.3 | 1.1 | 15.5 | 0.05 | 0.29 | 0.93 | 12.81 |
| 4% | 78°C | 0.2 | 0.5 | 2.2 | 50.8 | 0.08 | 0.19 | 0.57 | 4.03 |

Tables 5-13 and 5-14 show the percent recovery and non-recoverable creep compliance of PG 76-22M with and without Sasobit[®] at equal-stiffness temperature. With respect to percent recovery, at both lower creep stress and higher creep stress, Sasobit[®] increased the rutting resistance of PG 76-22M. With respect to non-recoverable creep compliance, at lower creep stress, Sasobit[®] increased the rutting resistance but at higher creep stress, no trend or effect of Sasobit[®] was observed.

Table 5-13. Percent recovery of PG 76-22M at equal-stiffness temperature

| PG 76-22M: Percent recovery at equal-stiffness ($G^*/\sin\delta$ value of 1 kPa) temperature | | | | | |
|--|---|-------------------------|----------------|---------------------------|----------------|
| Percent Sasobit[®] | 1 kPa stiffness Temperature (°C) | Percent recovery | | Standard deviation | |
| | | Creep stress | | Creep stress | |
| | | 0.1 kPa | 3.2 kPa | 0.1 kPa | 3.2 kPa |
| 0% | 76.8 | 34.7 | 13.0 | 3.2 | 1.1 |
| 1% | 78.7 | 67.5 | 26.3 | 1.1 | 2.5 |
| 2% | 81.2 | 86.4 | 20.3 | 1.7 | 2.5 |
| 4% | 82 | 74.3 | 22.4 | 3.2 | 3.2 |

Table 5-14. J_{nr} of PG 76-22M at equal-stiffness temperature

| PG 76-22M: Non-recoverable creep compliance at equal-stiffness ($G^*/\sin\delta$ value of 1 kPa) Temperature | | | | | |
|--|---|--|----------------|---------------------------|----------------|
| Percent Sasobit[®] | 1 kPa Stiffness Temperature (°C) | Non-recoverable creep Compliance, J_{nr} (1/kPa) | | Standard deviation | |
| | | Creep stress | | Creep stress | |
| | | 0.1 kPa | 3.2 kPa | 0.1 kPa | 3.2 kPa |
| 0% | 76.8 | 0.007 | 0.4 | 0.0005 | 0.0168 |
| 1% | 78.7 | 0.003 | 0.3 | 0.0002 | 0.0290 |
| 2% | 81.2 | 0.001 | 0.4 | 0.0002 | 0.0338 |
| 4% | 82 | 0.002 | 0.3 | 0.0003 | 0.0324 |

From the above MSCR analyses, it can be concluded that at high grading temperatures, (i.e. 64 °C for PG 64-22 and 76 °C for PG 76-22M), 1% and 2% Sasobit[®] increased the rutting resistance and the optimum percentage of Sasobit[®] lies between 2% and 4%. At equal stiffness (1 kPa of $G^*/\sin\delta$) temperature, the influence of Sasobit[®] was stress dependent.

In this regard, the MSCR test was performed at varying creep stresses, 0.1 kPa, 0.2 kPa, 0.5 kPa and 3.2 kPa at equal-stiffness temperature for PG 64-22. Table 5-15 shows that linear relationship between creep stress and percent recovery had the highest coefficient of determination (R^2) for 0% Sasobit[®]. As the percent of Sasobit[®] increased, the R^2 value decreased. The lowest R^2 obtained was 0.73 for 4% Sasobit[®]. On the other hand, overall, the R^2 values in all cases were good for log (creep stress) and percent recovery relationship. Therefore, it can be concluded that the effect of creep stress on percent recovery is logarithmic.

Table 5-15. Coefficient of determination values for creep stress and percent recovery relationships

| Asphalt binder | Percent Sasobit [®] | Coefficient of determination (R^2) | |
|----------------|------------------------------|--|---|
| | | Linear relationship: Creep stress and percent Recovery | Logarithmic relationship: Log (creep stress) and percent Recovery |
| PG 64-22 | 0% | 0.997 | 0.899 |
| | 1% | 0.91 | 0.998 |
| | 2% | 0.84 | 0.98 |
| | 4% | 0.73 | 0.96 |

5.7 Evaluation of Rutting Susceptibility of Sasobit[®] Modified WMA

Rutting was performed using an APA. AASHTO TP63 was followed in this regard. Figure 5-8 shows images of the test procedure. Six asphalt binder mix samples were prepared with $7.5 \pm 0.5\%$ air voids. In this method, three steel wheels each 100 lb ran over three pneumatic rubber hoses. APA measured the rut depth with LVDTs and a computer updated the rut depths every 10 cycles (also called strokes). As per the specifications, the first 50 cycles were used for setting of the samples, and deformation during the first 50 cycles was not counted towards rut depth. After the setting 50 cycles, another 8000 cycles were run for rut depth. In this study, manual measurements of rut were also obtained after 8000 cycles with a strain gauge as can be seen in Figure 5-8. In manual measurements, each of the six samples was measured at two points using the APA manual measurement template. Figure 5-9 shows typical rut depths with respect to stroke count obtained from the computer.

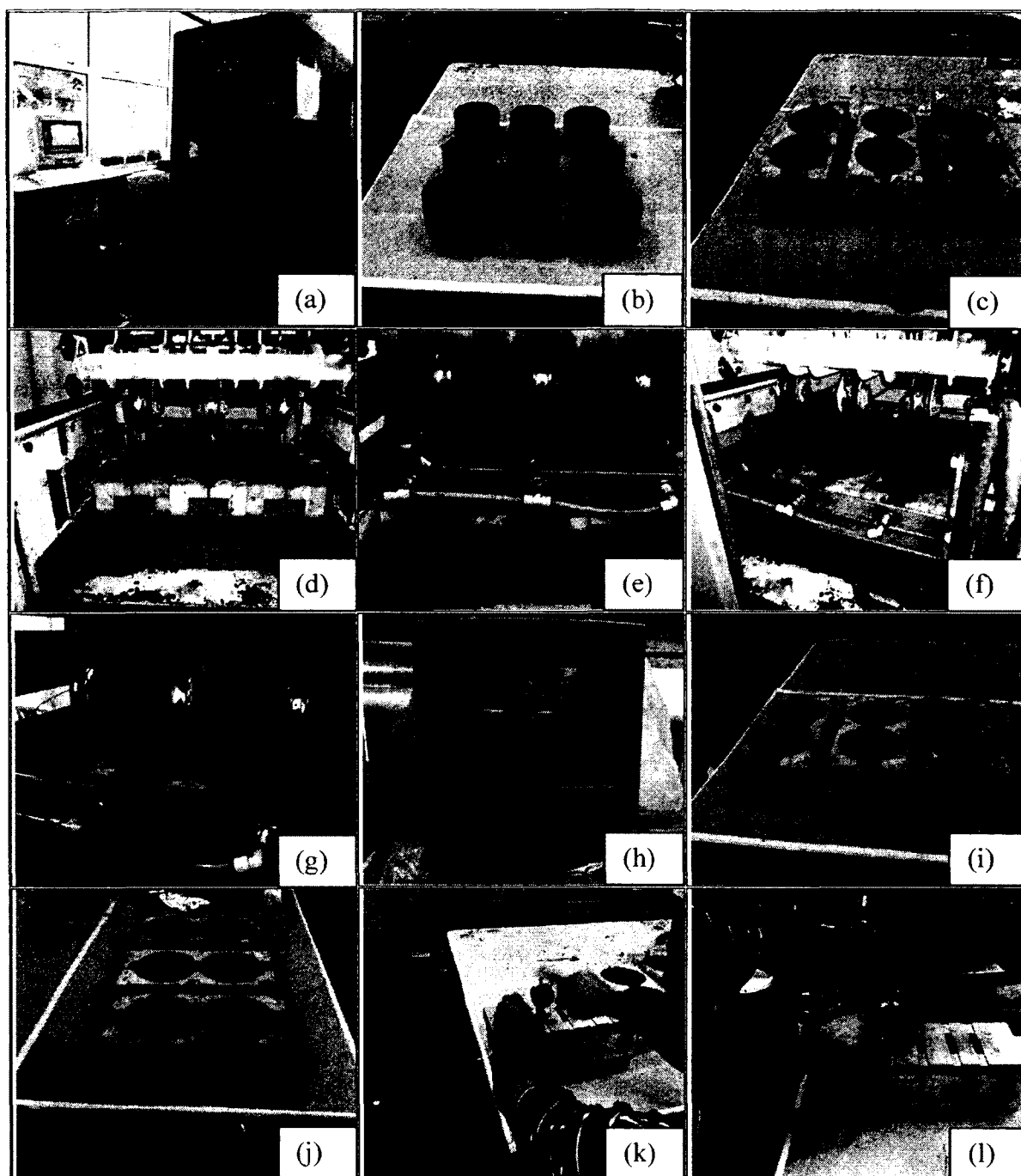


Figure 5-8. (a) Asphalt pavement analyzer (APA), (b) Gyratory rut samples, (c) Rut samples in mold, (d) Molds placed in the APA, (e) and (f) Rubber hose setup, (g) Steel wheel rolling, (h) Software taking rut measurements, (i) and (j) Rut samples after 8000 cycles (k) and (l) Manual rut measurement with a strain gauge

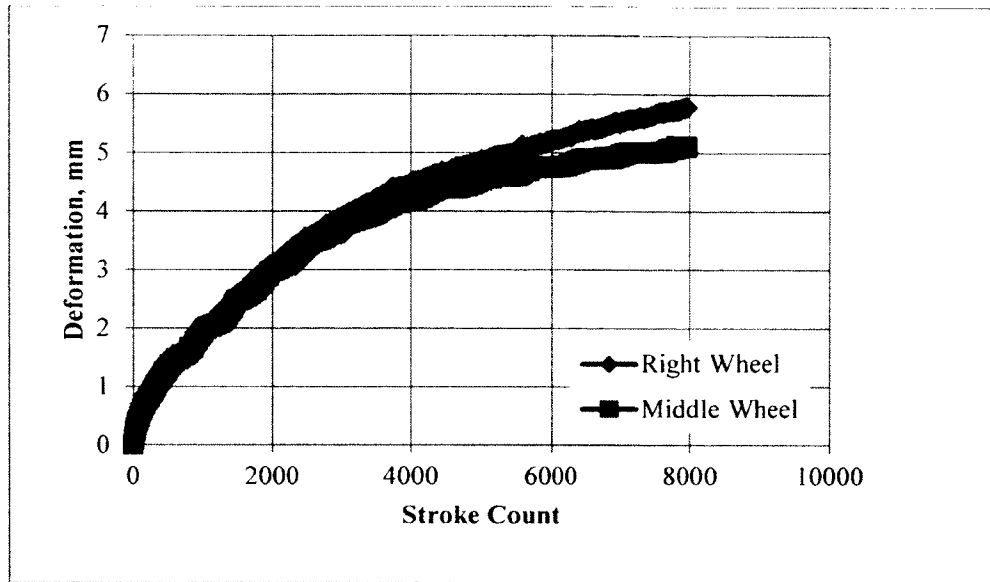


Figure 5-9. Typical rut depths data obtained from the APA

5.7.1 Effects of Sasobit[®] on Rutting Susceptibility of HMA

At first, effects of Sasobit[®] were evaluated at hot mix temperatures. In this regard, two sets of samples, Test 1 and Test 2 were prepared at hot mix temperatures. Both sets of samples have $7.5 \pm 0.5\%$ air voids, 4.8% asphalt content, 163 °C mixing and 150 °C compaction temperatures. The only difference between these two sets was that Test 1 samples do not have Sasobit[®] while Test 2 samples had 2% Sasobit[®] in it. Table 5-16 shows average air voids and average rut depths of Test 1 and Test 2. After 8000 cycles, each of the six samples (Test 1-a through Test 1-f) was measured for rut at two locations (see Appendix C for rut depths of individual samples). It can be observed in Table 5-16 that manually measured rut depths were higher than APA rut depths. This is because of the fact that manually measured rut depths include deformations from first 50 setting cycles while APA rut depths do not include the first 50 setting cycles. Table 5-16 shows a comparison of rutting susceptibility of Test 1 samples prepared without Sasobit[®] and Test

2 samples prepared with 2% Sasobit[®]. It can be observed that 2% Sasobit[®] reduced APA rut depth from 6.95 mm to 4.71 mm.

Table 5-16. Effects of Sasobit[®] on rutting of HMA

| Test ID | Avg. % air Voids | % AC | % Sasobit [®] | Mixing Temp., °C | Compaction Temp., °C | Manual Rut, mm | APA Rut, mm |
|---------|------------------|------|------------------------|------------------|----------------------|----------------|-------------|
| Test 1 | 7.33 | 4.8 | 0 | 163 | 150 | 8.62 | 6.95 |
| Test 2 | 7.53 | 4.8 | 2 | 163 | 150 | 5.38 | 4.71 |

Effects of Sasobit[®] on rutting of hot mix asphalt were further evaluated by another two sets of samples, Test 3 and Test 4. This time, the air voids of the samples were increased to about 10%. Tables 5-17 shows that both of these two sets had about 10% air voids, 4.8% asphalt content, 163 °C mixing and 150 °C compaction temperatures. Table 5-17 shows that APA rut depth of HMA without Sasobit[®] was 9.46 mm whereas, APA rut depth of HMA with 2% Sasobit[®] was 5.27 mm. Therefore, HMA with higher air voids also indicated that Sasobit[®] increased rutting resistance of asphalt mixes.

Table 5-17. Effects of Sasobit[®] on rutting of HMA with higher air voids

| Test ID | Avg. % Air Voids | % AC | % Sasobit [®] | Mixing Temp., °C | Compaction Temp., °C | Manual Rut, mm | APA Rut, mm |
|---------|------------------|------|------------------------|------------------|----------------------|----------------|-------------|
| Test 3 | 10.41 | 4.8 | 0 | 163 | 150 | 12.77 | 9.46 |
| Test 4 | 9.97 | 4.8 | 2 | 163 | 150 | 7.14 | 5.27 |

Effects of Sasobit[®] on rutting of hot mix asphalt were further evaluated by another two sets of samples, Test 5 and Test 6 as in Table 5-18. This time, the percent asphalt contents of samples were increased to 5.3% from 4.8%. Table 5-18 shows that both of these two sets had about 7.5% air voids, 5.3% asphalt content, 163 °C mixing and 150 °C compaction temperatures. It can be observed that APA rut depth of HMA without Sasobit[®] was 7.55 mm whereas, APA rut depth of HMA with 2% Sasobit[®] was 5.73 mm. Therefore, HMA with higher asphalt content further indicates that Sasobit[®] increased rutting resistance of asphalt mixes. Percent air voids and rut depth of individual samples are shown in Table C-1 to C-10 in Appendix C.

Table 5-18. Effects of Sasobit[®] on rutting of HMA with higher asphalt content

| Test ID | Avg. % Air Voids | % AC | % Sasobit [®] | Mixing Temp., °C | Compaction Temp., °C | Manual Rut, mm | APA Rut, mm |
|---------|------------------|------|------------------------|------------------|----------------------|----------------|-------------|
| Test 5 | 7.67 | 5.3 | 0 | 163 | 150 | 9.38 | 7.55 |
| Test 6 | 7.97 | 5.3 | 2 | 163 | 150 | 6.03 | 5.73 |

5.7.2 Evaluation of Rutting Susceptibility of Sasobit[®] Modified WMA

One of the objectives of this study was to evaluate rutting susceptibility of Sasobit[®] modified WMA. In this regard, six samples were prepared with 2% Sasobit[®] at warm mix temperatures, 143 °C mixing and 110 °C compaction. Another set of six samples were prepared without Sasobit[®] at the same warm mix temperatures, 143 °C mixing and 110 °C compaction. It can be seen that both of these two sets had about 7.5% air voids, 4.8% asphalt content, 143 °C mixing and 110 °C compaction temperatures. The

only difference between Test 7 and Test 8 is that one has 2% Sasobit[®] and the other set does not.

Table 5-19 shows that HMA has rut depth of 6.95 mm and manually measured rut depth of 8.62 mm while Sasobit[®] modified WMA has an APA rut depth of 5.32 mm and manually measured rut depth of 5.99 mm. It can be concluded here that Sasobit[®] modified WMA was not rutting susceptible rather Sasobit[®] increased rutting resistance.

Table 5-19. Rutting susceptibility of Sasobit[®] modified WMA

| Test ID | Avg. % air Voids | % AC | % Sasobit [®] | Mixing Temp., °C | Compaction Temp., °C | Manual Rut, mm | APA Rut, mm |
|---------|------------------|------|------------------------|------------------|----------------------|----------------|-------------|
| Test 1 | 7.33 | 4.8 | 0 | 163 | 150 | 8.62 | 6.95 |
| Test 7 | 7.16 | 4.8 | 0 | 143 | 110 | 6.05 | 6.93 |
| Test 8 | 7.49 | 4.8 | 2 | 143 | 110 | 5.99 | 5.32 |

Rutting susceptibility of Sasobit[®] modified WMA was further evaluated by reducing the previously used warm mix mixing temperature from 143 °C to 133 °C. Six samples were prepared with 2% Sasobit[®] at warm mix temperatures, 133 °C mixing and 110 °C compaction. Another set of six samples were prepared without Sasobit[®] at the same warm mix temperatures, 133 °C mixing and 110 °C compaction. It can be seen that both of these two sets had about 7.5% air voids, 4.8% asphalt content, 133 °C mixing and 110 °C compaction temperatures. The only difference between Test 9 and Test 10 is that one had 2% Sasobit[®] and the other set did not. Table 5-30 shows that Sasobit[®] modified WMA prepared at 133 °C and compacted at 110 °C has lower rutting depth than hot mix asphalt. Two percent Sasobit[®] reduced the rut depth from 8.62 mm to 5.98 mm in case of manual measurements and from 6.95 mm to 5.45 mm in case of LVDT measurements.

Therefore, Sasobit[®] modified WMA exhibited better rutting resistance than hot mix asphalt.

Table 5-20. Rutting susceptibility of Sasobit[®] modified WMA in case of warm mixing temperature of 133 °C

| Test ID | Avg. % Air Voids | % AC | % Sasobit [®] | Mixing Temp., °C | Compaction Temp., °C | Manual Rut, mm | APA Rut, mm |
|---------|------------------------|---------|---------------------------|------------------------|-------------------------|-------------------|-------------------|
| Test 1 | 7.33 | 4.8 | 0 | 163 | 150 | 8.62 | 6.95 |
| Test 9 | 7.74 | 4.8 | 2 | 133 | 110 | 5.98 | 5.45 |
| Test 10 | 7.47 | 4.8 | 0 | 133 | 110 | 8.17 | 6.69 |

5.7.3 Development of a Linear Multiple Variable Rutting Model

A linear multiple variable regression model for rut depth was developed in order to understand the comparative effects of various variables used in this study. A total of 10 sets (Test 1 through Test 10) of rut depths data were used to develop the linear regression model. The input variables were percent air voids, percent asphalt content, percent Sasobit[®], and mixing temperature in degree celsius. Table 5-21 shows that the coefficient of determination between actual rut depths and predicted rut depths using this multiple variable linear regression model was 0.89. The linear multiple variable regression model obtained can be described in Equation 5.1.

$$\begin{aligned} \text{Rut Depth (mm)} = & 0.6 * (\% AV) + 1.21 * (\% AC) - 1.15 * (\% \text{Sasobit}^{\text{®}}) \\ & - 0.01 * (MT \text{ } ^{\circ}\text{C}) - 1.729. \end{aligned} \quad 5.1$$

Where AV = Air Voids, AC = Asphalt content and MT = Mixing Temperature °C.

Table 5-21. Summary output of multiple regression model

| SUMMARY OUTPUT | | | | | |
|-----------------------|--------------|----------------|--------|---------|----------------|
| Regression Statistics | | | | | |
| Multiple R | 0.94 | | | | |
| R Square | 0.89 | | | | |
| Adjusted R Square | 0.80 | | | | |
| Standard Error | 0.64 | | | | |
| Observations | 10 | | | | |
| ANOVA | | | | | |
| | df | SS | MS | F | Significance F |
| Regression | 4 | 16.0 | 4.0 | 9.9 | 0.01 |
| Residual | 5 | 2.0 | 0.4 | | |
| Total | 9 | 18.0 | | | |
| | | | | | |
| | Coefficients | Standard Error | t Stat | P-value | |
| Intercept | -1.729 | 5.39 | -0.32 | 0.761 | |
| % Air Voids | 0.600 | 0.22 | 2.75 | 0.040 | |
| % AC | 1.210 | 1.16 | 1.04 | 0.346 | |
| % Sasobit® | -1.150 | 0.20 | -5.71 | 0.002 | |
| Mixing Temp °C | -0.010 | 0.02 | -0.48 | 0.650 | |

The regression model shows that an increase in percent air voids and/or an increase in percent asphalt content will increase rut depth. An increase in percent Sasobit® and/or an increase in mixing temperature will decrease rut depth. Table 5-22 shows the predicted rut values using this model and actual rut values obtained from the APA test. Table 5-21 shows that the coefficient of percent air voids has the estimated standard error of 0.22, t-statistic of 2.75 and p-value of 0.04. It was statistically significant at significance level $\alpha = 0.05$ as $p < 0.05$. The coefficient of percent Sasobit® has estimated standard error of 0.2, t-statistic of -5.71 and p-value of 0.002. It was statistically significant at significance level $\alpha = .05$ as $p < 0.05$. The other two factors,

percent asphalt content and mixing temperature, have p values larger than 0.05 and were statistically insignificant at the significance level $\alpha = 0.05$.

Table 5-22. Actual and predicted rut depths

| Test ID | % Air Voids | % AC | % Sasobit [®] | Mixing Temp °C | Actual APA rut, mm | Predicted Rut by the Model, mm |
|-----------------------|-------------|------|------------------------|----------------|--------------------|--------------------------------|
| Test 1 | 7.33 | 4.8 | 0 | 163 | 6.95 | 6.89 |
| Test 2 | 7.53 | 4.8 | 2 | 163 | 4.71 | 4.71 |
| Test 3 | 10.41 | 4.8 | 0 | 163 | 9.46 | 8.74 |
| Test 4 | 9.97 | 4.8 | 2 | 163 | 5.27 | 6.18 |
| Test 5 | 7.67 | 5.3 | 0 | 163 | 7.55 | 7.70 |
| Test 6 | 7.97 | 5.3 | 2 | 163 | 5.73 | 5.58 |
| Test 7 | 7.16 | 4.8 | 0 | 143 | 6.93 | 6.98 |
| Test 8 | 7.49 | 4.8 | 2 | 143 | 5.32 | 4.88 |
| Test 9 | 7.74 | 4.8 | 2 | 133 | 5.45 | 5.13 |
| Test 10 | 7.47 | 4.8 | 0 | 133 | 6.69 | 7.27 |
| R²= | | | | | 0.89 | |

5.8 Evaluation of Aging

For evaluation of aging a DSR was used to measure stiffness, $G^*/\sin\delta$ before and after aging. The following eight batches of extraction and recovery of asphalt binders were performed: two batches of 163 °C mix with 0% Sasobit[®], two batches of 163 °C mix with 2% Sasobit[®], two batches of 133 °C mix with 0% Sasobit[®] and two batches of 133 °C mix with 2% Sasobit[®]. From each batch two DSR samples were tested. Extraction and recovery were performed using a centrifuge and a rotary evaporator according to ASTM D 5404 followed by ASTM D 2172 (Test Method A).

Table 5-23 shows the $G^*/\sin\delta$ values and Table 5-24 shows the aging indices. The details of individual samples have been provided in Appendix D. It can be observed from these two tables that aging indices of Sasobit[®] mixes are lower than without Sasobit[®] mixes. For 163°C mixes, the aging index of 2% Sasobit[®] mix is 1.1 while the aging index of 0% Sasobit[®] mix is 1.72. Similar trend is observed for 133 °C mixes. This indicates that Sasobit[®] mixes do not age as much as without Sasobit[®] mixes. Another important observation of this study is that the aging indices of 163 °C mixes are higher than the aging indices of 133 °C mixes. This finding justifies the concern that lowering the production temperatures reduces aging and increases rutting susceptibility. Also, it can be noticed from these tables that reduction in aging index due to reduction in mixing temperature is higher for Sasobit[®] mixes than that of without Sasobit[®] mixes.

Table 5-23. $G^*/\sin\delta$ of original and extracted asphalt binders

| $G^*/\sin\delta$ in kPa of original PG 64-22 | | | | |
|--|-------------------------------|-------------------------------|-------------------------------|-------------------------------|
| | 64 °C | | 76 °C | |
| | 0% Sasobit[®] | 2% Sasobit[®] | 0% Sasobit[®] | 2% Sasobit[®] |
| Average | 1.46 | 3.84 | 0.36 | 0.97 |
| St. dev. | 0.09 | 0.17 | 0.00 | 0.06 |
| $G^*/\sin\delta$ in kPa of asphalt binders extracted from 163 °C mix | | | | |
| | 64 °C | | 76 °C | |
| | 0% Sasobit[®] | 2% Sasobit[®] | 0% Sasobit[®] | 2% Sasobit[®] |
| Average | 2.51 | 4.25 | 0.58 | 0.97 |
| St. dev. | 0.30 | 0.52 | 0.05 | 0.08 |

Table 5-23 continued...

| G*/sinδ in kPa of asphalt binders extracted from 133 °C mix | | | | |
|--|--------------------|--------------------|--------------------|--------------------|
| | 64 °C | | 76 °C | |
| | 0% Sasobit® | 2% Sasobit® | 0% Sasobit® | 2% Sasobit® |
| Average | 2.43 | 2.82 | 0.55 | 0.68 |
| St. dev. | 0.12 | 0.11 | 0.02 | 0.04 |

Table 5-24. Aging indices of extracted asphalt binders

| Aging index | | | | |
|--------------------|--------------------|--------------------|--------------------|--------------------|
| | 64 °C | | 76 °C | |
| | 0% Sasobit® | 2% Sasobit® | 0% Sasobit® | 2% Sasobit® |
| 163 °C Mix | 1.72 | 1.1 | 1.6 | 1.0 |
| 133 °C Mix | 1.66 | 0.7 | 1.5 | 0.7 |

5.9 Conclusions

From the study on rutting susceptibility of Sasobit® modified WMA an overall positive effect was observed. The following specific conclusions can be drawn on rutting susceptibility of Sasobit® modified WMA.

1. Evaluation of rutting factor $G^*/\sin\delta$ indicates that addition of 1%, 2% and 4% Sasobit® increases rutting resistance. However, evaluation of phase angle indicates that at one grading higher temperature of PG 76-22M, there exists an optimum percent of Sasobit® between 2% and 4% above which rutting resistance will start decreasing. Therefore, it can be concluded that if rut test is performed higher than grading temperature, an overdose of Sasobit® will increase rutting susceptibility.

2. In case of PG 64-22, for both 64 °C and 70 °C and for both 0.1 kPa and 3.2 kPa creep stress, an increase in percent of Sasobit[®] caused an increase in average percent recovery. However, 3.2 kPa J_{nr} measurements of PG 64-22 indicate that 1% and 2% Sasobit[®] reduced the rutting susceptibility while 4% Sasobit[®] increased the rutting susceptibility of asphalt pavements.
3. The positive effects of Sasobit[®] on rutting resistance of PG 76-22M was observed only at lower pavement service temperatures (70 °C and 76 °C and not at 82 °C). Analyses of 0.1 kPa creep stress data revealed that 1% and 2% Sasobit[®] increased the percent recovery of PG 76-22M and the addition of 4% Sasobit[®] started reducing it. This indicates that an optimum amount of Sasobit[®] was needed for increasing rutting resistance of PG 76-22M.
4. Overall conclusion from temperature sweep test and MSCR is that, addition of 1% and 2% Sasobit[®] increases the rutting resistance.
5. To understand if the increase in rutting resistance was caused by the increase in stiffness or by the internal molecular associations, a different set of MSCR test was performed. In this approach, equal-stiffness (1 kPa of $G^*/\sin\delta$) temperatures of 0%, 1%, 2% and 4% Sasobit[®] added asphalt binders were determined based on temperature sweep test results and MSCR test was performed on that equal-stiffness temperature. Results indicate that at higher stress Sasobit[®] will make PG 64-22 rutting susceptible and at lower stress it will make PG 64-22 rutting resistant. Therefore, the true influence of Sasobit[®] on rutting of PG 64-22 is stress dependent.

6. MSCR test was performed at varying creep stresses, 0.1 kPa, 0.2 kPa, 0.5 kPa and 3.2 kPa at equal-stiffness temperature for PG 64-22. A general trend observed was that as the creep stress increased, the percent recovery decreased. It was concluded that the effect of creep stress on percent recovery is logarithmic.
7. A total of 60 samples were tested using an APA. It was found in this study that 2% Sasobit[®] reduced rutting susceptibility of Sasobit[®] modified hot mix asphalt. This finding was verified with higher asphalt content mixes. The fact that Sasobit[®] reduced rutting susceptibility of HMA was further verified with higher air void mixes. Sasobit[®] modified WMA mixed at 143 °C and compacted at 110 °C showed better rutting resistance than HMA. Sasobit[®] modified asphalt mixes prepared at 133 °C and 110 °C also reduced rutting susceptibility. A multiple variable regression rutting model using 60 samples were developed that predicted rutting depths with coefficient of determination of 0.89. Statistical analyses showed that Sasobit[®] reduced rutting resistance at 5% level of significance.
8. From aging evaluation of extracted asphalt binders it can be observed that aging indices of Sasobit[®] mixes are lower than without Sasobit[®] mixes. This indicates that Sasobit[®] mixes do not age as much as without Sasobit[®] mixes. Another important observation of this study is that the aging indices of 163 °C mixes are higher than the aging indices of 133 °C mixes.

This finding justifies the concern that lowering the production temperatures reduces aging and increases rutting susceptibility. Also, it was observed that reduction in aging index due to reduction in mixing temperature is higher for Sasobit[®] mixes than that of without Sasobit[®] mixes.

CHAPTER 6

EVALUATION OF ATOMIC FORCE MICROSCOPE (AFM) AS A SCREENING TOOL FOR ASPHALTIC MATERIALS – AN EXPLORATORY STUDY

6.1 Introduction

Asphalt binder is identified as a complex mix of hydrocarbons (Asphalt Institute, 1989). It is such a ubiquitous material that it has been used since biblical times but the details of its properties are still unknown (Speight, 1999). For more than three centuries, microscopes have been used to study materials (Baker, 1987). Yet for opacity and adhesive properties, asphalt binder has not been studied much. With the advent of transmission electron microscopy, the asphaltenes which are the heaviest asphalt components have been studied by many researchers (Dykstra et al., 1944; Freund and Vajta, 1958; Dickie et al., 1969; Donnet et al., 1973; Peyrot, 1973).

With the help of low light optical microscopy, now it is possible to study asphalt binders in its solid state without the use of solvents. Claudy et al. (1992) studied the bi-phasic nature of asphalt binders using phase-contrast and polarized light microscopy and investigated birefringent region of about 10 μm . These regions are called “Crystalline saturated hydrocarbons.” By confocal laser-scanning microscopy 2-7 μm dispersion in asphalt binders have been observed by Bearsley et al. (2004). Recently, atomic force microscopy has been used to study asphalt binders by many researchers.

In 1996, Loeber et al. (1996) used AFM to study a heat-cast asphalt binder film. Pauli et al. (2001) observed the 'bee-like' appearance of asphalt binders under AFM. In this study, the samples were prepared by heat casting. Thus, solid state structure was maintained governing its rheological properties. High-resolution microscopic images were obtained by phase-detection microscopy (PDM). PDM is a non-contact AFM method (Zhong et al., 1993) and it prevents tip pollution by soft and adhesive asphalt binders. The image has been provided by the difference between the oscillation signal sent to the instrument cantilever and its actual oscillation which is affected by tip-sample interactions (Stark et al., 1999). Previous researches identified four different phase of asphalt binder using an AFM. To this end, this study has been initiated to characterize asphalt binders by its phases.

6.2 Objective

The objective of this exploratory study was to evaluate if an atomic force microscope can be used for evaluation of asphaltic materials.

6.3 Asphalt Binder Sample Preparation

The asphalt binders namely, PG 64-22 and PG 76-22M were used in this study. A commercially available paraffin wax was added to the asphalt binder at the rate of 1% (w/w). To understand the effect of aging, a limited no. of samples were prepared by heating the asphalt binder samples inside a forced draft oven for three minutes.

Initially toluene was used to dissolve the asphalt binder and to prepare spin-coated glass plate samples. Later, it was found that bee-like microstructure can also be observed on asphalt binder samples prepared by heat casting (without using solvent).

6.4 Results and Discussions

The atomic force microscope used was a Quescent Amscope. Figure 6-1 shows an asphalt binder sample under AFM. The images were obtained at room temperature and atmospheric pressure. For each asphalt binder, topographic AFM images of 20 μm x 20 μm were acquired in non-contact mode at several locations on the sample surface.

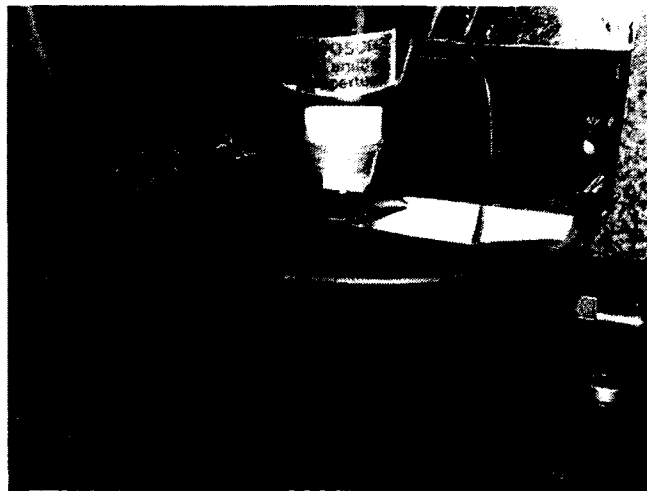


Figure 6-1. Asphalt binder under atomic force microscope

Loeber et al. (1996) identified the following four phases on an asphalt binder surface: (a) Catana phase, (b) Peri-phase, (c) Para-phase and (d) Sal-phase. Figure 6-2 shows topographic image and Figure 6-3 shows these four phases as identified in the present study. The white and black stripes in bee structure are referred to as high to low height as the catana or catanic phase, from the Greek “cata,” high to low, and “ana,” low to high.

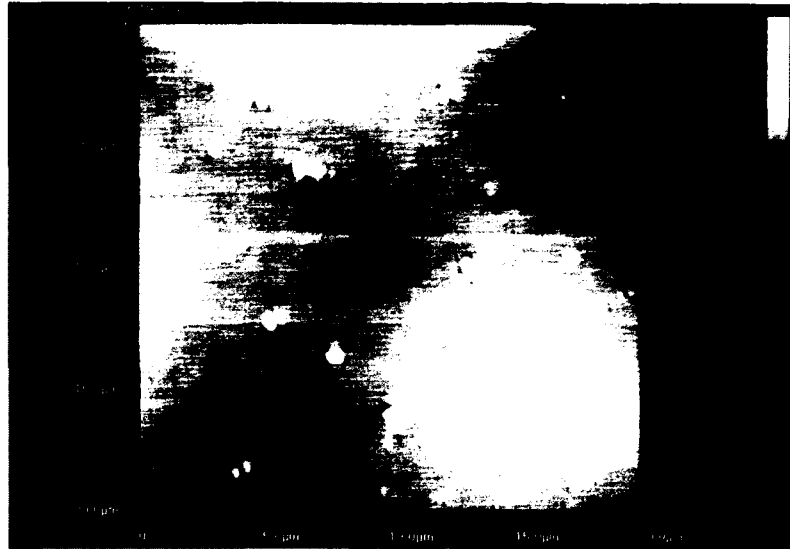


Figure 6-2. Topographic image of asphalt binders PG 64-22 (20µm x 20µm)

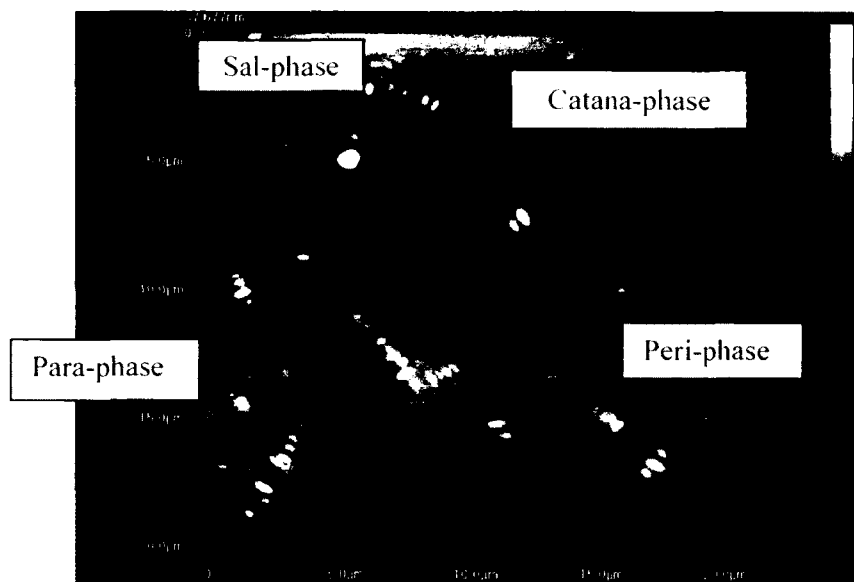
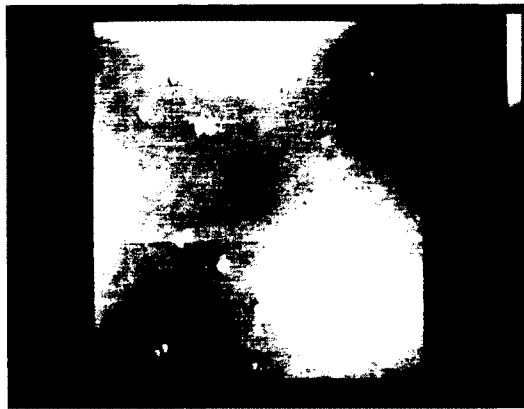


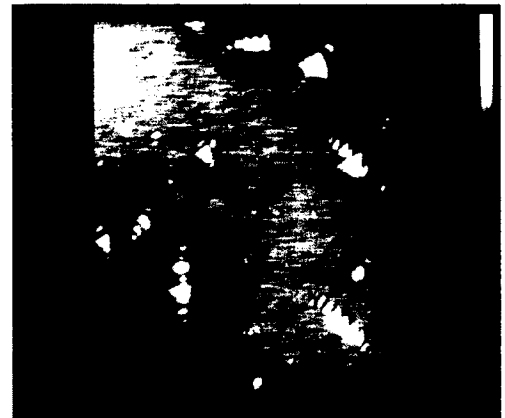
Figure 6-3. Phase identification

Just around the catana phase was a dark looking phase, separated here and there by another lighter shade phase. These phases are termed as "peri- and para-phases." (from the Greek "peri," around; and "para," neighboring). Also in each paraphrase there is a small quasi-spherical domains termed the "sal-phase" ("sal," Latin for salt). This phase was dispersed in the paraphrase and was easily detectable.

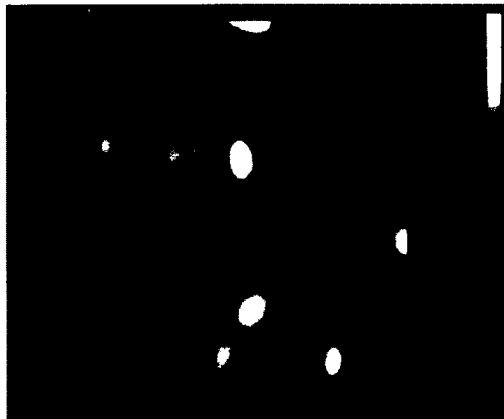
Figure 6-4 (a), (b) and (c) show PG 64-22 with 0%, 0.5% and 1% wax respectively. It was interesting since wax was making the bees longer in length, higher in height. One of the three minutes aged sample is shown in Figure 6-4(d). Aging samples were noisy and not as smooth as pure asphalt binders.



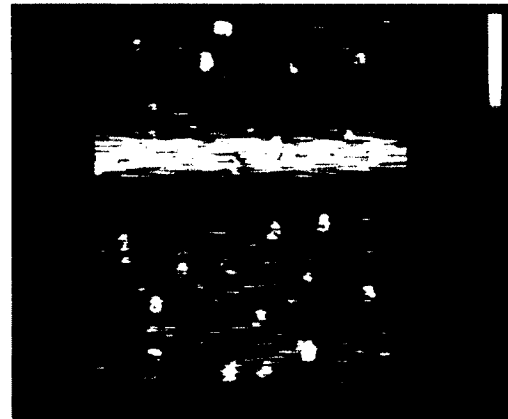
(a) PG 64-22 with 0% wax



(b) PG 64-22 with 0.5% wax



(c) PG 64-22 with 1% wax



(d) PG 64-22 three minutes aging

Figure 6-4. PG 64-22 samples with 0, 0.5, 1% wax and aged condition

Figure 6-5(a) and (b) show polymer modified binder images. Figure 6-5 (c) shows PG 76-22M sample with 1% wax while Figure 6-5(d) shows three minutes aged sample of PG 76-22M.

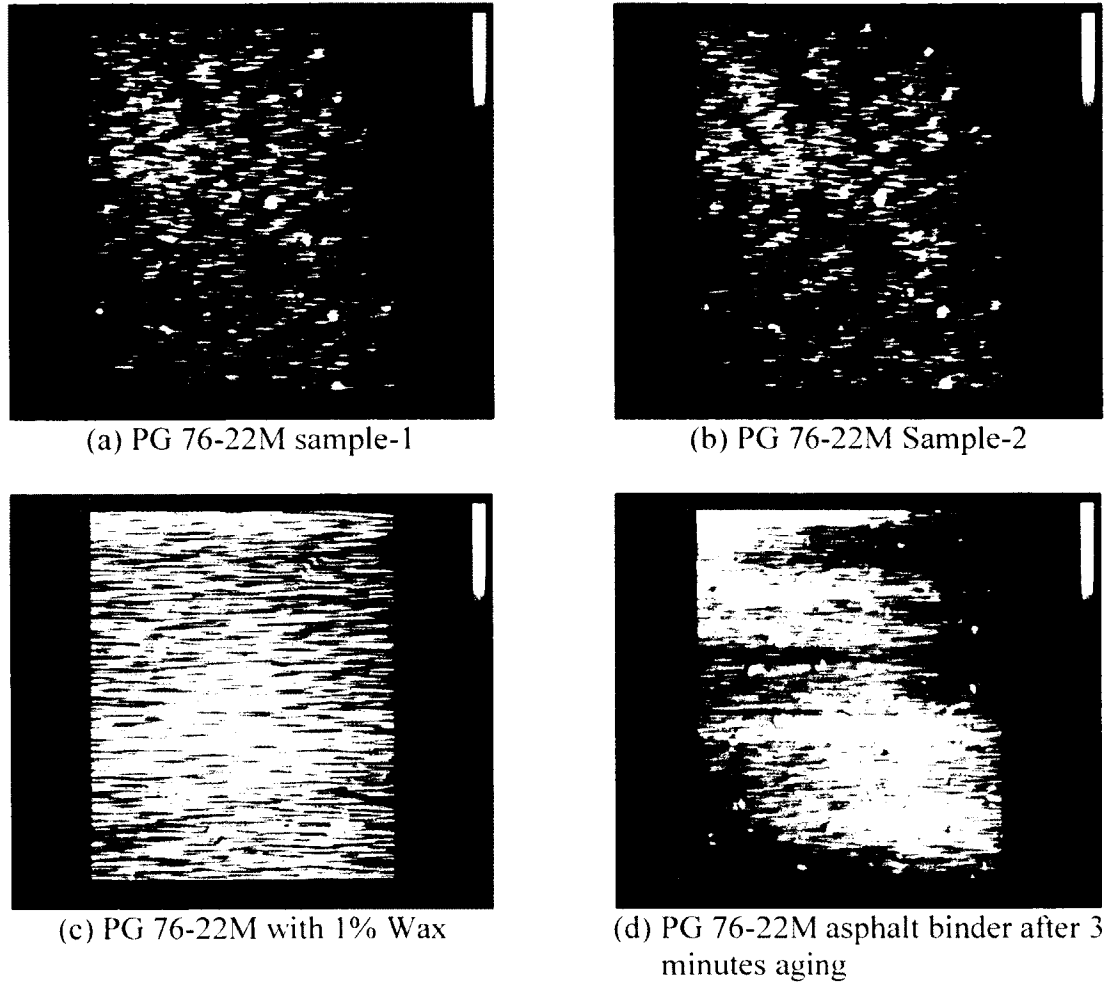


Figure 6-5. PG 76-22M with aging and 1% wax

To analyze the AFM data, scanning probe microscopic (SPM) image analysis software Gwyddion 2.29 was used in this study. Gwyddion 2.29 is an open source software and available online. Each bee area and height was obtained through the software. The masking tool was used in the software (as shown in Figure 6-6) to select each bee and then automatically calculated each bee area and height. Three neat binder samples and two 1% wax modified samples have been selected for the analysis. Table 6-1 to 6-5 show details of the SPM data analysis. Table 6-6 shows the summary of analysis.



(a) Image opened for analysis



(b) Bee area selected for calculation

Figure 6-6. Image analysis by Gwyddion**Table 6-1.** AFM data analysis for PG 64-22 +0% Wax - sample 1

| Sample Type | Surface Area of each Bee μm^2 | Average bee Height for Each bee, nm | Bee height Average, nm | Average bee Area, μm^2 | % Bee Area |
|-------------|--|-------------------------------------|------------------------|-----------------------------------|------------|
| PG 64-22 | 2.15 | 7.31 | 10.45 | 2.48 | 7.44 |
| | 2.37 | 9.32 | | | |
| | 1.91 | 11.33 | | | |
| | 1.73 | 10.73 | | | |
| | 1.90 | 5.24 | | | |
| | 3.30 | 15 | | | |
| | 2.72 | 10.81 | | | |
| | 2.62 | 11.72 | | | |
| | 3.56 | 9.33 | | | |
| | 1.88 | 7.33 | | | |
| | 1.33 | 13.75 | | | |
| | 1.53 | 13.83 | | | |

In Table 6-1 to 6-5 the average bee height of a bee was calculated by deducting the minimum height from average height in a bee area. Then the average height of the bee of each sample was calculated dividing the total height by the number of bees. Average bee area was calculated by dividing total bee area by the number of bees. The percent bee area was calculated from total bee area and total image area. It can be observed from these tables that wax increased the individual bee area, percent bee area. It is noticeable that wax increased the bee height significantly.

Table 6-2. AFM data analysis for PG 64-22 + 0% Wax - sample 2

| Sample Type | Surface area For each bee μm^2 | Average bee Height for Each bee, nm | Bee Height Average | Average bee Area, μm^2 | % Bee Area |
|-------------|---|-------------------------------------|--------------------|-----------------------------------|------------|
| PG 64-22 | 1.85 | 20.3 | 11.26 | 2.09 | 6.29 |
| | 1.61 | 16.21 | | | |
| | 3.4 | 9.72 | | | |
| | 1 | 82 | | | |
| | 1.77 | 9.13 | | | |
| | 2.44 | 8.43 | | | |
| | 3.27 | 15.84 | | | |
| | 1.83 | 10.95 | | | |
| | 2.41 | 8.66 | | | |
| | 1.50 | 6 | | | |
| | 2.35 | 12.4 | | | |
| | 1.67 | 9.8 | | | |

Table 6-3. AFM data analysis for PG 64-22 +0% Wax - sample 3

| Sample Type | Surface Area For each bee μm^2 | Average bee Height for each bee, nm | Bee Height Average | Average bee Area, μm^2 | % Bee Area |
|--------------------|---|--|---------------------------|---|-------------------|
| PG 64-22 | 2.63 | 6.05 | 10.86 | 2.40 | 8.38 |
| | 2.15 | 8.53 | | | |
| | 2.62 | 9.34 | | | |
| | 1.21 | 7.13 | | | |
| | 1.73 | 10.95 | | | |
| | 1.80 | 9.15 | | | |
| | 1.34 | 11.72 | | | |
| | 4.90 | 11.46 | | | |
| | 4.31 | 15.73 | | | |
| | 1.62 | 8.14 | | | |
| | 1.57 | 16.13 | | | |
| | 2.44 | 9.86 | | | |
| | 2.71 | 12.69 | | | |
| | 2.45 | 15.15 | | | |

Table 6-4. AFM data analysis for PG 64-22 + 1% Wax - sample 1

| Sample Type | Surface Area For each bee μm^2 | Average Bee Height for each bee, nm | Bee Height Average | Average bee Area, μm^2 | % Bee Area |
|--------------------|---|--|---------------------------|---|-------------------|
| PG 64-22-1% Wax | 1.56 | 8.71 | 27.04 | 3.7 | 6.46 |
| | 3.00 | 17.33 | | | |
| | 2.16 | 20.14 | | | |
| | 4.92 | 30.54 | | | |
| | 5.04 | 55.65 | | | |
| | 4.49 | 21 | | | |
| | 4.64 | 36.1 | | | |

Table 6-5. AFM data analysis for PG 64-22 + 1% wax - sample 2

| Sample Type | Surface Area For each bee μm^2 | Average Bee Height for Each bee, nm | Bee Height Average | Average Bee Area, μm^2 | % Bee Area |
|---------------------|---|--|---------------------------|---|-------------------|
| PG 64-22- 1% Wax | 3.54 | 28.8 | 36.76 | 7.07 | 12.37 |
| | 4.59 | 22.6 | | | |
| | 5.21 | 29.2 | | | |
| | 8.37 | 34.1 | | | |
| | 9.05 | 80 | | | |
| | 9.63 | 45.2 | | | |
| | 9.06 | 17.4 | | | |

Table 6-6. Summary of analysis

| Sample Type | Bee height Average, nm | Average Bee area, μm^2 | % Bee area |
|--------------------|-------------------------------|---|-------------------|
| PG 64-22 | 10.86 | 2.32 | 7.37 |
| PG 64-22 1% Wax | 31.9 | 4.95 | 9.42 |

6.5 Conclusions

It can be concluded from this exploratory study that wax modified asphalt may be differentiated by its morphology using an AFM. Most importantly, the data obtained in an AFM can be quantified and asphalt has a unique bee-shape microstructure that can be used for evaluation. However, analyses of asphalt microstructure using the AFM still remains tedious and a standard method of testing is yet to be established for using it as a screening tool.

CHAPTER 7

CONCLUSIONS AND RECOMMENDATIONS

In this study, dynamic viscosity (η') of asphalt binders with and without a wax-based warm mix asphalt (WMA) additive, Sasobit[®] was measured at temperature ranges from 28 °C to 130 °C at six degree celsius interval. Laboratory densities of Superpave gyratory samples compacted at different temperatures, at different gyrations and at different asphalt contents were determined to evaluate the effect of viscosity on density. Also, field densities after different compaction steps were analyzed to evaluate the effect of Sasobit[®] on viscosity. The following specific conclusions can be drawn from the dynamic viscosity study:

1. An increase in percent of Sasobit[®] increases the rutting factor of PG 64-22 thereby increasing the potential for rutting resistance. For PG 76-22M at 76 °C, up to 2% Sasobit[®] increases the rutting factor $G^*/\sin\delta$ and addition of 4% Sasobit[®] starts reducing it. Firstly, this suggests that rate of Sasobit[®] must be optimized before its use. Secondly, this effect can be justified by the fact that the Sasobit[®] is an asphalt flow improver and it reduces viscosity at production temperatures. Addition of excess Sasobit[®] may reduce stiffness properties. In this regard, rate effect can be explained by temperature effect. And it can be observed that changes of PG 64-22 is similar to PG 76-22M at 76 °C with the addition of Sasobit[®].

2. Sasobit[®] reduces viscosity at higher compaction temperatures but it increases viscosity at lower compaction temperatures. There exists a critical temperature for each asphalt binder below which viscosity will increase with addition of Sasobit[®]. Therefore, compaction below the critical temperature can negatively impact density. For PG 64-22, the critical temperature is 104 °C and for PG 76-22M, the critical temperature is about 101 °C.
3. The gyratory compacted samples exhibit that Sasobit[®] added samples have higher densities than without Sasobit[®] samples at higher compaction temperature whereas, Sasobit[®] added samples have lower densities than without Sasobit[®] samples at lower compaction temperature.
4. Sasobit[®] indeed reduced the viscosity of binder as well as the mix at higher compaction temperature as can be seen from the density directly behind the screed. Sasobit[®] mix as monitored in this study has 3.5% more density than the PG 76-22M mix without Sasobit[®]. As the compaction continues, the mixes cool down and the beneficial effects of Sasobit[®] cannot be seen anymore. By the time the finisher roller completes, both mixes produce similar densities, 93.3% and 93.0% respectively for Sasobit[®] and PG 76-22M mixes. This strongly justifies the findings of this study that the beneficial effect of Sasobit[®] in viscosity reduction can only be obtained at higher compaction temperatures.

For effect of shear rate on steady state viscosity, three temperatures, namely 64 °C, 100 °C and 124 °C for PG 64-22 and three temperatures, 76 °C, 100 °C and 124 °C were used for PG 76-22M. Shear rates were used in the range between 0.0025 s⁻¹ to 250 s⁻¹. The following specific conclusions can be obtained from steady state viscosity at different temperatures at different shear rates:

1. PG 64-22 is a Newtonian fluid at 124 °C, 100 °C and at 64 °C it is Newtonian up to shear rate 10 s⁻¹. Polymer-modified asphalt binders, such as PG 76-22M used in this study, exhibit shear-thinning behavior even at asphalt mix compaction temperatures, such as 124 °C where unknown shear rates are utilized and shear rate dependency is of practical interests. Similar trends are observed at 100 °C and at 76 °C except that the shear rate dependency increases with reduced temperatures.
2. With the addition of Sasobit[®], PG 64-22 at 64 °C becomes a shear-thinning liquid. The shear rate dependency increases with an increase in percent of Sasobit[®]. Similar effects of Sasobit[®] are observed at 100 °C in reduced level and shear rate dependency with the addition of Sasobit[®] is almost negligible at 124 °C. The shear rate dependency in general reduces with an increase in temperatures. Also, the rate of change of viscosity is higher at higher shear rates and lower at lower shear rates. For PG 76-22M, the shear rate dependency increases with an increase in percent of Sasobit[®] at all the three temperatures. This indicates if the actual shear rate during the compaction process is higher than 6.8 s⁻¹, then the currently recommended viscosity as well as temperature is overestimated and compaction temperature can be

reduced. On the other hand, if the actual shear rate during the compaction process is lower than 6.8 s^{-1} , then the currently recommended viscosity as well as temperature is underestimated and a higher compaction temperature should be used.

3. The coefficient of determination, R^2 values for simplified CROSS model fit show that both the binders with and without Sasobit[®] fit the model very well with coefficient of determination varying between 0.8627 and 0.9369 for PG 64-22 and between 0.8804 and 0.9712 for PG 76-22M.
4. The zero shear viscosity were determined at 64 °C for PG 64-22 and at 76 °C for PG 76-22M. The correlation between zero shear viscosity and $G^*/\sin\delta$ is better in case of PG 64-22 binders. For both the binders, the correlation is better between zero shear viscosity and $G^*/\sin\delta$ at 34 °C.

At all the temperatures used in this study, dynamic viscosity is higher than steady state viscosity. Overall; on the comparison between steady state and dynamic viscosity, it can be concluded that the viscosity from the two methods are better comparable at higher temperature, such as 124 °C and because the influence of Sasobit[®] reaches a turning point at around 100 °C, the coefficient of determination values are below 0.95 except in one case. From the study on rutting susceptibility of Sasobit[®] modified WMA an overall positive effect was observed. The following specific conclusions can be drawn on rutting susceptibility of Sasobit[®] modified WMA.

1. Evaluation of rutting factor $G^*/\sin\delta$ indicates that addition of 1%, 2% and 4% Sasobit[®] increases rutting resistance. However, evaluation of phase angle indicates that at one grading higher temperature of PG 76-22M, there exists an

optimum percent of Sasobit[®] between 2% and 4% above which rutting resistance will start decreasing. Therefore, it can be concluded that if rut test is performed higher than grading temperature, an overdose of Sasobit[®] will increase rutting susceptibility.

2. In case of PG 64-22, for both 64 °C and 70 °C and for both 0.1 kPa and 3.2 kPa creep stress, an increase in percent of Sasobit[®] caused an increase in average percent recovery. However, 3.2 kPa J_{nr} measurements of PG 64-22 indicate that 1% and 2% Sasobit[®] reduced the rutting susceptibility while 4% Sasobit[®] increased the rutting susceptibility of asphalt pavements.
3. The positive effects of Sasobit[®] on rutting resistance of PG 76-22M was observed only at lower pavement service temperatures (70 °C and 76 °C and not at 82 °C). Analyses of 0.1 kPa creep stress data revealed that 1% and 2% Sasobit[®] increased the percent recovery of PG 76-22M and the addition of 4% Sasobit[®] started reducing it. This indicates that an optimum amount of Sasobit[®] was needed for increasing rutting resistance of PG 76-22M.
4. Overall conclusion from temperature sweep test and MSCR is that, addition of 1% and 2% Sasobit[®] increases the rutting resistance.
5. To understand if the increase in rutting resistance was caused by the increase in stiffness or by the internal molecular associations, a different set of MSCR test was performed. In this approach, equal-stiffness (1 kPa of $G^*/\sin\delta$) temperatures of 0%, 1%, 2% and 4% Sasobit[®] added asphalt binders were determined based on temperature sweep test results and MSCR test was performed on that equal-stiffness temperature. Results indicate that at higher

stress Sasobit[®] will make PG 64-22 rutting susceptible and at lower stress it will make PG 64-22 rutting resistant. Therefore, the true influence of Sasobit[®] on rutting of PG 64-22 is stress dependent.

6. MSCR test was performed at varying creep stresses, 0.1 kPa, 0.2 kPa, 0.5 kPa and 3.2 kPa at equal-stiffness temperature for PG 64-22. A general trend observed was that as the creep stress increased, the percent recovery decreased. It was concluded that the effect of creep stress on percent recovery is logarithmic.
7. A total of 60 samples were tested using an APA. It was found in this study that 2% Sasobit[®] reduced rutting susceptibility of Sasobit[®] modified hot mix asphalt. This finding was verified with higher asphalt content mixes. The fact that Sasobit[®] reduced rutting susceptibility of HMA was further verified with higher air void mixes. Sasobit[®] modified WMA mixed at 143 °C and compacted at 110 °C showed better rutting resistance than HMA. Sasobit[®] modified asphalt mixes prepared at 133 °C and 110 °C also reduced rutting susceptibility. A multiple variable regression rutting model using 60 samples were developed that predicted rutting depths with coefficient of determination of 0.89. Statistical analyses showed that Sasobit[®] reduced rutting resistance at 5% level of significance.
8. From aging evaluation of extracted asphalt binders it can be observed that aging indices of Sasobit[®] mixes are lower than without Sasobit[®] mixes. This indicates that Sasobit[®] mixes do not age as much as without Sasobit[®] mixes. Another important observation of this study is that the aging indices of 163 °C

mixes are higher than the aging indices of 133 °C mixes. This finding justifies the concern that lowering the production temperatures reduces aging and increases rutting susceptibility. Also, it was observed that reduction in aging index due to reduction in mixing temperature is higher for Sasobit[®] mixes than that of without Sasobit[®] mixes.

From an exploratory study it can be concluded that wax modified asphalt binders may be differentiated by its morphology using an AFM. Most importantly, the data obtained in an AFM can be quantified and asphalt has a unique bee-shape microstructure that can be used for evaluation. However, analyses of asphalt microstructure using the AFM still remains tedious and a standard method of testing is yet to be established for using it as a screening tool.

The following general conclusions and recommendations can be drawn from this study.

1. There exists a critical temperature for each asphalt binder below which viscosity will increase with addition of Sasobit[®]. Therefore, compaction below the critical temperature can negatively impact density. For PG 64-22, the critical temperature is 104 °C and for PG 76-22M, the critical temperature is about 101 °C.
2. With the addition of Sasobit[®], asphalt binders become a shear-thinning liquid even at compaction temperature ranges. The shear rate dependency increases with an increase in percent of Sasobit[®]. This indicates if the actual shear rate during the compaction process is higher than 6.8 s^{-1} , then the currently recommended viscosity as well as temperature is overestimated and

compaction temperature can be reduced. On the other hand, if the actual shear rate during the compaction process is lower than 6.8 s^{-1} , then the currently recommended viscosity as well as temperature is underestimated and a higher compaction temperature should be used.

3. An optimum amount of Sasobit[®] exists between 2% and 4% based on phase angle and non-recoverable creep compliance analyses of PG 64-22 and based on percent recovery of PG 76-22M. Currently used rutting factor $G^*/\sin\delta$ fails to indicate any optimum amount. Phase angle values suggest if rutting is performed at one grading higher temperature, an overdose of Sasobit[®] will increase rutting potential. Addition of Sasobit[®] increases rutting resistance at lower stress while it increases rutting potential at higher stress. APA rut depths indicate that Sasobit[®] mixes prepared at WMA temperatures performed better than HMA without Sasobit[®]. From aging evaluation of extracted asphalt binders it was revealed that reduced production temperatures reduces aging and may increase rutting susceptibility.
4. From very limited data it can be concluded that wax modified asphalt binders may be differentiated by its morphology using an AFM.

REFERENCES

- AASHTO T166. "Bulk Specific Gravity of Compacted Bituminous Mixtures Using Saturated Surface Dry Specimens." In *AASHTO Standards*. Washington, D.C.: American Association of State and Highway Transportation Officials, 2004.
- AASHTO T315. "Determining the Rheological Properties of Asphalt Binder Using a Dynamic Shear Rheometer (DSR)." In *AASHTO Standards*. Washington, D.C.: American Association of State and Highway Transportation Officials, 2004.
- AASHTO T316. "Standard Method of Test for Viscosity Determination of Asphalt Binder Using Rotational Viscometer." In *AASHTO Standards*. Washington, D.C.: American Association of State and Highway Transportation Officials, 2004.
- AASHTO T340. "Determining Rutting Susceptibility of Hot Mix Asphalt using the Asphalt Pavement Analyzer." In *AASHTO Standards*. Washington, D.C.: American Association of State and Highway Transportation Officials, 2004.
- AASHTO TP 30. "Standard Practice for Mixture conditioning of Hot Mix Asphalt." In *AASHTO Standards*. Washington, D.C.: American Association of State and Highway Transportation Officials, 2004.
- AASHTO TP 70. "Standard Method of Test for Multiple Stress Creep Recovery Test of Asphalt Binder using a Dynamic Shear Rheometer." In *AASHTO Standards*. Washington, D.C.: American Association of State and Highway Transportation Officials, 2009.
- Ali, Ayman W. "Laboratory Evaluation of Warm Asphalt Binders using Foamed Asphalt." Masters Thesis, Civil Engineering, University of Akron, 2010.
- Anderson, D.A., Y.M. Le Hir, J.P. Planche, and D. Martin. "Zero Shear Viscosity of Asphalt Binders." *Transportation Research Record: Journal of the Transportation Research Board* (Transportation Research Board of the National Academies) 1810 (2002): 54-62.
- Asphalt Institute*. 2012. <http://www.asphaltinstitute.org> (accessed 7/22/2012).
- Asphalt Institute. *The Asphalt Handbook, Manual Series No. 4*. Kentucky: The Asphalt Institute, 1989.
- Aspha-Min*[®]. 2012. <http://www.aspha-min.com/asphamin-en.html> (accessed 7/25/2012).

- ASTM. *Annual Book of ASTM standards: Road and Paving Materials; Traveled Surface Characteristics*. Vol. 04.03. West Conshohocken, PA, 2005.
- Azari, H., R.H. McCuen, and K.D. Stuart. "Optimum Compaction Temperature for Modified Binders." *Journal of Transportation Engineering* (American Society of Civil Engineers) 129, no. 5 (2003): 531-537.
- Bahia, H.U. *Recommendations for Mixing and Compaction Temperatures of Modified Asphalt Binders*. National Cooperative Highway Research Program, Report 9-10, Washington, D.C.: Transportation Research Council, 2000.
- Baker, H. *The Microscope Made Easy*. Lincolnwood, IL: Science Heritage Ltd. , 1987.
- Barthel, W., J.P. Machand, and M. Von Devivere. *Warm Asphalt Mixes by Adding a Synthetic Zeolite*. Vienna: Third Eurasphalt and Eurobitumen Congress, 2004.
- Bearsley, S., A. Forbes, and R.G. Haverkamp. "Direct Observation of the Asphaltene Structure in Paving Grade Bitumen Using Confocal Laser Microscopy." *Journal of Microscopy* 215 (2004): 149-155.
- Biro, S., T. Gandhi, and S. Amirkhanian. "Midrange Temperature Rheological Properties of Warm Asphalt Binders." *Journal of Materials in Civil Engineering* 21, no. 7 (July 2009): 316-323.
- Bonaquist, Ramon. *Mix Design Practices for Warm Mix Asphalt*. Technical Report, Sterling, VA: National Centre for Highway Research Program, 2011.
- Branthaver, J.F., M.W. Catalfomo, and J.C. Petersen. "Ion Exchange Chromatography Separation of SHRP Asphalts." *Fuel Science Technology International* 10 (1992): 855-885.
- Butz, T., I. Rahimian, and G. Hilderbrand. "Modifications of Road Bitumens with the Fischer-Tropsch Paraffin Sasobit®." *Journal of Applied Asphalt Binder Technology*, no. 2 (2001): 70-86.
- Claudy, P., J.M. Létoffé, G.N. King, and J.P. Planche. "Characterization of Asphalts Cements by Thermo Microscopy and Differential Scanning Calorimetry correlations to Classical Physical Properties." *Fuel Science Technology International* 10 (1992): 735-765.
- Cooper, S.B. Jr. *Evaluation of HMA Mixtures containing Sasobit®*. Baton Rouge, Louisiana: Louisiana Transportation Research Center, 2009.
- Corrigan, M. "Warm Mix Asphalt Technologies and Research." *Federal Highway Administration, Office of Pavement Technology, Washington D.C.* 2012. <http://www.fhwa.dot.gov/pavement/asphalt/wma.cfm> (accessed 7/25/2012).

- Cotton, F.A., G. Wiskinson, C.A. Murillo, and M. Bochmann. *Advanced Inorganic Chemistry*. Sixth edition. Newyork: Wiley-Interscience, n.d.
- D'Angelo, J, R. Kluttz, R. Dongre, K. Stephens, and L. Zanzotto. "Revision of the Superpave High Temperature binder Specification: The Multiple Stress Creep Recovery Test." *Journal of the Association of Asphalt Paving Technologists* 76 (2007): 123-162.
- D'Angelo, J., and R. Dongre. "Practical use of Multiple Stress Creep and Recovery Test Characterization of Styrene-Butadiene-Styrene Dispersion and other Additives in Polymer Modified Asphalt Binders." *Transportation Research Record: Journal of the Transportation Research Board* (Transportation Research Board of the National Academies) 2126 (2009): 73-82.
- D'Angelo, John. "Multiple Stress Creep and Recovery Test Method: New Specification." Federal Highway Administration, 2008.
- D'Angelo, John, et al. *Warm Mix Asphalt: European Practice*. Technical Report, Federal Highway Administration, 2008.
- Dickie, J.P., M.N. Haller, and T.F. Yen. "Electron Microscopic Investigations of the Nature of Petroleum Asphaltics." *Journal of Colloid Interface Science* 29 (1969): 475-484.
- Diefenderfer, S., and A. Hearon. *Laboratory Evaluation of a Warm Mix Asphalt Technology for use in Virginia*. Research Report, Virginia Transportation Research Council, 2008.
- Donnet, J.P., J. Ducret, E. Papirer, and M. Kennel. "Étude des bitumes routiers par microscopie électronique." *Journal of Microscopie* 17 (1973): 139-144.
- Dykstra, H., K. Beu, and D.L. Karz. "Precipitation of Asphalt from Crude Oil by Flow through Silica." *Oil and Gas Journal* 43, 79, 82, 102, 104 (1944).
- Edwards, Y., and P. Redelius. "Rheological Effects of Waxes in Bitumen." *Energy and Fuel* 17, no. 3 (2003): 511-520.
- Edwards, Y., Y. Tasdemir, and P. Redelius. "Rheological Effects of Commercial Waxes and Polyphosphoric Acid in Bitumen 160/220 Low Temperature Performance." *Fuel* 85 (2006): 989-997.
- Estakhri, C.P., J. Button, and A.E. Alvarez. "Field and Laboratory Investigation of Warm Mix Asphalt in Texas." Austin, Texas 78763-5080, 2010.
- Eurovia Services*. 2012. <http://www.eurovia.com/en/produit/135.aspx> (accessed 7/22/2012).

- Federal Highway Administration*. 2012.
<http://www.fhwa.dot.gov/pavement/asphalt/wma.cfm> (accessed 7/25/2012).
- Ferry, J.D. *Viscoelastic Properties of Polymers*. New York: John Wiley & Sons, 1980.
- Freund, M., and S. Vajta. *Untersuchung der Bitumen Struktur Mitdem Elecktronen Mikroskop*. Vols. 13-18. ErdölKhole, 1958.
- Gandhi, T. "Effects of Warm Asphalt Additives on Asphalt Binder and Mixtures Properties." PhD Thesis, Clemson, South Carolina, 2008.
- Haggag, M.M., W.S. Mogawer, and R. Bonaquist. "Fatigue Evaluation of Warm-Mix Asphalt Mixtures." *Transportation Research Record: Journal of the Transportation Research Board* (Transportation Research Board of the National Academies) 2208 (2011): 26-32.
- Hossain, Z., A. Bhudhala, M. Zaman, E. O'Rear, and S. Cross. "Evaluation Of The Use Of Warm Mix Asphalt As A Viable Paving Material In The United States." A report submitted to the Federal Highway Administration, Oklahoma State University, 2009.
- Hurley, G., and B. Prowell. "Evaluation of Potential Process for use in Warm Mix Asphalt." *Journal of the Association of Asphalt Paving Technologist* 75 (2006): 41-90.
- Hurley, G.C., and B.D. Prowell. *Evaluation of Aspha-Min[®] Zeolite for use in Warm Mix Asphalt*. NCAT Report 05-04, Auburn, Ala: National Center for Asphalt Technology, 2005.
- Hurley, G.C., and B.D. Prowell. *Evaluation of Sasobit[®] for use in Warm Mix Asphalt*. NCAT Report 05-06, Auburn, Ala: National Center for Asphalt Technology, 2005.
- Kanitpong, K., S. Sonthong, K. Nam, W. Martono, and H. Bahia. *Laboratory Study on Warm Mix Asphalt Additives*. Washington, D.C.: Presented at the 86th Annual Meeting of the Transportation Research Board, 2007.
- Kenndy, T. W., Y. Yildirim, and M. Slaimanian. "Mixing and Compaction Temperatures for Superpave Mixes." *Association of Asphalt Paving Technologist*, 2000.
- Khatri, A., H.U. Bahia, and D. Hanson. "Mixing and Compaction Temperatures for Modified Binders Using the Superpave Gyrotory Compactor." *Journal of the Association of Asphalt Paving Technologists* 70 (2001): 368-402.
- Kim, H.S., S.J. Lee, and S.N. Amirkhanian. "Effects of Warm Mix Asphalt Additives on Performance Properties of Polymer Modified Asphalt Binders." *Canadian Journal of Civil Engineering* 37 (2010): 17-24.

- Koenders, B G., et al. "Innovative Process in Asphalt Production and Application to Obtain Lower Operating Temperatures." *Second Eurasphalt & Eurobitumen Congress*. Barcelona, Spain, 2000.
- Kristansdottir, O., S.T. Muench, L. Michael, and G. Burke. "Assessing the Potential for Warm Mix Asphalt Technology Adoption." *Presented at the 86th Annual Meeting of the Transportation Research Board*. Washington D.C., 2007.
- Kuennen, T. *Warm Mixes are a Hot Topic*. Des Plaines, Illinois: Better Roads, James Informational Media, Inc., 2004.
- Lange, C.R., and M. Stroup-Gardiner. "Temperature-Dependent Chemical-Specific Emission Rates of Aromatics and Polyaromatic Hydrocarbons (pahs) in Bitumen Fume." *Journal of Occupational and Environmental Hygiene*, 2007: 72-76.
- Lee, S-J., S. Amirkhani, C. Thodesen, and K. Shantanawi. "Effects of Compaction Temperature on Rubberized Asphalt Mixes." *Proceedings of the Asphalt Rubber*. California: Pam Springs, 2006: 583-597.
- Levy, D.F. "Fundamental Viscosity and How it is Measured." *ASTM Special Technical Publication*. New York: American Society of Testing and Materials, 1962: 3-20.
- Liu, J., S. Sabounddijan, P. Li, B. Connor, and B. Brunette. "Laboratory Evaluation of Sasobit[®]-modified Warm Mix Asphalt for Alaskan Conditions." *Journal of Materials in Civil Engineering* 23, no. 11 (2011): 1498-1505.
- Loeber, L., O. Sutton, J. Morel, J.M. Valleton, and G. Muller. "New Direct Observations of Asphalts and Asphalt binders by Scanning Electron Microscopy and Atomic Force Microscopy." *Journal of Microscopy* 182 (1996): 32-39.
- Maupin, G.W., and D.W. Mokarem. *Investigation of Proposed AASHTO Rut Test Procedure Using the Asphalt Pavement Analyzer*. Final Report, Charlottesville: Virginia Transportation Research Council, 2006.
- MeadWestvaco*. 2007. <http://www.meadwestvaco.com/asphalt.nsf/v/evotherm> (accessed 7/22/2012).
- Menard, K.P. *Dynamic Mechanical Analysis: A Partial Introduction*. CRC Press, 1999.
- Middleton, B., and R.W. Forfylyow. "Evaluation Of Warm Mix Asphalt Produced With The Double Barrel Green Process." *Transportation Research Record: Journal of the Transportation Research Board* (Transportation Research Board of the National Academies) 2126 (2009): 19-26.

- Mogawer, W.S., A.J. Austerman, and H.U. Bahia. "Evaluating the Effect of Warm-Mix Asphalt Technologies on Moisture Characteristics of Asphalt Binders and Mixtures." *Transportation Research Record: Journal of the Transportation Research Board* (Transportation Research Board of the National Academies) 2209 (2011): 52-60.
- Pauli, A.T., J.F. Branthaver, R.E. Robertson, and W. Grimes. "Atomic Force Microscopy Investigation of SHRP Asphalts." *Symposium on Heavy Oil and Resid Compatibility and Stability, Petroleum Chemistry Division*. San Diego, California, USA: American Chemical Society, 2001.
- Pavement Interactive*. 2012. <http://www.pavementinteractive.com> (accessed 7/25/2012).
- Peyrot, J. "Nouvelle méthode d'étude des bitumes par microscopie électronique." *Bull. Liasion Labo. Ponts Chaussees* 68 (1973): 12-15.
- Pfeffer, J.P., and R.N.J. Saal. "Asphaltic Bitumen as a Colloid System." *Journal of Physics Chemistry*, 1940: 139-149.
- Pieri, N., and J.P. Planche. "Caractérisation structurale des bitumes routiers par IRTF et fluorescence UV en mode excitation-émission synchrones." *Analisis* 24 (1996): 13-122.
- Prowell, B.D., G.C. Hurley, and B. Frank. *Warm Mix Asphalt: Best Practices Third Edition*. Quarterly Improvement Publication, Lanham, Maryland: National Asphalt Pavement Association, 2012.
- Prowell, B.D., G.C. Hurley, and E. Crews. "Field Performance of Warm Mix asphalt at National Center for Asphalt Technology Test Track." *Transportation Research Record: Journal of the Transportation Research Board* (Transportation Research Board of the National Academies) 1998 (2007): 96-102.
- Rajagopal, A. *Comparison and Definition of State DOT's Practices in Selection of Materials for Pavements*. Technical Report, Ohio Department of Transportation and the Federal Highway Administration, 2004.
- Reinke, G. *Use of Hamburg Rut Testing Data to Validate the Use of J_{nr} as a Performance Parameter for High Temperature Permanent Deformation*. Transportation Research Circular No. EC 147, 2010.
- Sargand, S., M.D. Nazzal, A. Al-Rawashdeh, and D. Powers. "Field Evaluation of Warm Mix Asphalt Technologies." *Journal of Materials in Civil Engineering* (American Society of Civil Engineers), 2011.
- Sasol Wax*. 2012. http://www.sasolwax.com/Sasobit_Technology.html (accessed 7/22/2012).

- Shen, J., S.N. Amirkhani, and S.J. Lee. *Effects of Rejuvenating Agents on Recycled Aged Rubber Modified Binders*. Transportation Research Board, 84th Annual Meeting, Compendium of Papers CD ROM, 2005.
- Speight, J.G. "The Chemistry and Technology of Petroleum." Edited by 3rd. *Marcel Dekker*, 1999: 237-404.
- Stark, M., and R. Guckengerger. "Fast Low Cost Phase Detection Setup for Tapping-Mode Atomic Force Microscopy." *Review of Scientific Instruments*, 1999: 3614-3619.
- Stuart, K.D. *Methodology for Determining Compaction Temperatures for Modified Asphalt Binders*. Draft FHWA Report, McLean, VA.: Federal Highway Administration, 2000.
- Sutton, C.L. *Hot Mix Blue Smoke Emissions*. Technical Paper T-143, Astec Industries, Inc, 2002.
- Sybliski, D. "Zero-Shear Viscosity of Bituminous Binder and its Relation to Bituminous Mixture's Rutting Resistance." *Transportation Research Record: Journal of the Transportation Research Board* (Transportation Research Board of the National Academies) 1535 (1996): 15-21.
- Tabatabaee, N., and H.A. Tabatabaee. "Multiple Stress Creep and Recovery and Time Sweep Fatigue Tests: Crumb Rubber Modified Binder and Mixture Performance." *Transportation Research Record: Journal of the Transportation Research Board* (Transportation Research Board of the National Academies) 2180 (2010): 67-74.
- Tao, M., and R. Mallick. "An Evaluation of the Effects of Warm Mix Asphalt Additives on Workability and Mechanical Properties of Reclaimed Asphalt Pavement Material." *Transportation Research Record: Journal of the Transportation Research Board* (Transportation Research Board of the National Academies) 2126 (2009): 151-160.
- USEPA. *Hot Mix Asphalt Plants - Emissions Assessment Report*. Technical Report, Research Triangle Park, NC: Emissions Monitoring and Analysis Division, Office of Air Quality Planning and Standards, United States Environmental Protection Agency, 2000.
- Warm Mix Asphalt: European Practice*. 2008.
http://international.fhwa.dot.gov/pubs/pl08007/wma_08_d.cfm (accessed 7/22/2012).
- Wasiuddin, N.M., M.M. Zaman, and E.A. O'Rear. "Effect of Sasobit® and Aspha-Min® on Wettability and Adhesion between Asphalt Binders and Aggregates." *Transportation Research Record: Journal of the Transportation Research Board* (Transportation Research Board of the National Academies) 2051 (2008): 80-89.

- Wasiuddin, N.M., R. Saha, and B. Jr. King. "Effects of a Wax-based Warm Mix Additive on Lower Compaction Temperatures." *Geotechnical Special Publication (211 GSP)*. 2011: 4614-4623.
- Wasiuddin, N.M., S. Selvamohan, M.M. Zaman, and M.L.T. Guegan. "A Comparative Laboratory Study of Sasobit[®] and Aspha-Min[®] in Warm Mix Asphalt." *Transportation Research Record: Journal of the Transportation Research Board* (Transportation Research Board of the National Academies) 1998 (2007): 82-88.
- Witczak, M.W., K. Kaloush, T. Pellinen, M. El-Basyouny, and V.H. Quintus. *Simple Performance Test for Superpave Mix Design*. NCHRP Report 465, Washington D.C.: National Cooperative Highway Research Program, 2002.
- Xiao, F., J. Jordan, and S.N. Amirkhanian. "Laboratory Investigation of Moisture Damage in Warm Mix Asphalt containing Moist Aggregate." *Transportation Research Record: Journal of the Transportation Research Board* (Transportation Research Board of the National Academies) 2126 (2009): 151-160.
- Xiao, F., J. Jordan, and S.N. Amirkhanian. "Laboratory Investigation of Moisture Damage in Warm Mix Asphalt containing Moist Aggregate." *88th Annual Meeting of the Transportation Research Board*. Washington, D.C.: Transportation Research Board of the National Academies, 2009.
- Xiao, F., S. Amirkhanian, B. Putman, and J. Shen. "Laboratory Investigation of Engineering Properties of Rubberized Asphalt Mixtures Containing Reclaimed Asphalt Pavement." *Candaian Journal of Civil Engineering* 37, no. 11 (November 2010): 1414-1422.
- Xiao, F., S.N. Amirkhanian, and B.J. Putman. "Evaluation of Rutting Resistance in Warm Mix Asphalt Containing Moist Aggregate." *Transportation Research Record: Journal of the Transportation Research Board* (Transportation Research Board of the National Academies) 2180 (2010): 75-84.
- Xiao, F., S.N. Amirkhanian, and C.H. Juang. "Rutting Resistance of Rubberized Asphalt Concrete Pavements Containing Reclaimed Asphalt Pavement Mixtures." *Journal of Materials in Civil Engineering* 19 (6) (June 2007): 475-483.
- Yildirim, Y., M. Solaimanian, and T.W. Kennedy. "Mixing and Compaction Temperatures for Superpave Mixes." *Proceedings of the Association of Asphalt Paving Technologists*. 2000. 34-71.
- Zaumanis, M. "Warm Mix Asphalt Investigation." Master of Science Thesis, Civil Engineering, Technical University of Denmark, 2010.
- Zhong, Q., D. Inness, K. Kjoller, and V.B. Elings. "Fractured Polymer/Silica Fiber Surface Studied by Tapping Mode Atomic Force Microscopy." *Surface Science Letters* 290 (1993): L688-L692.

APPENDIX A

RHEOLOGICAL DATA

MEASUREMENT OF ASPHALT BINDER VISCOSITY

Asphalt binders are visco-elastic. They behave partly like an elastic solid (deformation due to loading is recoverable – it is able to return to its original shape after a load is removed) and partly like a viscous liquid (deformation due to loading is non-recoverable – it cannot return to its original shape after a load is removed) (Pavement Interactive, 2012).

Currently, rotational viscometer has been in use for the measurement of viscosity. The viscosity of asphalt binder at high temperatures is important because it can control pumpability, mixability and workability. The basic rotational viscometer test measures the torque required to maintain a constant rotational speed (20 rpm) of a cylindrical spindle submerged in an asphalt binder at a constant temperature (typically 275 °F (135 °C)). This torque is converted to a dynamic viscosity and automatically displayed by the Rotational viscometer. Viscosity is calculated by the following equations (Pavement Interactive, 2012):

$$\eta = \frac{\tau}{\gamma}, \quad \text{eqn - 1}$$

$$\tau = \frac{T}{2\pi R_s^2 L}, \quad \text{eqn - 2}$$

$$\gamma = \frac{2\omega R_c^2 R_s^2}{x^2 (R_c^2 - R_s^2)}, \quad \text{eqn - 3}$$

where

η = Viscosity (Pa s),

τ = Shear Stress (N/cm²),

γ = Shear Rate (sec^{-1}),

T = Torque (in N m),

L = Effective spindle length (m),

R_s = Spindle Radius (m),

R_c = Container Radius (m),

ω = Rotational Speed (radians/second),

x = radial location where shear rate is being calculated (m).

However, the field compaction temperature may go down to as low as 80 °C which is far below the practical range of a rotational viscometer to be used. In the present study, a DSR has been used to find asphalt binder viscosity at compaction temperatures.

The DSR measures a specimen's complex shear modulus (G^*) and phase angle (δ). The G^* means the sample's total resistance to deformation when repeatedly sheared, while δ , is the lag between the applied shear stress and the resulting shear strain (As shown in Figure A-1 and A-2)

The larger the δ , the more viscous the material. δ limiting values are:

- Purely elastic material: $\delta = 0^\circ$
- Purely viscous material: $\delta = 90^\circ$

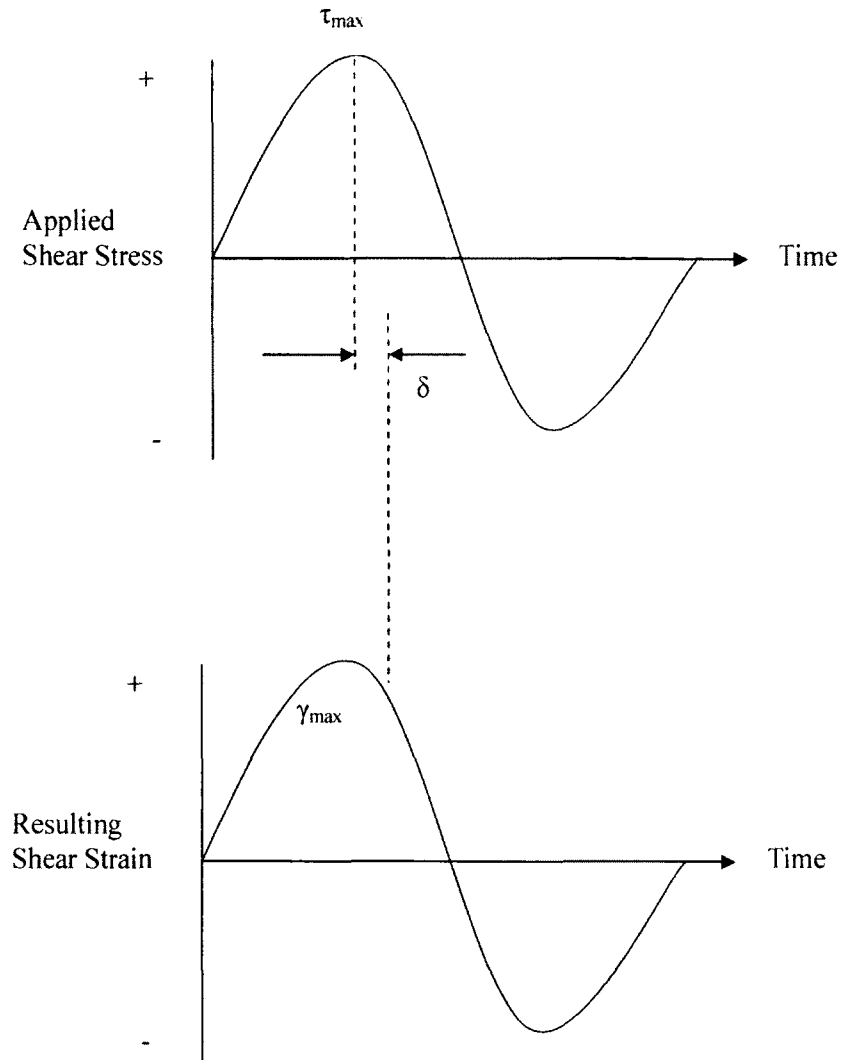


Figure A-1. DSR applied shearing stress and strain

The specified DSR oscillation rate of 10 radians/second (1.59 Hz) is meant to simulate traffic speed of about 55 mph (90 km/hr) shearing action. G^* and δ are used as predictors of HMA rutting and fatigue cracking. Early in pavement life rutting is the main concern, while later in pavement life fatigue cracking becomes the major concern (Pavement Interactive, 2012).

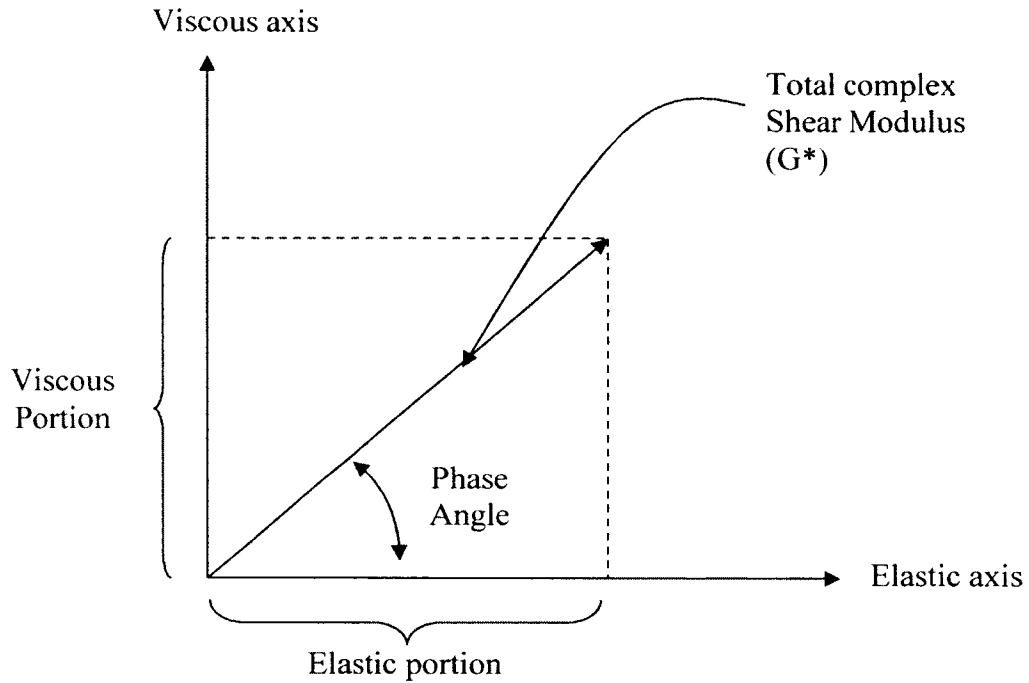


Figure A-2. Complex modulus elaboration

Dynamic viscosity as defined in Equation 4 has been used in this study to characterize lower compaction temperature characteristics of asphalt binder.

$$\eta' = \frac{G''}{\omega}, \quad \text{eqn - 4}$$

where

G'' = Elastic Modulus, Pa; ω = Angular velocity, radian/sec.

Table A-1. PG 64-22 with 0% Sasobit[®] sample 1

| Temperature °C | Angular frequency (rad/sec) | % Strain | Delta, degrees | η' Pas | $G^*/\sin\delta$ kPa |
|-------------------|--------------------------------|----------|----------------|----------------|-------------------------|
| 28 | 10 | 12 | 66.63 | 60100 | 713.3 |
| 34 | | | 71.25 | 21830 | 243.5 |
| 40 | | | 74.31 | 9020 | 97.32 |
| 46 | | | 77.29 | 3664 | 38.51 |
| 52 | | | 80.16 | 1508 | 15.53 |
| 58 | | | 82.64 | 646.2 | 6.569 |
| 64 | | | 84.63 | 291.8 | 2.943 |
| 70 | | | 86.26 | 137.8 | 1.384 |
| 76 | | | 87.54 | 68.44 | 0.6856 |
| 82 | | | 88.46 | 36.03 | 0.3605 |
| 88 | | | 89.03 | 20.21 | 0.2021 |
| 94 | | | 89.17 | 11.9 | 0.119 |
| 100 | | | 89.09 | 7.323 | 0.07325 |
| 106 | | | 89.15 | 4.684 | 0.04685 |
| 112 | | | 88.69 | 3.108 | 0.0311 |
| 118 | | | 88 | 2.151 | 0.02153 |
| 124 | | | 87.83 | 1.528 | 0.0153 |
| 130 | 87.1 | 1.11 | 0.01113 | | |

Table A-2. PG 64-22 with 0% Sasobit[®] sample 2

| Temperature °C | Angular frequency (rad/sec) | % Strain | Delta, degrees | η' Pas | $G^*/\sin\delta$ kPa |
|-------------------|--------------------------------|----------|----------------|----------------|-------------------------|
| 28 | 10 | 12 | 66.12 | 58270 | 696.8 |
| 34 | | | 70.97 | 22090 | 247.2 |
| 40 | | | 74.08 | 9211 | 99.61 |
| 46 | | | 77.07 | 3781 | 39.8 |
| 52 | | | 79.95 | 1569 | 16.19 |
| 58 | | | 82.46 | 674.7 | 6.865 |
| 64 | | | 84.49 | 307 | 3.099 |
| 70 | | | 86.11 | 147.1 | 1.478 |
| 76 | | | 87.39 | 73.37 | 0.7352 |
| 82 | | | 88.34 | 38.94 | 0.3897 |
| 88 | | | 88.94 | 21.81 | 0.2182 |
| 94 | | | 88.96 | 12.85 | 0.1286 |
| 100 | | | 88.88 | 7.934 | 0.07937 |
| 106 | | | 88.72 | 5.114 | 0.05117 |
| 112 | | | 88.22 | 3.41 | 0.03413 |
| 118 | | | 87.86 | 2.383 | 0.02386 |
| 124 | | | 86.35 | 1.707 | 0.01714 |
| 130 | 86.13 | 1.262 | 0.01268 | | |

Table A-3. PG 64-22 with 1% Sasobit[®] sample 1

| Temperature °C | Angular frequency (rad/sec) | % Strain | Delta, degrees | η' Pa s | $G^*/\sin\delta$ kPa |
|---------------------------|--|-----------------|-----------------------|------------------------------------|--|
| 28 | 10 | 12 | 63.98 | 67050 | 830.4 |
| 34 | | | 70.10 | 23230 | 262.9 |
| 40 | | | 73.12 | 9434 | 103 |
| 46 | | | 75.86 | 3943 | 41.92 |
| 52 | | | 78.43 | 1700 | 17.71 |
| 58 | | | 80.65 | 777.3 | 7.984 |
| 64 | | | 82.23 | 385.2 | 3.922 |
| 70 | | | 83.89 | 191.2 | 1.934 |
| 76 | | | 84.88 | 97.12 | 0.9789 |
| 82 | | | 85.72 | 49.94 | 0.5021 |
| 88 | | | 86.11 | 25.9 | 0.2603 |
| 94 | | | 85.69 | 14.05 | 0.1412 |
| 100 | | | 85.19 | 7.597 | 0.07651 |
| 106 | | | 83.59 | 4.263 | 0.04317 |
| 112 | | | 80.70 | 2.891 | 0.0297 |
| 118 | | | 81.88 | 2.344 | 0.02391 |
| 124 | | | 71.83 | 1.468 | 0.01625 |
| 130 | 65.18 | 1.07 | 0.01299 | | |

Table A-4. PG 64-22 with 1% Sasobit[®] sample 2

| Temperature °C | Angular frequency (rad/sec) | % Strain | Delta, degrees | η' Pa s | $G^*/\sin\delta$ kPa |
|---------------------------|--|-----------------|-----------------------|------------------------------------|--|
| 28 | 10 | 12 | 63.22 | 67130 | 842.2 |
| 34 | | | 69.39 | 23280 | 265.6 |
| 40 | | | 72.48 | 9609 | 105.6 |
| 46 | | | 75.24 | 4053 | 43.34 |
| 52 | | | 77.97 | 1743 | 18.22 |
| 58 | | | 80.35 | 790 | 8.129 |
| 64 | | | 82.18 | 390.7 | 3.98 |
| 70 | | | 83.73 | 198.5 | 2.009 |
| 76 | | | 84.93 | 101.5 | 1.023 |
| 82 | | | 85.84 | 52.74 | 0.5302 |
| 88 | | | 86.54 | 27.28 | 0.2738 |
| 94 | | | 86.34 | 14.63 | 0.1469 |
| 100 | | | 85.65 | 7.932 | 0.07978 |
| 106 | | | 83.83 | 4.443 | 0.04495 |
| 112 | | | 80.86 | 2.994 | 0.03072 |
| 118 | | | 76.96 | 2.1 | 0.02212 |
| 124 | | | 71.84 | 1.541 | 0.01707 |
| 130 | 66.38 | 1.092 | 0.01301 | | |

Table A-5. PG 64-22 with 2% Sasobit[®] sample 1

| Temperature °C | Angular frequency (rad/sec) | % Strain | Delta, degrees | η' Pa s | $G^*/\sin\delta$ kPa |
|---------------------------|--|-----------------|-----------------------|------------------------------------|--|
| 28 | 10 | 12 | 57.27 | 1.61E+05 | 2274 |
| 34 | | | 68.68 | 58080 | 669.4 |
| 40 | | | 71.52 | 15870 | 176.5 |
| 46 | | | 73.43 | 7128 | 77.58 |
| 52 | | | 75.57 | 3211 | 34.23 |
| 58 | | | 77.57 | 1465 | 15.35 |
| 64 | | | 79.83 | 660.1 | 6.814 |
| 70 | | | 81.81 | 307.1 | 3.135 |
| 76 | | | 83.48 | 152.7 | 1.547 |
| 82 | | | 84.72 | 79.51 | 0.8019 |
| 88 | | | 85.51 | 42.07 | 0.4233 |
| 94 | | | 86.12 | 21.76 | 0.2187 |
| 100 | | | 86.51 | 10.77 | 0.1081 |
| 106 | | | 88.77 | 4.349 | 0.04351 |
| 112 | | | 90.00 | 2.494 | 0.02495 |
| 118 | | | 90.00 | 1.736 | 0.01737 |
| 124 | 87.71 | 1.249 | 0.0125 | | |
| 130 | 87.63 | 0.9307 | 9.32E-03 | | |

Table A-6. PG 64-22 with 2% Sasobit[®] sample 2

| Temperature °C | Angular frequency (rad/sec) | % Strain | Delta, degrees | η' Pa s | $G^*/\sin\delta$ kPa |
|---------------------------|--|-----------------|-----------------------|------------------------------------|--|
| 28 | 10 | 12 | 58.78 | 1.74E+05 | 2379 |
| 34 | | | 68.32 | 47460 | 549.6 |
| 40 | | | 71.36 | 19430 | 216.5 |
| 46 | | | 73.48 | 8469 | 92.14 |
| 52 | | | 75.67 | 3648 | 38.86 |
| 58 | | | 77.82 | 1564 | 16.37 |
| 64 | | | 80.05 | 678.2 | 6.991 |
| 70 | | | 81.96 | 313.2 | 3.194 |
| 76 | | | 83.52 | 156 | 1.58 |
| 82 | | | 84.75 | 81.35 | 0.8203 |
| 88 | | | 85.55 | 42.71 | 0.4296 |
| 94 | | | 85.95 | 21.8 | 0.2191 |
| 100 | | | 86.36 | 10.77 | 0.1081 |
| 106 | | | 88.11 | 4.365 | 0.0437 |
| 112 | | | 88.27 | 2.58 | 0.02582 |
| 118 | | | 88.13 | 1.806 | 0.01808 |
| 124 | | | 87.01 | 1.317 | 0.01321 |
| 130 | 87.22 | 0.9774 | 9.80E-03 | | |

Table A-7. PG 64-22 with 4% Sasobit[®] sample 1

| Temperature °C | Angular frequency (rad/sec) | % Strain | Delta, degrees | η' Pa s | $G^*/\sin\delta$ kPa |
|-------------------|--------------------------------|----------|----------------|-----------------|-------------------------|
| 28 | 10 | 12 | 56.76 | 1.49E+05 | 2131 |
| 34 | | | 69.06 | 39660 | 454.6 |
| 40 | | | 72.07 | 15530 | 171.5 |
| 46 | | | 73.49 | 6719 | 73.09 |
| 52 | | | 74.7 | 2950 | 31.7 |
| 58 | | | 76.03 | 1297 | 13.77 |
| 64 | | | 77.97 | 570.6 | 5.965 |
| 70 | | | 79.78 | 265.1 | 2.737 |
| 76 | | | 81.12 | 133.1 | 1.363 |
| 82 | | | 81.9 | 71.84 | 0.733 |
| 88 | | | 81.96 | 39.7 | 0.4049 |
| 94 | | | 81.82 | 20.66 | 0.2108 |
| 100 | | | 81.74 | 9.415 | 0.09614 |
| 106 | | | 84.96 | 3.245 | 0.0327 |
| 112 | | | 87.61 | 1.606 | 0.01609 |
| 118 | | | 86.81 | 1.165 | 0.01168 |
| 124 | | | 86.15 | 0.8813 | 8.85E-03 |
| 130 | 84.68 | 0.6719 | 6.78E-03 | | |

Table A-8. PG 64-22 with 4% Sasobit[®] sample 2

| Temperature °C | Angular frequency (rad/sec) | % Strain | Delta, degrees | η' Pa s | $G^*/\sin\delta$ kPa |
|---------------------------|--|-----------------|-----------------------|------------------------------------|--|
| 28 | 10 | 12 | 58.78 | 1.63E+05 | 2228 |
| 34 | | | 70.08 | 42810 | 484.3 |
| 40 | | | 72.68 | 16860 | 185 |
| 46 | | | 74.25 | 7261 | 78.38 |
| 52 | | | 75.74 | 3152 | 33.55 |
| 58 | | | 77.35 | 1375 | 14.44 |
| 64 | | | 79.37 | 602.8 | 6.24 |
| 70 | | | 81.33 | 276.2 | 2.827 |
| 76 | | | 82.85 | 134.1 | 1.362 |
| 82 | | | 83.82 | 71.26 | 0.721 |
| 88 | | | 84.22 | 39.4 | 0.398 |
| 94 | | | 84.1 | 21.06 | 0.2129 |
| 100 | | | 83.87 | 10.26 | 0.1038 |
| 106 | | | 84.08 | 3.805 | 0.03846 |
| 112 | | | 82.75 | 1.962 | 0.01994 |
| 118 | | | 85.71 | 1.596 | 0.01605 |
| 124 | | | 84.8 | 1.037 | 0.01045 |
| 130 | 84.74 | 0.7597 | 7.66E-03 | | |

Table A-9. PG 76-22M with 0% Sasobit[®] sample 1

| Temperature °C | Angular frequency (rad/sec) | % Strain | Delta, degrees | η' Pa s | $G^*/\sin\delta$ kPa |
|---------------------------|--|-----------------|-----------------------|------------------------------------|--|
| 28 | 10 | 12 | 61.37 | 52490 | 681.4 |
| 34 | | | 64.64 | 19420 | 237.7 |
| 40 | | | 65.43 | 8864 | 107.2 |
| 46 | | | 65.59 | 4286 | 51.68 |
| 52 | | | 65.74 | 2185 | 26.28 |
| 58 | | | 66.08 | 1168 | 13.97 |
| 64 | | | 66.78 | 644.6 | 7.631 |
| 70 | | | 67.93 | 364.3 | 4.243 |
| 76 | | | 69.48 | 214.3 | 2.443 |
| 82 | | | 71.38 | 126.9 | 1.413 |
| 88 | | | 73.75 | 77.26 | 0.8382 |
| 94 | | | 76.23 | 47.58 | 0.5044 |
| 100 | | | 78.58 | 30.08 | 0.313 |
| 106 | | | 80.94 | 19.54 | 0.2004 |
| 112 | | | 82.86 | 12.71 | 0.1291 |
| 118 | | | 84.61 | 8.295 | 0.08367 |
| 124 | | | 85.48 | 5.758 | 0.05793 |
| 130 | 87.10 | 3.892 | 0.03903 | | |

Table A-10. PG 76-22M with 0% Sasobit[®] sample 2

| Temperature °C | Angular frequency (rad/sec) | % Strain | Delta, degrees | η' Pa s | $G^*/\sin\delta$ kPa |
|---------------------------|--|-----------------|-----------------------|------------------------------------|--|
| 28 | 10 | 12 | 61.37 | 52490 | 681.4 |
| 34 | | | 64.64 | 19420 | 237.7 |
| 40 | | | 65.43 | 8864 | 107.2 |
| 46 | | | 65.59 | 4286 | 51.68 |
| 52 | | | 65.74 | 2185 | 26.28 |
| 58 | | | 66.08 | 1168 | 13.97 |
| 64 | | | 66.78 | 644.6 | 7.631 |
| 70 | | | 67.93 | 364.3 | 4.243 |
| 76 | | | 69.48 | 214.3 | 2.443 |
| 82 | | | 71.38 | 126.9 | 1.413 |
| 88 | | | 73.75 | 77.26 | 0.8382 |
| 94 | | | 76.23 | 47.58 | 0.5044 |
| 100 | | | 78.58 | 30.08 | 0.313 |
| 106 | | | 80.94 | 19.54 | 0.2004 |
| 112 | | | 82.86 | 12.71 | 0.1291 |
| 118 | | | 84.61 | 8.295 | 0.08367 |
| 124 | | | 85.48 | 5.758 | 0.05793 |
| 130 | 87.10 | 3.892 | 0.03903 | | |

Table A-11. PG 76-22M with 1% Sasobit® sample 1

| Temperature °C | Angular frequency (rad/sec) | % Strain | Delta, degrees | η' Pa s | $G^*/\sin\delta$ kPa |
|---------------------------|--|-----------------|-----------------------|------------------------------------|--|
| 28 | 10 | 12 | 57.42 | 70040 | 986.5 |
| 34 | | | 62.62 | 25190 | 319.4 |
| 40 | | | 63.7 | 11520 | 143.4 |
| 46 | | | 63.9 | 5634 | 69.87 |
| 52 | | | 64.05 | 2861 | 35.39 |
| 58 | | | 64.4 | 1478 | 18.17 |
| 64 | | | 65.23 | 766.2 | 9.294 |
| 70 | | | 66.36 | 426.3 | 5.08 |
| 76 | | | 67.86 | 251 | 2.926 |
| 82 | | | 69.8 | 147.7 | 1.677 |
| 88 | | | 72.05 | 86.96 | 0.9609 |
| 94 | | | 74.52 | 50.39 | 0.5426 |
| 100 | | | 77.11 | 28.94 | 0.3046 |
| 106 | | | 80.1 | 16.59 | 0.171 |
| 112 | | | 82.33 | 10.75 | 0.1095 |
| 118 | | | 84.08 | 7.186 | 0.07263 |
| 124 | | | 85.41 | 4.909 | 0.04941 |
| 130 | 86.26 | 3.434 | 0.03449 | | |

Table A-12. PG 76-22M with 1% Sasobit[®] sample 2

| Temperature °C | Angular frequency (rad/sec) | % Strain | Delta, degrees | η' Pa s | $G^*/\sin\delta$ kPa |
|---------------------------|--|-----------------|-----------------------|------------------------------------|--|
| 28 | 10 | 12 | 57.32 | 84840 | 1198 |
| 34 | | | 62.68 | 27270 | 345.5 |
| 40 | | | 63.81 | 12060 | 149.8 |
| 46 | | | 63.98 | 5837 | 72.28 |
| 52 | | | 64.12 | 2944 | 36.37 |
| 58 | | | 64.46 | 1546 | 18.98 |
| 64 | | | 65.23 | 825.5 | 10.01 |
| 70 | | | 66.34 | 467.7 | 5.575 |
| 76 | | | 67.86 | 275 | 3.205 |
| 82 | | | 69.81 | 160.1 | 1.817 |
| 88 | | | 72.09 | 93.05 | 1.028 |
| 94 | | | 74.59 | 53.94 | 0.5804 |
| 100 | | | 77.17 | 31.63 | 0.3327 |
| 106 | | | 80.14 | 18.35 | 0.1891 |
| 112 | | | 82.42 | 11.94 | 0.1215 |
| 118 | | | 84.25 | 7.961 | 0.08042 |
| 124 | | | 85.69 | 5.438 | 0.05469 |
| 130 | 86.6 | 3.792 | 0.03806 | | |

Table A-13. PG 76-22M with 2% Sasobit[®] sample 1

| Temperature °C | Angular frequency (rad/sec) | % Strain | Delta, degrees | η' Pa s | $G^*/\sin\delta$ kPa |
|---------------------------|--|-----------------|-----------------------|------------------------------------|--|
| 28 | 10 | 12 | 55.48 | 1.13E+05 | 1664 |
| 34 | | | 63.29 | 42760 | 535.8 |
| 40 | | | 63.91 | 12900 | 159.9 |
| 46 | | | 63.66 | 6402 | 79.71 |
| 52 | | | 63.68 | 3298 | 41.05 |
| 58 | | | 63.98 | 1748 | 21.65 |
| 64 | | | 64.82 | 925.7 | 11.3 |
| 70 | | | 66.17 | 505.6 | 6.042 |
| 76 | | | 67.65 | 302.1 | 3.532 |
| 82 | | | 69.53 | 177.5 | 2.022 |
| 88 | | | 71.71 | 103.9 | 1.153 |
| 94 | | | 74.16 | 59.27 | 0.6404 |
| 100 | | | 76.85 | 32.07 | 0.3382 |
| 106 | | | 79.8 | 17.11 | 0.1767 |
| 112 | | | 82.41 | 10.57 | 0.1075 |
| 118 | | | 84.25 | 7.087 | 0.07159 |
| 124 | | | 85.68 | 4.853 | 0.04881 |
| 130 | 86.58 | 3.426 | 0.03438 | | |

Table A-14. PG 76-22M with 2% Sasobit[®] sample 2

| Temperature °C | Angular frequency (rad/sec) | % Strain | Delta, degrees | η' Pa s | $G^*/\sin\delta$ kPa |
|-------------------|--------------------------------|----------|----------------|-----------------|-------------------------|
| 28 | 10 | 12 | 55.69 | 1.41E+05 | 2068 |
| 34 | | | 63.08 | 37450 | 471 |
| 40 | | | 64.18 | 15920 | 196.5 |
| 46 | | | 64.02 | 7788 | 96.37 |
| 52 | | | 63.93 | 3956 | 49.03 |
| 58 | | | 64.18 | 2038 | 25.15 |
| 64 | | | 65.04 | 1024 | 12.46 |
| 70 | | | 66.64 | 503.7 | 5.978 |
| 76 | | | 68.5 | 272.4 | 3.146 |
| 82 | | | 70.45 | 158.4 | 1.784 |
| 88 | | | 72.5 | 93.86 | 1.032 |
| 94 | | | 74.71 | 54.93 | 0.5903 |
| 100 | | | 77.05 | 30.42 | 0.3203 |
| 106 | | | 80.06 | 14.33 | 0.1477 |
| 112 | | | 82.97 | 8.412 | 0.08541 |
| 118 | | | 84.54 | 5.685 | 0.05737 |
| 124 | 85.68 | 3.908 | 0.0393 | | |
| 130 | 86.4 | 2.761 | 0.02772 | | |

Table A-15. PG 76-22M with 4% Sasobit[®] sample 1

| Temperature °C | Angular frequency (rad/sec) | % Strain | Delta, degrees | η' Pa s | $G^*/\sin\delta$ kPa |
|---------------------------|--|-----------------|-----------------------|------------------------------------|--|
| 28 | 10 | 12 | 53.48 | 1.34E+05 | 2073 |
| 34 | | | 62.83 | 37710 | 476.5 |
| 40 | | | 64.04 | 16250 | 201 |
| 46 | | | 63.94 | 7975 | 98.82 |
| 52 | | | 63.88 | 4073 | 50.53 |
| 58 | | | 64.15 | 2100 | 25.93 |
| 64 | | | 65.03 | 1046 | 12.73 |
| 70 | | | 66.68 | 509.7 | 6.045 |
| 76 | | | 68.58 | 274.9 | 3.172 |
| 82 | | | 70.57 | 159.6 | 1.794 |
| 88 | | | 72.67 | 94.26 | 1.034 |
| 94 | | | 74.87 | 55.4 | 0.5945 |
| 100 | | | 77.16 | 30.8 | 0.324 |
| 106 | | | 80.11 | 14.7 | 0.1514 |
| 112 | | | 82.95 | 8.612 | 0.08744 |
| 118 | | | 84.54 | 5.838 | 0.05891 |
| 124 | 85.68 | 4.039 | 0.04062 | | |
| 130 | 86.31 | 2.862 | 0.02874 | | |

Table A-16. PG 76-22M with 4% Sasobit[®] sample 2

| Temperature °C | Angular frequency (rad/sec) | % Strain | Delta, degrees | η' Pa s | $G^*/\sin\delta$ kPa |
|-------------------|--------------------------------|----------|----------------|-----------------|-------------------------|
| 28 | 10 | 12 | 55.69 | 1.41E+05 | 2068 |
| 34 | | | 63.08 | 37450 | 471 |
| 40 | | | 64.18 | 15920 | 196.5 |
| 46 | | | 64.02 | 7788 | 96.37 |
| 52 | | | 63.93 | 3956 | 49.03 |
| 58 | | | 64.18 | 2038 | 25.15 |
| 64 | | | 65.04 | 1024 | 12.46 |
| 70 | | | 66.64 | 503.7 | 5.978 |
| 76 | | | 68.5 | 272.4 | 3.146 |
| 82 | | | 70.45 | 158.4 | 1.784 |
| 88 | | | 72.5 | 93.86 | 1.032 |
| 94 | | | 74.71 | 54.93 | 0.5903 |
| 100 | | | 77.05 | 30.42 | 0.3203 |
| 106 | | | 80.06 | 14.33 | 0.1477 |
| 112 | | | 82.97 | 8.412 | 0.08541 |
| 118 | | | 84.54 | 5.685 | 0.05737 |
| 124 | | | 85.68 | 3.908 | 0.0393 |
| 130 | 86.4 | 2.761 | 0.02772 | | |

Table A-17. Sample density data 1

| 0 % Sasobit[®], 85 °C, 4.8% AC, 120 Gyration | Dry weight gm | Weight in water gm | SSD wt | G_{mb} |
|--|--------------------------|-------------------------------|---------------|-----------------------|
| Sample 1 | 4595.7 | 2621.5 | 4606.4 | 2.32 |
| Sample 2 | 4598.1 | 2626 | 4607.1 | 2.32 |
| Sample 3 | 4599.8 | 2615.8 | 4613.1 | 2.30 |
| 2% Sasobit[®], 85 °C, 4.8% AC, 120 Gyration | | | | |
| Sample 1 | 4604 | 2618.9 | 4612.4 | 2.31 |
| Sample 2 | 4602.8 | 2618.4 | 4614.7 | 2.31 |
| Sample 3 | 4606.9 | 2616.3 | 4619.4 | 2.30 |
| Sample 4 | 4616.6 | 2628 | 4624 | 2.31 |
| 0% Sasobit[®], 120 °C, 4.8% AC, 120 Gyration | | | | |
| Sample 1 | 4553.6 | 2601.5 | 4559.5 | 2.33 |
| Sample 2 | 4599.1 | 2629 | 4610 | 2.32 |
| Sample 3 | 4601.7 | 2631.8 | 4612.5 | 2.32 |
| 2% Sasobit[®], 120 °C, 4.8% AC, 120 Gyration | | | | |
| Sample 1 | 4604.7 | 2635 | 4612.4 | 2.33 |
| Sample 2 | 4609.8 | 2633 | 4619.7 | 2.32 |
| Sample 3 | 4514.9 | 2588 | 4526.6 | 2.33 |

Table A-18. Sample density data 2

| 0 % Sasobit[®], 85 °C, 5% AC, 75 Gyrations | Dry weight gm | Weight in water gm | SSD wt | G_{mb} |
|--|--------------------------|-------------------------------|---------------|-----------------------|
| Sample 1 | 4615 | 2623.6 | 4624 | 2.31 |
| Sample 2 | 4616.5 | 2621.4 | 4625 | 2.30 |
| Sample 3 | 4611.4 | 2623.3 | 4620.8 | 2.31 |
| 2% Sasobit[®], 85 °C, 5% AC, 75 Gyrations | | | | |
| Sample 1 | 4611.3 | 2614.4 | 4622.8 | 2.29 |
| Sample 2 | 4606.2 | 2623.9 | 4616.3 | 2.31 |
| Sample 3 | 4610.6 | 2614.2 | 4620.5 | 2.29 |
| 0% Sasobit[®], 120 °C, 5% AC, 75 Gyrations | | | | |
| Sample 1 | 4610.9 | 2631 | 4617.1 | 2.32 |
| Sample 2 | 4604.2 | 2621.2 | 4609.6 | 2.31 |
| Sample 3 | 4606.7 | 2630.2 | 4617 | 2.32 |
| 2% Sasobit[®], 120 °C, 5% AC, 75 Gyrations | | | | |
| Sample 1 | 4605.5 | 2640.2 | 4614.4 | 2.33 |
| Sample 2 | 4603.6 | 2631.3 | 4613 | 2.32 |
| Sample 3 | 4609 | 2636.5 | 4616.3 | 2.33 |

APPENDIX B
MIX DESIGN DATA

| | | | | | |
|------------|----------------------|------------|----------------------|---------|----------------------|
| Prj. No. | | Mix Type | 0.5 inch NMS | Project | Superpave Mix Design |
| Producer | Amethyst, Ruston, LA | Highway | Homer Street, Ruston | ESALs | 0.3 - 3 M |
| Plant Type | Drum Mixer | Plant Code | | H529 | |

| Materials Type | Materials Source Code | % USED |
|-------------------------|-----------------------|--------|
| Crushed Gravel - Coarse | STANDARD, AA97 | 12 |
| Crushed Gravel - Small | STANDARD, AA97 | 53 |
| Coarse Sand | BIDENHARN, A505 | 18 |
| Fine Sand | RICHARD'S | 17 |
| Perma Tac 99 | LION OIL, 41BF | 0.8 |
| PG 64-22 | AKZO NOBEL, 5753 | 4.8 |

| Sieve Size | Coarse Gravel | Small Gravel | Coarse Sand | Fine Sand | Comb. Agg. | JMF Tolerance (Extracted) |
|------------|---------------|--------------|-------------|-----------|------------|---------------------------|
| 19 mm | 100 | 100 | 100 | 100 | 100.0 | (±4) |
| 12.5 mm | 54 | 99.12 | 100 | 100 | 94.0 | (±4) |
| 9.5 mm | 2.66 | 83.59 | 100 | 100 | 79.6 | (±4) |
| 4.75 mm | 0 | 44.02 | 100 | 100 | 58.3 | (±4) |
| 2.36 mm | 0 | 21 | 91.9 | 100 | 44.7 | (±3) |
| 0.6 mm | 0 | 12 | 55.3 | 99.4 | 33.2 | (±2) |
| 0.15 mm | 0 | 3.1 | 5 | 40.4 | 9.4 | (±2) |
| 0.075 mm | 0.1 | 2.3 | 2.4 | 28 | 6.4 | (±0.7) |

Asphalt Binder (Extracted)

(±0.2)

Tests on Asphalt Cement**Found**

Specific Gravity 1.03

Tests on Aggregates**Req.**

Fine Agg. Angularity, % 46 min. 45

Coarse Agg. Angularity, % 100 min. 95

Flat or Elongated Particles <1 Max. 10

Gse 2.600

Gsb 2.554

Specimen Weight 4600 gm

Tests on Compressed Mixtures (@ Design AC)

| | # Gyr. | Density % of G _{mm} | Density Req. |
|------|--------|------------------------------|--------------|
| Nini | 7 | 88.8 | 90% max. |
| Ndes | 75 | 95.8 | 96.5±1% |
| Nmax | 115 | 96.4 | 98% max. |

Tensile Strength Ratio

Tensile Strength, Control, psi >145

Tensile Strength Ratio (TSR), % >100%

Tests on Compressed Mixtures

| % AC | Gmb | Gmm | Dens. % of Gmm | Density Req. | % VMA | VMA Min Req | % VFA | % VFA Req. | Dust Prop. | DP Req. |
|------|-------|-------|----------------|--------------|-------|-------------|-------|------------|------------|-----------|
| 4.20 | 2.326 | 2.444 | 95.2 | | 12.8 | | 62.2 | | 1.8 | |
| 4.40 | 2.317 | 2.437 | 95.1 | 96.5±1% | 13.3 | 13 | 63.0 | 68-78 | 1.7 | 0.6 - 1.6 |
| 4.80 | 2.321 | 2.423 | 95.8 | | 13.5 | | 69.1 | | 1.55797 | |
| 5.3 | 2.344 | 2.406 | 97.4 | | 13.1 | | 80.9 | | 1.4 | |

Mix Layer Depth 2 in. binder course

MEETS SPECIFICATION REQUIREMENTS

APPENDIX C

RUT TEST DATA

Table C-1. APA rut samples and rut depths of test 1

| Sample ID | %, Air Void | % AC | % Sasobit® | Mixing Temp. °C. | Compaction Temp. °C | Manual Rut, mm | Wheel | Avg. Manual Rut, mm | APA Rut, mm |
|-----------|-------------|-------|------------|------------------|---------------------|----------------|--------|---------------------|-------------|
| Test 1-a | 7.37 | 4.8 | 0 | 163 | 150 | 6.13 | Left | 7.02 | * |
| Test 1-b | 7.37 | | | | | 6.85 | | | |
| Test 1-c | 7.52 | | | | | 7.61 | | | |
| | | | | | | 7.47 | | | |
| Test 1-d | 7.18 | | | | | 8 | Middle | 7.88 | 6.18 |
| | | | | | | 8.01 | | | |
| | | 7.70 | | | | | | | |
| Test 1-e | 7.58 | 7.83 | Right | 9.35 | 7.73 | | | | |
| | | 9.10 | | | | | | | |
| Test 1-f | 7.03 | 10.46 | | | | | | | |
| | | 9.17 | | | | | | | |
| | | | | | | 8.67 | | | |

Table C-2. APA rut samples and rut depths of test 2

| Sample ID | %, Air Void | % AC | % Sasobit® | Mixing Temp. °C. | Compaction Temp. °C | Manual Rut, mm | Wheel | Avg. Manual Rut, mm | APA Rut, mm |
|-----------|-------------|------|------------|------------------|---------------------|----------------|-------|---------------------|-------------|
| Test 2-a | 7.94 | 4.8 | 2 | 163 | 150 | 5.52 | Left | 4.64 | * |
| | 4.64 | | | | | | | | |
| Test 2-b | 7.43 | | | | | 4.34 | | | |
| | 4.08 | | | | | | | | |
| Test 2-c | 7.28 | | | | | Middle | 5.80 | 5.44 | |
| | 5.44 | | | | | | | | |
| Test 2-d | 7.53 | | | | | | 5.12 | | |
| | 5.38 | | | | | Right | 6.34 | 5.31 | |
| Test 2-e | 7.58 | | | | | | 6.10 | | |
| | 4.61 | | | | | | | | |
| Test 2-f | 7.398 | | | | | | 4.19 | | 4.62 |

Table C-3. APA rut samples and rut depths of test 3

| Sample ID | %, Air Void | % AC | % Sasobit® | Mixing Temp. °C. | Compaction Temp. °C | Manual Rut, mm | Wheel | Avg. Manual Rut, mm | APA Rut, mm | |
|------------------|--------------------|-------------|-------------------|-------------------------|----------------------------|-----------------------|--------------|----------------------------|--------------------|------|
| Test 3-a | 9.96 | 4.8 | 0 | 163 | 150 | 9.71 | Left | 9.96 | | |
| Test 3-b | 10.55 | | | | | 9.11 | | | | |
| | | | | | | 10.98 | | | | |
| | | | | | | 10.04 | | | | |
| Test 3-c | 10.72 | | | | | 11.05 | Middle | 12.93 | | 9.42 |
| | | | | | | 11.15 | | | | |
| Test 3-d | 10.5 | 15.50 | | | | | | | | |
| | | 14 | Right | 12.61 | 9.50 | | | | | |
| Test 3-e | 10.29 | 10.27 | | | | | | | | |
| | | 11.23 | | | | | | | | |
| Test 3-f | 10.43 | 16 | | | | | | | | |
| | | 12.95 | | | | | | | | |

Table C-4. APA rut samples and rut depths of test 4

| Sample ID | %, Air Void | % AC | % Sasobit® | Mixing Temp. °C. | Compaction Temp. °C | Manual Rut, mm | Wheel | Avg. Manual Rut, mm | APA Rut, mm | |
|------------------|--------------------|-------------|-------------------|-------------------------|----------------------------|-----------------------|--------------|----------------------------|--------------------|------|
| Test 4-a | 9.36 | 4.8 | 2 | 163 | 150 | 4.41 | Left | 7.58 | | |
| | | | | | | 4.26 | | | | |
| Test 4-b | 11.18 | | | | | 11.20 | | | | |
| | | | | | | 10.48 | | | | |
| Test 4-c | 9.57 | | | | | 6.45 | Middle | 6.76 | | 5.11 |
| | | | | | | 6.68 | | | | |
| Test 4-d | 9.57 | 6.73 | | | | | | | | |
| | | 7.18 | Right | 7.52 | 5.43 | | | | | |
| Test 4-e | 10.02 | 7.54 | | | | | | | | |
| | | 7.64 | | | | | | | | |
| Test 4-f | 10.09 | 7.51 | | | | | | | | |
| | | 7.39 | | | | | | | | |

Table C-5. APA rut samples and rut depths of test 5

| Sample ID | %, Air Void | % AC | % Sasobit® | Mixing Temp. °C. | Compaction Temp. °C | Manual Rut, mm | Wheel | Avg. Manual Rut, mm | APA Rut, mm |
|-----------|-------------|------|------------|------------------|---------------------|----------------|--------|---------------------|-------------|
| Test 5-a | 7.55 | 5.3 | 0 | 163 | 150 | 5.74 | Left | 6.94 | |
| Test 5-b | 8.31 | | | | | 6.82 | | | |
| | | | | | | 7.74 | | | |
| | | | | | | 7.45 | Middle | 10.03 | |
| Test 5-c | 7.70 | | | | | 10.24 | | | |
| | | | | | | 10.39 | | | |
| Test 5-d | 7.70 | | | 9.48 | Right | 8.73 | 7.04 | | |
| | | | | 10 | | | | | |
| Test 5-e | 7.18 | | | 10.12 | | | | | |
| | | | | 9.56 | | | | | |
| | | | | 7.71 | | | | | |
| Test 5-f | 7.58 | | | | | 7.52 | | | |

Table C-6. APA rut samples and rut depths of test 6

| Sample ID | %, Air Void | % AC | % Sasobit® | Mixing Temp. °C. | Compaction Temp. °C | Manual Rut, mm | Wheel | Avg. Manual Rut, mm | APA Rut, mm |
|-----------|-------------|------|------------|------------------|---------------------|----------------|--------|---------------------|-------------|
| Test 6-a | 8.16 | 5.3 | 2% | 163 | 150 | 7.56 | Left | 7.36 | |
| Test 6-b | 9.24 | | | | | 6.88 | | | |
| Test 6-c | 8.07 | | | | | 6.85 | | | |
| Test 6-d | 7.46 | | | | | 8.15 | Middle | 6.66 | |
| | | | | | | 7.22 | | | |
| Test 6-e | 7.43 | | | | | 6.53 | Right | 5.39 | |
| | | 6.19 | | | | | | | |
| Test 6-f | 7.46 | 6.68 | | | | | | | |
| | | 6.04 | | | | | | | |
| | | 5.30 | | | | | | | |
| | | 5.19 | | | | | | | |
| | | 5.01 | | | | | | | |

Table C-7. APA rut samples and rut depths of test 7

| Sample ID | %, Air Void | % AC | % Sasobit® | Mixing Temp. °C. | Compaction Temp. °C | Manual Rut, mm | Wheel | Avg. Manual Rut, mm | APA Rut, mm | |
|-----------|-------------|------|------------|------------------|---------------------|----------------|-------|---------------------|-------------|------|
| Test 7-a | 7.31 | 4.8 | 0 | 143 | 110 | 8.16 | Left | 7.71 | | |
| | | | | | | 8.31 | | | | |
| Test 7-b | 6.93 | | | | | 7.16 | | | | |
| | | | | | | 7.23 | | | | |
| Test 7-c | 6.69 | | | | | Middle | 7.21 | 6.65 | | 6.49 |
| | | | | | | | 6.46 | | | |
| Test 7-d | 7.43 | | | | | | 6.25 | | | |
| | | | | | | 6.68 | | | | |
| Test 7-e | 7.06 | | | | | Right | 6.18 | 5.45 | | 7.38 |
| | | | | | | | 5.08 | | | |
| | | | | | | | 5.31 | | | |
| Test 7-f | 7.55 | | | | | | 5.23 | | | |

Table C-8. APA rut samples and rut depths of test 8

| Sample ID | %, Air Void | % AC | % Sasobit® | Mixing Temp. °C. | Compaction Temp. °C | Manual Rut, mm | Wheel | Avg. Manual Rut, mm | APA Rut, mm |
|-----------|-------------|------|------------|------------------|---------------------|----------------|--------|---------------------|-------------|
| Test 8-a | 7.57 | 4.8 | 2 | 143 | 110 | 6.23 | Left | 5.23 | 5.13 |
| Test 8-b | 7.49 | | | | | 6.03 | | | |
| | | | | | | 4.52 | | | |
| | | | | | | 4.13 | | | |
| Test 8-c | 7.69 | | | | | 6.45 | Middle | 5.94 | |
| Test 8-d | 7.10 | | | | | 6.38 | | | |
| | | | | | | 5.58 | | | |
| | | | | | | 5.33 | Right | 6.04 | |
| Test 8-e | 7.55 | 6.84 | | | | | | | |
| | | 6.20 | | | | | | | |
| Test 8-f | 7.52 | 6.03 | | | | | | | |
| | | 5.10 | | | | | | | |

Table C-9. APA rut samples and rut depths of test 9

| Sample ID | %, Air Void | % AC | % Sasobit® | Mixing Temp. °C. | Compaction Temp. °C | Manual Rut, mm | Wheel | Avg. Manual Rut, mm | APA Rut, mm | |
|-----------|-------------|-------|------------|------------------|---------------------|----------------|--------|---------------------|-------------|------|
| Test 9-a | 8.04 | 4.8 | 2 | 133 | 110 | 6.55 | Left | 5.39 | | |
| Test 9-b | 7.71 | | | | | 4.71 | | | | |
| Test 9-c | 7.67 | | | | | 5.26 | | | | |
| | | | | | | 5.06 | | | | |
| Test 9-d | 7.69 | | | | | 6.81 | Middle | 6.36 | | 6.29 |
| | | | | | | 6.47 | | | | |
| | | 5.86 | | | | | | | | |
| Test 9-e | 7.65 | Right | 5.59 | 5.78 | 6.01 | | | | | |
| Test 9-f | 7.67 | | | | 6.12 | | | | | |
| | | | | | 5.71 | | | | | |
| | | | | | | 4.51 | | | | |

Table C-10. APA rut samples and rut depths of test 10

| Sample ID | %, Air Void | % AC | % Sasobit® | Mixing Temp. °C. | Compaction Temp. °C | Manual Rut, mm | Wheel | Avg. Manual Rut, mm | APA Rut, mm |
|-----------|-------------|-------|------------|------------------|---------------------|----------------|-------|---------------------|-------------|
| Test 10-a | 7.28 | 4.8 | 0 | 133 | 110 | 7.92 | Left | 8.25 | |
| | 7.70 | | | | | | | | |
| Test 10-b | 7.77 | | | | | | | | |
| | 8.76 | | | | | | | | |
| | 8.63 | | | | | | | | |
| Test 10-c | 7.43 | | | | | Middle | 7.40 | 5.82 | |
| | 8.91 | | | | | | | | |
| Test 10-d | 7.15 | | | | | | | | |
| | 7.13 | Right | 8.93 | 7.56 | 5.75 | | | | |
| Test 10-e | 8.04 | | | | | | | | |
| | 8.01 | | | | | | | | |
| | 8.34 | | | | | | | | |
| | 10.42 | | | | | | | | |
| Test 10-f | 7.18 | | | | 8.96 | | | | |

APPENDIX D

AGING DATA

Table D-1. Phase angle, dynamic modulus and stiffness of asphalt binders extracted from 166 °C mix with 0% Sasobit[®]

| Asphalt binders extracted from 166 °C mix with 0% Sasobit[®] | | | |
|--|-------------------|------------|------------------------|
| | δ , degree | G^* , Pa | $G^*/\sin\delta$, kPa |
| 64°C | | | |
| Sample 1 | 86.6 | 2208.0 | 2.2 |
| Sample 2 | 86.6 | 2285.0 | 2.3 |
| Sample 3 | 86.3 | 2696.0 | 2.7 |
| Sample 4 | 86.2 | 2816.0 | 2.8 |
| Average | 86.5 | 2501.3 | 2.5 |
| St. Dev. | 0.19 | 299.86 | 0.30 |
| 76°C | | | |
| sample 1 | 88.6 | 527.8 | 0.5 |
| Sample 2 | 88.6 | 531.4 | 0.5 |
| Sample 3 | 88.5 | 609.8 | 0.6 |
| Sample 4 | 88.4 | 636.0 | 0.6 |
| Average | 88.5 | 576.3 | 0.6 |
| St. Dev. | 0.08 | 54.94 | 0.05 |

Table D-2. Phase angle, dynamic modulus and stiffness of asphalt binders extracted from 166 °C mix with 2% Sasobit[®]

| Asphalt binders extracted from 166 °C mix with 2% Sasobit[®] | | | |
|--|-------------------|------------|------------------------|
| | δ , degree | G^* , Pa | $G^*/\sin\delta$, kPa |
| 64°C | | | |
| Sample 1 | 82.8 | 4377.0 | 4.4 |
| Sample 2 | 82.1 | 4690.0 | 4.7 |
| Sample 3 | 82.5 | 4293.0 | 4.3 |
| Sample 4 | 83.3 | 3481.0 | 3.5 |
| Average | 82.7 | 4210.3 | 4.2 |
| St. Dev. | 0.50 | 515.31 | 0.52 |
| 76°C | | | |
| Sample 1 | 84.3 | 959.3 | 1.0 |
| Sample 2 | 83.5 | 1037.0 | 1.0 |
| Sample 3 | 83.7 | 1006.0 | 1.0 |
| Sample 4 | 84.3 | 856.3 | 0.9 |
| Average | 83.9 | 964.7 | 1.0 |
| St. Dev. | 0.41 | 78.98 | 0.08 |

Table D-3. Phase angle, dynamic modulus and stiffness of asphalt binders extracted from 133 °C mix with 0% Sasobit®

| Asphalt binders extracted from 133 °C mix with 0% Sasobit® | | | |
|---|------------------------------------|---------------|---------------------------------------|
| | δ, degree | G*, Pa | G*/sinδ, kPa |
| 64°C | | | |
| Sample 1 | 87.2 | 2543.0 | 2.5 |
| Sample 2 | 87.3 | 2308.0 | 2.3 |
| Sample 3 | 87.3 | 2328.0 | 2.3 |
| Sample 4 | 87.1 | 2511.0 | 2.5 |
| Average | 87.2 | 2422.5 | 2.4 |
| St. Dev. | 0.08 | 121.65 | 0.12 |
| 76°C | | | |
| Sample 1 | 89.0 | 571.8 | 0.6 |
| Sample 2 | 89.0 | 528.4 | 0.5 |
| Sample 3 | 89.0 | 533.0 | 0.5 |
| Sample 4 | 88.9 | 563.9 | 0.6 |
| Average | 89.0 | 549.3 | 0.5 |
| St. Dev. | 0.04 | 21.77 | 0.02 |

Table D-4. Phase angle, dynamic modulus and stiffness of asphalt binders extracted from 133 °C mix with 2% Sasobit®

| Asphalt binders extracted from 133 °C mix with 2% Sasobit® | | | |
|---|------------------------------------|---------------|---------------------------------------|
| | δ, degree | G*, Pa | G*/sinδ, kPa |
| 64°C | | | |
| Sample 1 | 84.5 | 2645.0 | 2.7 |
| Sample 2 | 82.9 | 2872.0 | 2.9 |
| Sample 3 | 84.9 | 2876.0 | 2.9 |
| Sample 4 | 85.2 | 2842.0 | 2.9 |
| Average | 84.4 | 2808.8 | 2.8 |
| St. Dev. | 1.04 | 110.22 | 0.11 |
| 76°C | | | |
| Sample 1 | 85.9 | 623.9 | 0.6 |
| Sample 2 | 83.8 | 700.9 | 0.7 |
| Sample 3 | 86.0 | 694.7 | 0.7 |
| Sample 4 | 86.3 | 678.1 | 0.7 |
| Average | 85.5 | 674.4 | 0.7 |
| St. Dev. | 1.13 | 35.02 | 0.04 |

Table D-5. Phase angle, dynamic modulus and stiffness of original PG 64-22 with 0% Sasobit[®]

| Original PG 64-22 with 0% Sasobit[®] | | | |
|--|------------------------------------|---------------|---------------------------------------|
| | δ, degree | G*, Pa | G*/sinδ, kPa |
| 64°C | | | |
| Sample 1 | 88.2 | 1536.0 | 1.5 |
| Sample 2 | 88.2 | 1380.0 | 1.4 |
| Sample 3 | 88.2 | 1383.0 | 1.4 |
| Sample 4 | 88.2 | 1532.0 | 1.5 |
| Average | 88.2 | 1457.8 | 1.5 |
| St. Dev. | 0.04 | 88.07 | 0.09 |
| 76°C | | | |
| Sample 1 | 89.4 | 360.3 | 0.4 |
| Sample 2 | 89.3 | 357.0 | 0.4 |
| Sample 3 | 89.3 | 355.3 | 0.4 |
| Sample 4 | 89.4 | 357.6 | 0.4 |
| Average | 89.3 | 357.6 | 0.4 |
| St. Dev. | 0.02 | 2.08 | 0.00 |

Table D-6. Phase angle, dynamic modulus and stiffness of original PG 64-22 with 2% Sasobit[®]

| Original PG 64-22 with 2% Sasobit[®] | | | |
|--|------------------------------------|---------------|---------------------------------------|
| | δ, degree | G*, Pa | G*/sinδ, kPa |
| 64°C | | | |
| Sample 1 | 79.4 | 3707.0 | 3.8 |
| Sample 2 | 78.1 | 3875.0 | 4.0 |
| Sample 3 | 77.5 | 3891.0 | 4.0 |
| Sample 4 | 77.9 | 3555.0 | 3.6 |
| Average | 78.2 | 3757.0 | 3.8 |
| St. Dev. | 0.81 | 158.31 | 0.17 |
| 76°C | | | |
| Sample 1 | 81.3 | 894.0 | 0.9 |
| Sample 2 | 79.6 | 992.7 | 1.0 |
| Sample 3 | 78.9 | 1004.0 | 1.0 |
| Sample 4 | 79.7 | 911.7 | 0.9 |
| Average | 79.8 | 950.6 | 1.0 |
| St. Dev. | 0.99 | 55.80 | 0.06 |